CARDIAC AND VALVE-GAPING ACTIVITY OF MUSSELS IN RESPONSE TO COMMON STRESSORS IN SAN DIEGO ESTUARIES

A Thesis

Presented to the

Faculty of

San Diego State University

In Partial Fulfillment

of the Requirements for the Degree

Master of Science in Biology

with a Concentration in

Ecology

---

by

Monica Jayne Klopp

Fall 2025

SAN DIEGO STATE UNIVERSITY

The Undersigned Faculty Committee Approves the

Thesis of Monica Jayne Klopp:

Cardiac and Valve-Gaping Activity of Mussels in Response to Common Stressors in San Diego Estuaries

Luke Miller, Chair
Department of Biology

Kevin Hovel
Department of Biology

Trent Biggs
Department of Geography

10/22/2025

Approval Date

DEDICATION

To my parents. Thank you for “shipping” me off to marine science camp every summer growing up.

ABSTRACT OF THE THESIS

Cardiac and Valve-Gaping Activity of Mussels in Response to
Common Stressors in San Diego Estuaries
by
Monica Jayne Klopp
Master of Science in Biology with a Concentration in Ecology
San Diego State University, 2025

Urban estuaries face mounting pressures from anthropogenic activity and climate change. However, effective tools for monitoring biological responses alongside abiotic stressors remain limited. The need for robust monitoring is especially prevalent in San Diego, CA, where urbanized, low-inflow estuaries frequently experience stressful conditions. One promising approach is the use of bivalve biosentinels. Monitoring the behavior and physiology of bivalve biosentinels within these estuaries can provide a detailed understanding of ecosystem stress in real time. In my thesis, I aimed to understand how the Mediterranean mussel (*M. galloprovincialis*) responds to common stressors in three San Diego estuaries (Los Peñasquitos Lagoon, San Diego Bay, and the Tijuana River Estuary) by measuring their heart rate and gaping behavior in the laboratory and comparing those results to what is observed in the field. Mussels were equipped with custom infrared heart rate sensors and Hall-effect gape sensors to continuously monitor cardiac activity and valve behavior. To evaluate mussel responses to stressors, I conducted laboratory experiments exposing individuals to either hypoxia (≤ 3 mg L^{-1}) or low salinity (< 3 psu). I also conducted field deployments to track cardiac and gaping responses under natural conditions at two depths within the three estuaries. During the lab trials, hypoxia increased heart rate variability and short bursts of gaping activity. Exposure to low salinity induced prolonged valve closure and decreased average heart rate. Both stressors elicited pronounced spikes in cardiac activity during recovery, likely in response to oxygen debt accrued during a transition to anaerobic metabolism during stressful periods. Mussels from the different estuaries responded similarly during laboratory trials, suggesting that gene flow may homogenize traits along the San Diego coastline. Field deployments, however, revealed strong site-specific differences: mussels in San Diego Bay and Los Peñasquitos Lagoon experienced relatively benign conditions, while mussels in the Tijuana River Estuary experienced chronic hypoxia, salinity crashes, and elevated turbidity that reduced overall survival and growth. Collectively, these findings highlight the value of bivalve biosentinels for capturing biologically meaningful responses to estuarine stress and demonstrate their potential as a complementary tool to abiotic monitoring for managing and conserving urban estuaries.

TABLE OF CONTENTS

PAGE

LIST OF TABLES

PAGE

LIST OF FIGURES

PAGE

INTRODUCTION

ENVIRONMENTAL STRESSORS IN URBAN ESTUARIES

Amidst rapid environmental change due to anthropogenic activity, there is a growing urgency to direct research efforts toward developing new tools for ecosystem monitoring (Sparrow et al., 2020). Ecosystems impacted by urbanization require robust monitoring systems that provide information on the health and functioning of these ecosystems. Estuaries are one such ecosystem that is vulnerable and in need of monitoring. An estuary is a coastal ecosystem where freshwater from rivers and streams meets and mixes with saltwater from the ocean. Because estuaries sit at the interface between freshwater and saltwater systems, they tend to be dynamic and highly productive ecosystems that experience strong temporal variation (Shen et al., 2022). They act as buffers protecting shoreline communities from extreme weather and waves that can lead to coastal erosion (Barbier et al., 2011). They are also critical habitats for the life cycle completion of many species, including crabs, flatfish, and salmonids (Armstrong et al., 2003; Brown et al., 2006; Davis et al., 2022; Guerreiro et al., 2021). However, many estuaries are vulnerable to both anthropogenic and climate impacts. Estuaries located near or within highly developed areas are at a particularly high risk of ecosystem collapse due to contamination from urban runoff, eutrophication, overexploitation, hypoxia, and habitat loss due to shoreline manipulation (Kennish, 2002; Levin et al., 2023; Tronske et al., 2018). Increased temperatures and more frequent and severe weather events caused by climate change exacerbate the adverse effects experienced by these coastal areas (Harvey et al., 2020).

San Diego estuaries are heavily impacted by both urbanization and climate change. All estuaries along the San Diego coastline are classified as low-inflow, where the rate of freshwater inflow is low enough that the estuary is predominantly influenced by oceanic processes (Doughty et al., 2019; Largier, 2023). Some low-inflow estuaries experience closure of the tidal inlet, as wave action and tidal fluctuations that move water in and out of

the estuary can deposit sediment and increase the sill elevation at the tidal inlet (Gale et al., 2006). Closure of the tidal inlet increases temperatures, decreases salinity, and reduces dissolved oxygen (DO) within the estuary (Behrens et al., 2016; Cousins et al., 2010). These conditions can lead to biodiversity loss, flooding, poor water quality, and habitat loss (Kennish, 2002; Largier et al., 2019; Ludka et al., 2018; Nordby and Zedler, 1991; Zedler, 2010). In recent decades, increases in urban activity, such as beach nourishment, wetland fill, infrastructure placement, and dam impoundments have all resulted in an increased risk of mouth closures (Coats et al., 1989; Ludka et al., 2018). These effects are exacerbated by sea-level rise, wave action, and extreme weather events, which have led to more frequent and prolonged mouth closures (Harvey et al., 2020). Overall, interruptions in natural ocean-estuary exchange can lead to a significant decline in the health of an estuary over time. As these threats to urban estuaries continue to increase, it is imperative that robust abiotic and organismal monitoring efforts be implemented to successfully mitigate negative impacts.

BIVALVES AS ESTUARY BIOSENTINELS

Traditionally, San Diego estuary conditions have been monitored using abiotic parameters such as temperature, nutrients, pH, salinity, and DO (O'Higgins and Rumril, 2007). Although these factors are important for understanding estuarine dynamics, they often fail to capture the full status of organismal health in the estuary. Abiotic factors alone miss the crucial biological responses to subtle changes in water quality that may pose harm to the organisms living in an estuary. It is therefore vital to augment existing monitoring tools with novel approaches to better understand ecosystem health and support more effective mitigation efforts.

One way to gain valuable information on the health of an ecosystem is to use a biosentinel. A biosentinel is an organism that provides measurable responses to ecosystem changes in a timely fashion (Hazen et al., 2019). A classic example of a biosentinel is the use of the canary in coal mines in the early 20th century. A dead canary alerted coal mine workers to lethal levels of carbon monoxide in the surrounding area. In aquatic environments, the diversity of invertebrates has historically been measured as a bioindicator of ecosystem health (Wilhm and Dorris, 1968). Biosentinels can also be used to detect and elucidate harmful changes in water quality. During some harmful algal blooms, *Pseudo-*

nitzschia diatoms produce domoic acid, which can have neurotoxic effects on mammals and birds. The California sea lion (*Zalophus californianus*) is a useful biosentinel for the presence of domoic acid, as exposed animals exhibit distinct neurological symptoms (McClain et al., 2023). Ultimately, an organism that is used as a biosentinel species can provide crucial information on the status of its environment.

The decision on which organism to use as a biosentinel species in a particular environment depends on what data will be collected and how those data will be used. In an estuarine system, bivalves are an ideal option for biosentinels. Bivalves filter-feed, bioaccumulate, are abundant, easy to collect, and sessile, so they can provide feedback about water quality in their habitat. Bivalves have been used in many scenarios as biosentinels. For example, NOAA's National Mussel Watch Project presents annual metrics on the contamination levels at nearly 300 national monitoring sites by collecting mussels from each site and transporting them to contract labs for analysis (Melwani et al., 2014). Bivalves have also been used in San Diego estuaries as indicators of contaminated water. In San Diego Bay, non-native Pacific oysters (*Crassostrea* (*Magallana*) *gigas*) have been collected and analyzed for contaminants that would pose a risk to food webs and human health (Talley et al., 2022).

Ideally, native bivalves would be used as biosentinels in San Diego estuaries; however, the native Olympia oyster *Ostrea lurida* is not available in high enough abundance in San Diego, and the native bay mussel *Mytilus trossulus* has been displaced by the non-native Mediterranean mussel *Mytilus galloprovincialis* (Geller, 1999). For my project, I used the Mediterranean mussel *M. galloprovincialis* as a biosentinel due to its high abundance in the local estuaries (McDonald and Koehn, 1988). I also attempted to use the Pacific oyster, *C. gigas*, but found that population abundances were too low in the Tijuana River Estuary, where the oyster has all but vanished since 2023 (*personal observation*), despite increases in population abundances elsewhere (Wolfe et al., 2024). Furthermore, the thicker shell of the Pacific oyster makes it more challenging to place infrared heart sensors successfully.

M. galloprovincialis is an invasive marine bivalve that has spread successfully around the world through both accidental (ship ballast water; Geller et al., 1994) and intentional (aquaculture) introductions (McDonald and Koehn, 1988). *M. galloprovincialis* was not noted to be an invasive species along the Southern California coastline until the 1980s (Geller, 1999; McDonald and Koehn, 1988). However, the mussel was likely introduced

earlier in the 20th century due to shipping activity. Since *M. galloprovincialis* is morphologically similar to its native congener *M. trossulus*, the invasion initially went unnoticed (Geller, 1999). However, *M. galloprovincialis* is more heat-tolerant and has a growth rate nearly ten times greater than *M. trossulus*, which likely allowed for the invasive mussel to quickly outgrow and replace native populations of *M. trossulus* (Lockwood and Somero, 2011; Shinen and Morgan, 2009). Currently, *M. galloprovincialis* is widely cultivated for aquaculture purposes all along the West Coast (Wonham, 2004) and also exists in self-sustaining populations within San Diego estuaries. Since *M. galloprovincialis* is highly successful in exploiting these highly urbanized areas, it can be used as a biosentinel species to provide management agencies with information on water quality and the overall health of estuarine biota.

MUSSEL PERFORMANCE IN DIFFERENT ABIOTIC CONDITIONS

If mussels are to be used as biosentinels, it is essential to understand how various abiotic conditions will affect their physiological and behavioral performance. In estuarine ecosystems, mussels are exposed to various environmental stressors. Their responses to changes in factors such as temperature, food availability, turbidity, DO, and salinity must be carefully characterized to ensure they serve as reliable indicators of ecosystem health. By identifying the environmental thresholds that affect mussel performance, we can better interpret biosentinel data and assess the ecological significance of observed physiological and behavioral changes.

Changes in water temperature can impact the physiology of mussels. *M. galloprovincialis* is a eurythermal species that displays tolerance to water temperatures ranging from near freezing to ~31 °C (Lockwood and Somero, 2011). This is a potential driver behind the widespread invasion of this mussel into San Diego's coastal areas. However, depending on acclimation conditions, cardiac failure can occur for this species at temperatures as low as 26 °C (Braby and Somero, 2006). These mussels also begin synthesizing heat shock proteins at temperatures as low as 25 °C, indicating that physiological changes occur at this temperature threshold (Hofmann and Somero, 1996). Although water temperatures infrequently exceed 25 °C along the San Diego coastline,

climate change is likely to increase the frequency and intensity of warming events in the future.

As a filter feeder, *M. galloprovincialis* depends on a relatively constant supply of phytoplankton and other organic matter. Reductions in chlorophyll *a*, a proxy for phytoplankton biomass, can lower the frequency of valve gaping and reduce growth. The threshold at which the blue mussel *Mytilus edulis* closes its valves is ~0.9µg chl *a* L^{-1}, which is likely a similar concentration at which valve closure occurs for *M. galloprovincialis* (Riisgård et al., 2006). *M. edulis* also closes its valves at high concentrations of chlorophyll *a*, likely due to its gut capacity being exceeded (Riisgård, 1991). In either scenario, suboptimal concentrations of chlorophyll *a* result in reduced performance overall. Chlorophyll *a* is especially important in the context of eutrophication resulting from urban runoff. Rain events can flush urban runoff into estuaries, resulting in an influx of nutrients. This influx can trigger algal blooms, leading to an increase in algal and phytoplankton biomass and, consequently, higher chlorophyll *a* levels within the estuary (Boyer et al., 2009). Understanding how mussel biosentinels respond to increased chlorophyll *a* can provide insight into when urban runoff influxes occur and when algal blooms are likely to happen.

Turbidity, a measure of water clarity influenced by suspended particles, can also significantly affect mussel performance. High amounts of chlorophyll *a* in the water column can contribute to inflated turbidity measurements. However, in the absence of high chlorophyll *a* fluorescence, high turbidity measurements can indicate an increased presence of inorganic and low-quality organic particles. Increases in turbidity are particularly prominent in estuaries during flood events associated with storms (Fahey and Coker, 1992). In the Tijuana River Estuary, chronic urban runoff and wastewater plumes also contribute substantially to higher turbidity measurements (Ayad et al., 2020). When bivalves actively filter-feed, elevated amounts of suspended inorganic particles can increase pseudofeces production, decrease nutrient absorption efficiency, and damage gill tissue (Ellis et al., 2002). To mitigate these impacts, mussels may close their valves and decrease their heart rates more frequently (Newell et al., 2001). Over time, chronic exposure to increased concentrations of suspended particles can lead to a decrease in the amount of energy available for growth and

reproduction. Given these impacts, monitoring mussel responses to turbidity can provide valuable insight into the ecological consequences of storm-driven runoff and pollution.

Hypoxic events, characterized by a decrease in DO in the water column, are also common in low-inflow estuaries. Often associated with eutrophication and stratified water, hypoxia can significantly impact the physiology and behavior of bivalves. Although intertidal mussels experience hypoxia regularly during aerial exposure at low tide, aqueous hypoxia can be much more harmful. Altieri (2006) demonstrated that while it took 70 hours of aerial exposure for intertidal mussels to experience 50% mortality, aqueous hypoxia caused 50% mortality in just 50 hours. This suggests that mussels exposed to aqueous hypoxia employ a different metabolic strategy than those exposed to aerial hypoxia, and that aqueous hypoxia is more stressful to mussels than aerial exposure (Altieri, 2006). Bivalve performance metrics are also impacted by hypoxia. Both tissue and shell growth decrease in *M. galloprovincialis* mussels exposed to hypoxia (Roberts and Carrington, 2023). In another study, exposure to hypoxia significantly reduced the settlement of eastern oyster (*Crassostrea virginica*) larvae (Baker and Mann, 1992). Physiological and behavioral performance metrics, including cardiac activity and gaping behavior, also change in response to hypoxic conditions (Peterson et al., 2025). As estuaries are becoming hypoxic more frequently due to climate change and increased nutrient loads (Breitburg et al., 2018), it is crucial to understand how bivalves respond (Altieri and Diaz, 2019; Diaz and Rosenberg, 2008; Seibel, 2023).

Bivalve molluscs such as *M. galloprovincialis* are osmoconformers. Their internal osmolarity fluctuates to mirror the salinity of the surrounding environment (Gostyukhina et al., 2023). These mussels can survive in a wide range of salinities (Boukadida et al., 2024); however, extreme fluctuations can negatively impact their behavior, physiology, and survival. Prolonged low salinity exposure (~10 psu) increased mortality in populations of *M. galloprovincialis* in the Black Sea, and exposure to low salinity decreased biomass, growth rates, and juvenile recruitment (Shurova, 2001). *M. edulis* individuals from sites experiencing high salinity fluctuations (10 to 30 psu) in the Baltic Sea had the lowest growth rates (Landes et al., 2015). Elevated salinity levels have also been associated with increases in instances of larval malformation (Boukadida et al., 2024). Physiological and behavioral performance metrics, such as cardiac activity and gaping behavior, also change in response to abnormal salinity (Addis et al., 2021; Andrews et al., 1959; Braby and Somero, 2006). Low salinity

events are a significant concern in urban estuaries due to increases in runoff and more intense rainfall activity during the wet season (Luković et al., 2021; White and Greer, 2006). Monitoring the responses of bivalve biosentinels to salinity fluctuations can provide crucial insight into how these estuarine ecosystems are changing over time.

CARDIAC AND VALVE-GAPING ACTIVITY AS MEASUREMENTS OF BIVALVE PERFORMANCE

Obtaining timely data is a key component of a biosentinel monitoring program. Traditional methods to obtain bivalve performance metrics have included measuring length, weight, recruitment rates, and tissue samples (Livingston et al., 2000; Talley et al., 2022). However, these variables are only able to encapsulate the long-term responses of bivalves. More recent studies have included heart rate and valve gape metrics (Cheng et al., 2025; Miller and Dowd, 2019; Porter and Breitburg, 2016), which can serve as a proxy for immediate physiological responses to changes in environmental conditions (Bayne, 2000; Miller and Dowd, 2017).

Valve gape serves as an indicator of feeding and respiratory activity. It can be easily measured and provides crucial metrics for gauging behavioral responses in bivalves (Frank et al., 2007). Stressful conditions such as elevated temperatures, low DO, low salinity, or chemical contamination can trigger bivalves to close their valves (Bamber, 2018; Borcherding, 2006; Porter and Breitburg, 2016; Tran et al., 2003; de Zwart et al., 1995). Valve-closure frequency tends to increase as water quality decreases (Bamber, 2023; Dowd and Somero, 2013; Porter and Breitburg, 2016; de Zwart et al., 1995). This ultimately leads to slower growth and reproductive rates, as the bivalves spend less time feeding and respiring (Ballesta-Artero et al., 2017). In contrast, bivalves may increase gaping activity in response to stressors, possibly as an effort to enhance metabolism and excrete harmful substances (Clements et al., 2018; Tran et al., 2010). In either case, a sustained change in valve gaping frequency indicates a stressful environment.

Heart rate sensors can also give valuable physiological information in cases where the environmental stressor is not severe enough to cause complete valve closure (Curtis et al., 2000). Both high and low heart rates can indicate harmful conditions depending on the stressor (Andrews et al., 1959; Widdows, 1973). For example, *M. galloprovincialis* exhibits

increased heart rates as water temperatures increase, while low salinity tends to lead to decreased heart rates (Braby and Somero, 2006). Decreased heart rates have also been observed in conditions with low DO levels (Gurr et al., 2018). Bivalves decrease their heart rates when their valves are closed to reduce energy usage as metabolism switches from aerobic to anaerobic respiration (Meng et al., 2018; Trueman, 1967). However, in cases when the valves open during or immediately following a stressful event, bivalves may increase their heart rates in an attempt to increase metabolism for excreting toxicants (Byrne et al., 1990; Trueman and Lowe, 1971). Since bivalves can experience both high and low heart rates under stressful conditions, an individual with a wider ranging or more variable heart rate may be exhibiting lower overall performance (Hui et al., 2020). It is crucial to tease out any patterns in heart rate and gaping behavior so that the information gathered from bivalve biosentinels can be more accurately understood.

COMBINING LAB AND FIELD APPROACHES TO ASSESS STRESSOR EFFECTS

In urban estuaries, long-term monitoring is essential for understanding the environmental changes that occur in the wake of anthropogenic and climate impacts. Advancements in both technology and methodology are crucial for enhancing the effectiveness of these monitoring efforts. Laboratory experiments are key to improving the tools used in long-term monitoring. When using a biosentinel, experimentally testing the organism's physiological and behavioral responses to specific stressors can provide a valuable baseline for responses observed in the field. Those baseline responses can significantly improve the successful implementation of a biosentinel monitoring system. My lab experiments will analyze the individual impact of low salinity and hypoxia on mussel valve gaping and heart rate in the context of long-term bivalve biosentinel monitoring in San Diego estuaries.

OBJECTIVES AND PREDICTIONS

The objective of my thesis is to understand how *M. galloprovincialis* responds to common stressors in San Diego estuaries by measuring heart rate and gaping behavior in the laboratory and comparing those results to what is observed in the field. Measures of higher performance included high proportions of open valves, higher gape opening %, moderate

average heart rates, and less variable heart rates. For the animals in the field, I also included higher shell growth rates and decreased mortality as indicators of high performance.

In the field, I deployed mussels on moorings and monitored them *in situ* in three different San Diego estuaries. I deployed one mooring in each estuary, submerging mussels at both the surface and the bottom of the water column. The frequency and intensity of stressors can differ between depths. For example, rainfall decreases salinity more at the surface of the water column compared to near the benthos. Deploying biosentinels at both depths provided heart rate and valve-gaping data under a gradient of estuarine conditions. I expected that mussels deployed in an estuary with more frequent and intense stressful events would have lower performance than mussels in an estuary with more benign conditions.

I also conducted controlled laboratory experiments designed to mimic stressful events that occur in the field. In the lab experiments, *M. galloprovincialis* collected from each estuary were exposed to either low salinity or hypoxia, and the resulting changes in the gaping and cardiac activity were recorded. I predicted that mussels exposed to low salinity or hypoxia would exhibit lower overall performance compared to mussels in unmanipulated seawater. There is debate about whether increasingly frequent and intense stressors will have a positive or negative impact on bivalve resilience in estuaries (Altieri, 2006; Gurr et al., 2021). Since mussels grown in different environmental conditions may have differing tolerances to stress, I also predicted that mussels from an estuary that experiences stressful conditions more frequently than other estuaries will perform better than mussels gathered from less stressful estuaries.

METHODS

SITE SELECTION AND BIVALVE COLLECTION

I conducted my field experiments in three low-inflow estuaries (Figure 1) along the San Diego coastline: Los Peñasquitos Lagoon (LPL; 32.933350 N, 117.257079 W), San Diego Bay (SDB; 32.710072 N, -117.174416 W), and the Tijuana River Estuary (TRE; 32.556920 N, -117.126148 W). LPL covers ~2 km^2 and is a shallow estuary that sits at the outlet of a 255km^2 watershed (Harvey et al., 2023). SDB is a much larger estuary, spanning 57 km^2, that drains a 660 km^2 watershed (Komoroske et al., 2012). The TRE covers ~10 km^2 and drains a large 4483 km^2 watershed—27% of which originates from the United States and 73% from Mexico (Biggs et al., 2022). I chose these sites based on their geographical separation and the differing frequencies of tidal inlet closure they experience. The tidal inlet closes annually at LPL, occasionally at the TRE, and SDB remains open to the ocean throughout the year. SDB was my reference site since conditions are relatively stable all year round. The TRE had the potential to exhibit more frequent stressful conditions due to the occasional inlet closures and chronic sewage spills. In both 2017 and 2022, heavy rainfall caused significant damage to Tijuana's sewage system, resulting in the spill of over 500 million liters of raw sewage into the TRE across the Mexican border (McLamb et al., 2024). Since 2022, the TRE has been heavily inundated with chronic sewage flow. LPL also had the potential to exhibit more frequent stressful conditions due to annual inlet closures. These sites are all monitored by the Tijuana River National Estuarine Research Reserve (TRNERR).

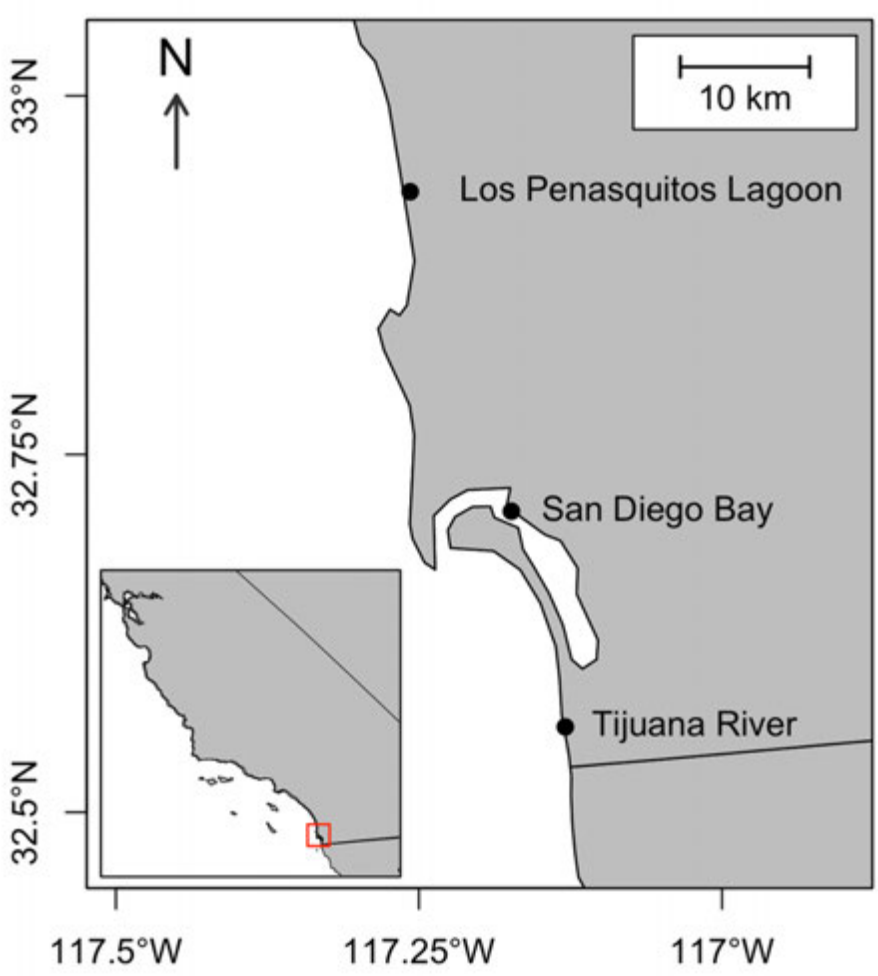

Figure 1. Map of Los Peñasquitos Lagoon (LPL), San Diego Bay (SDB), and the Tijuana River Estuary (TRE).

I periodically collected mussels for both my field and laboratory experiments from naturally occurring beds at each of my three sites between February 2023 and September 2024. After collection, I transported them to San Diego State University's Coastal and Marine Institute Laboratory for sensor attachment. I collected mussels ranging in length from 44 to 89 mm. I collected the largest mussels possible from each site to allow sufficient space for attaching the sensors. I obtained permission to collect at these sites from the California Department of Fish and Wildlife.

DEVELOPMENT OF PHYSIOLOGICAL SENSORS

Each mussel was equipped with two custom-built sensors to measure gaping and heart rate activity. Previously, monitoring the cardiac activity of a bivalve involved cutting

into the shell to expose the heart or implant electrodes into its pericardial cavity (Braby and Somero, 2006; Lowe, 1974). This highly invasive method has now been replaced by more modern techniques that involve sensors that emit infrared light to illuminate the heart through the shell and measure the amount of light reflected back (Burnett et al., 2013; Hellicar et al., 2015). As the heart beats, the amount of light absorbed by the sensor changes, permitting the user to estimate the heart rate of the bivalve based on the frequency at which the reflected light changes (Miller, 2022). These new sensors are more cost-effective and allow for continuous measurements over longer periods.

Magnetic reed switches (Borcherding, 2006), electromagnetic coils (de Zwart et al., 1995), and Hall effect sensors (Comeau, 2018; Miller and Dowd, 2017, 2019) have been commonly used to measure the gaping behavior—and thus physiological performance—of bivalves. I used Hall effect sensors, and for each bivalve, attached one to the posterior end of the valves opposite a magnet. As the valves open and close, the strength of the magnetic field detected by the sensor changes (Miller and Dowd, 2017). The sensor output is then calibrated to correspond to millimeter distances.

For each respective field deployment at a given location, I attached both gape and heart rate sensors to 8 mussels. I also occasionally replaced individual mussels. In total, I deployed 17 mussels at LPL, 17 mussels at SDB, and 28 mussels at the TRE. For both the hypoxia and low salinity laboratory experiments, I attached sensors to 16 mussels from each location, resulting in a total of 32 mussels from each location across all experimental trials. Before placing the sensors, I cleaned and sanded the valves to provide a smoother surface. I then used cyanoacrylate glue or UV resin to secure the sensors and magnets to the outside of the shell and fully coated each sensor and magnet with A-788 Splash Zone epoxy (Carboline, St. Louis, MO, USA). This makes them waterproof and resistant to fouling. I placed the heart rate sensors over the location on the shell that provided the strongest heart rate signal, as indicated by a pulse wave plot. The best place for heart sensor attachment is on the bottom left of the left valve, parallel to the hinge (Figure 2). I attached gape sensors to the posterior end of the right valve and glued a magnet directly across from it on the left valve (Figure 2). All sensors were calibrated using a custom BivalveBit circuit board (Miller, 2022).

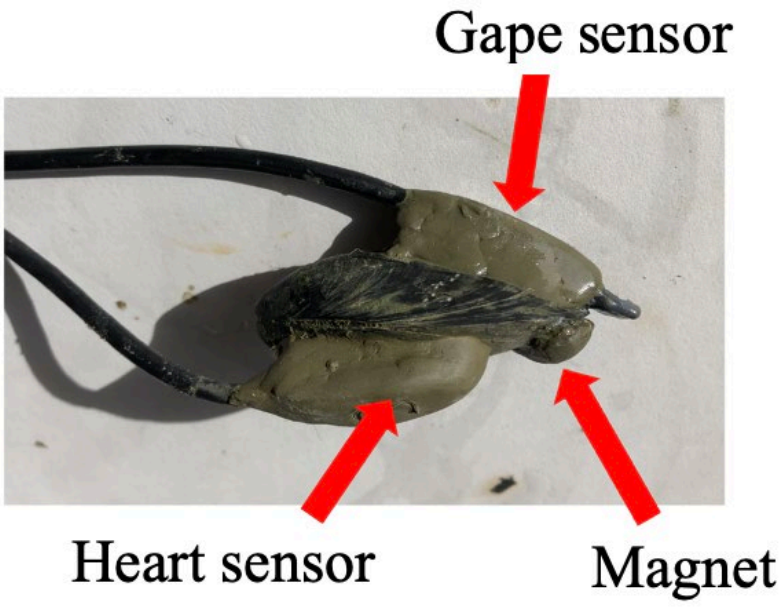

Figure 2. A mussel with a heart sensor, a gape sensor, and a magnet.

FIELD DEPLOYMENTS

In each of the three estuaries, I deployed a mooring containing biosentinel bivalves alongside other sensors collecting data on abiotic conditions. The moorings were deployed near the mouth of each estuary. Each held sixteen bivalves at two different heights in the water column: eight bivalves 0.5m above the substrate and eight bivalves at the surface attached to a buoy. Each set of eight bivalves consisted of four *C. gigas* and four *M. galloprovincialis* individuals. Only data from the *M. galloprovincialis* individuals will be reported in this thesis due to noisy, unreliable data from the oysters. Sensors attached to the surface bivalves were plugged into a separate data logger box from the sensors attached to the bottom bivalves. Each box held an EnviroDIY Mayfly v1.1 data logger (Stroud Water Research Center, Avondale, PA) for gape sensing and a Teensy 3.5 data logger (PJRC.com, Sherwood, OR) for heart sensing. Both boxes were equipped with custom circuit boards to interface with the multiple attached sensors.

The moorings also included directly co-located high-resolution water quality sensors at the surface and at the bottom. The sensors included a conductivity, temperature, and depth sensor (CTD, Sea-Bird SBE-37, Bellevue, WA, USA), a DO sensor (MiniDOT, Precision Measurement Engineering, Vista, CA, USA), and a fluorometer to measure chlorophyll *a*

(CFLUOR, Precision Measurement Engineering, Vista, CA, USA). All sensors were set to take readings at five-minute intervals. The sensors were used to track water conditions that could be associated with changes in heart rate or gaping.

Deployed bivalves and their attached sensors were serviced as needed. During maintenance visits, dead bivalves and malfunctioning water quality sensors were replaced, malfunctioning wires were removed, and data were downloaded from each SD card. Occasionally, the moorings were brought back into the lab since certain repairs could not be carried out during field visits. Due to necessary maintenance and replacement, the moorings were not able to collect both heart and gape data continuously. The mooring at LPL collected data from October 2024 to May 2025, and the mooring at SDB collected data from January 2024 to December 2024. The mooring at the TRE collected data from February 2025 to April 2025 (although there were viable gape data for the TRE mooring between January 2024 and September 2024).

I measured bivalve length using calipers (to the nearest 0.5 mm) before and after deployment for any bivalves brought back to the Coastal and Marine Institute Laboratory. Bivalves that were still on the moorings at the time of this writing were not measured a second time. Length was measured as the distance between the anterior and posterior ends of the animal. Growth rates were then calculated by finding the difference in length of individual bivalves between each measurement and dividing that by the number of days between measurements.

LAB EXPERIMENTS

I conducted experimental trials manipulating salinity and DO to reflect the most common abiotic stressors measured from the moorings. *M. galloprovincialis* individuals gathered from all three sites were used for the lab trials to allow for multiple site comparisons. Although *C. gigas* was included on the moorings, they were in short supply in the estuaries, so only mussels were used in the lab. All laboratory experiments were performed at the San Diego State University Coastal and Marine Institute Laboratory.

During the trials, the treatment mussels were exposed to either low salinity or hypoxia. I conducted six replicate trials exposing mussels to hypoxia from July 2024 to October 2024, and 6 replicate trials exposing mussels to low salinity from October 2024 to

February 2025. During each trial, four mussels were exposed to treatment conditions, and four mussels were exposed to unmanipulated seawater. Replicates were limited due to the limited space within the data-logging system. At the beginning of a trial, each mussel was placed into an isolated container supplied with a continuous flow of unmanipulated seawater (~35 psu) from a header tank. The mussels were then left to acclimate to their containers for at least 24 hours.

During the low salinity trials, the salinity was then slowly lowered to < 3 psu for the treatment mussels over the course of 2-3 hours. Lowering salinity in this manner mimics rain events in which freshwater flows into an estuary, decreasing salinity at the surface for a few days (Addis et al., 2021). After sitting at < 3 psu for 3 days, the salinity was then slowly ramped back up to control conditions over another 2-3 hours. The mussels were then left to recover for 48 hours.

Trials manipulating DO levels follow a similar protocol. After acclimation, nitrogen gas was bubbled into the header tank so that the treatment containers reached a DO level of ≤ 3.0 mg L^{-1} after 2-3 hours. The commonly used threshold of 2.0 mg L^{-1} of DO as an indicator for hypoxia is well below the true lethal threshold for many marine organisms (Vaquer-Sunyer and Duarte, 2008). Therefore, I used the more conservative threshold of 3.0 mg L^{-1}. The treatment mussels were then held in hypoxic conditions for 3 days and subsequently returned to normal DO conditions (~8 mg L^{-1}) over the course of another 2-3 hours. The mussels were then left to recover for 48 hours. To reduce oxygen exchange at the water's surface in the header tank, polystyrene sheets were placed on top of the water during treatment. Plastic wrap was also placed on the surface of the water for each container during treatment to minimize any potential oxygen exchange. The polystyrene and plastic wrap were removed prior to recovery.

For all trials, conductivity, temperature, and DO measurements were taken from each container every 30 minutes with a YSI ProSolo sensor during the decline and incline phases. Between the end of the decline phase and the start of the incline phase (during treatment), the YSI sensor was placed in the header tank and set to automatically collect conductivity, temperature, and DO measurements once every minute.

Heart rate values were recorded at 8Hz for 50 seconds every 2 minutes, and gape values were recorded once every minute. An aquarium chiller maintained the seawater

temperature at ~22°C. Mussels were fed a shellfish algae diet (Shellfish Diet 1800, Reed Mariculture, Campbell, CA, USA) at the beginning of acclimation, treatment, and recovery during the experimental trials and *ad libitum* in lab holding tanks before and after the experimental trials.

CALIBRATIONS AND DATA PROCESSING

The Hall effect sensor signal was used to estimate the distance between the two valves at the posterior end of the shell. Live bivalves and dead bivalves with working sensors attached were used for calibrations. The calibrations related the sensor's magnetic field output to an estimate of valve gape distance in millimeters. For both live and dead bivalves, aluminum or plastic rods of known diameter were placed between the valves adjacent to the Hall effect sensor and magnet while the sensor output was recorded. Sensor output was also recorded when the valves were fully closed (0 mm). Including the baseline calibration, each individual received at least three calibration measurements.

The slope of the regression line between the raw Hall sensor outputs and the measured distance calibrations was used to determine the gaping distance between the valves of an individual at any given moment. After gape data were collected and all individuals were calibrated, all gape distance estimates (in millimeters) were converted into a percentage opening (0 to 100%) to provide a standardized metric for comparison between individuals. For the following analyses, bivalves were classified as "Closed" or "Open" using an estimated gape value threshold of 5% of maximum gape width. Bivalves that were < 5% open at the time of measurement were classified as "Closed", while bivalves that were > 5% open at the time of measurement were classified as "Open". This binary variable was used instead of continuous percentage values because small differences in opening do not have clear implications for mussel physiology. Although some species of clams reduce respiration and feeding activity at around the 20% gape threshold (Jou et al., 2013), as long as there is an exchange of water across the mantle, the bivalve is considered to be open, feeding, and respiring. I chose a 5% threshold as a conservative value for valve opening. If an individual is below that 5% threshold at any point, I can be confident that they are not actively filtering water, and aerobic gas exchange is likely minimized. Therefore, the binary dichotomy I have

chosen for analysis is informative regarding an individual's ability to feed, respire, eliminate waste, and reproduce during stressful conditions.

Heart rate data were processed to obtain the average beats per minute (bpm) from an individual over repeated time intervals. Sensors attached to bivalves in the field recorded the amount of infrared light reflected back to the sensor at 10Hz for 60 seconds every 5 minutes. Sensors attached to bivalves used in the lab experiments recorded at 8Hz for 50 seconds every 2 minutes. Raw sensor data were processed using peak-detection algorithms to determine the bpm for an individual by counting the peaks in each round of measurements. The peak counts for the lab data were scaled up to one minute to account for the 50-second sampling period. Three algorithms (*pracma* package, Borchers, 2022; *forecast* package, Hyndman et al., 2023; *signal* package, Signal Developers, 2013) with slightly different peak detection sensitivities were used simultaneously and flagged if the results varied by more than two bpm from each other. The light reflection plots of the flagged results were then visually inspected to determine true beats or were categorized as "NA" if the plot showed no pattern to the peaks, or if the amplitude of the peaks was too low (range < 20 units as returned from the heart sensor's onboard analog-to-digital voltage converter). The short sampling durations somewhat limited the ability to discern very slow heart rates, so all plots with fewer than two peaks in the sampling window were removed.

STATISTICAL ANALYSIS

Statistical analysis was conducted in R (version 4.4.3; R Development Core Team, 2025). An α level of 0.05 was used for all statistical tests.

For the lab experiments, I used linear mixed effects models using the *lmerTest* package (Kuznetsova et al., 2017) to analyze the difference in average heart rate across treatment group (hypoxia/normoxia or low salinity/control salinity), trial phase (Acclimation, Treatment, or Recovery), and location (TRE, LPL, or SDB), and their interactions. Treatment group, trial phase, and location were treated as fixed factors with individual mussel ID as a random factor to account for repeated measures. The *DHARMa* package (Hartig, 2024) was used to check mixed models for equal variance, uniformity, outliers, and overdispersion. If the model fixed effects were significant, pairwise analyses of values within each treatment

group and trial phase were conducted using the *emmeans* package (Lenth, 2025) with Bonferroni adjustments.

I also used linear mixed-effects models to analyze the difference in the coefficient of variation (CV) in heart rate across treatment group, trial phase, and location. I used the following equation to calculate CV, where s is the standard deviation of heart rate values for one individual during a given trial phase and $\bar{x}$ is the mean heart rate for that individual during the same trial phase:

$$CV\% = \left(\frac{s}{\bar{x}}\right) * 100$$

Lower CV values indicate less variability in heart rate, while higher CV values indicate more variability in heart rate. Pairwise analyses of values within each treatment group and trial phase were conducted using the *emmeans* package with Bonferroni adjustments. I also conducted linear mixed-effects models to assess how heart rate CV for hypoxia mussels varied by location within each trial phase. Pairwise analyses of interaction values were conducted using the *emmeans* package with Bonferroni adjustments.

I then analyzed how the proportion of observations with open valves varied by treatment group, trial phase, and location. I calculated the proportion of observations with open valves by averaging the binary response data from individual mussels (0 = "Closed" and 1 = "Open" based on the 5% gaping threshold) across the trial phases. I conducted Kruskal-Wallis rank sum tests to test whether the proportion of observations with open valves varied between groups and among locations within the same trial phase, as the data did not meet the assumptions of normality. Dunn's post hoc tests with Holm adjustment methods were used to measure differences between factors. To analyze how the proportion of observations with open valves varied among trial phases, I conducted Friedman tests, as the data contained repeated measures. Wilcoxon signed rank tests with Holm adjustment methods were used to calculate pairwise comparisons.

For the field data, I used repeated measures correlation analyses (*rmcorr* package; Bakdash and Marusich, 2024) to assess relationships between mussel heart rate, gape opening, and environmental variables at each depth and location. This method accounts for the non-independence of repeated observations by estimating a common within-individual slope while allowing subject-specific intercepts. To align sampling frequencies, I averaged

raw measurements of gape opening, heart rate, DO, salinity, temperature, and turbidity into 15-minute intervals, matching the temporal resolution of turbidity (the least frequently sampled variable). Chlorophyll fluorescence was excluded due to its limited temporal coverage at LPL and SDB. Turbidity was removed from analyses at LPL because values were near zero for more than 95% of observations. Although salinity showed relatively low variability at LPL and SDB compared to the TRE, it was retained for reference. Heart rate or gape opening was treated as the response variable in each correlation analysis. To account for potential violations of normality and homoscedasticity, I estimated the repeated measures correlation coefficient (r_{rm}) and 95% confidence intervals using 1,000 bootstrapped resamples. From each analysis, I extracted the bootstrapped r_{rm}, bootstrapped confidence intervals, p-value, and shared slope to quantify the strength and direction of associations.

I analyzed repeated measures of gape in the field deployments using generalized linear mixed-effects models (GLMM) from the *lme4* package (Bates et al., 2015) at each depth within each location. I transformed average gape % into a binary variable (0 = "Closed" and 1 = "Open" based on the 5% gaping threshold). To facilitate model convergence and interpretability, I centered and scaled the averaged environmental variables. For each gape measurement model, I analyzed the additive relationship of open/closed values versus DO, salinity, temperature, and—if collected at that location—turbidity and chlorophyll fluorescence using a binomial error distribution. I used binary gape response data from individual mussels as the response variable. Environmental variables were fixed factors, and individual mussel ID was a random factor to account for repeated measures. I used Type II Wald χ^2 tests in the *car* package (Fox and Weisberg, 2019) to test the significance of the fixed factors. Model residuals were evaluated using the nonparametric dispersion and bootstrapped outlier tests in the *DHARMa* package. I also calculated marginal and conditional R^2 values using the *MuMIn* package (Bartoń, 2025) to assess the proportion of variance explained by the variables within the model.

RESULTS

For all boxplot graphs in my thesis, the box or interquartile range (IQR) represents the data lying within the 25^{th}-75^{th} percentile of the dataset. The black bar within the IQR represents the median of the data. The whiskers on the lower end and upper end represent either the most extreme data points or points within 1.5x the IQR, while points outside the whiskers represent outliers of the data. The red diamond symbols represent the mean of the data.

HYPOXIA TRIALS

DO (mg L^{-1}) was recorded throughout the six laboratory hypoxia trials to characterize the exposure conditions (Figure 3). During the first 24 hours (the Acclimation phase), DO levels in the individual containers across all trials averaged 7.2 mg L^{-1}. DO was then dropped to the 3 mg L^{-1} threshold over the course of ~3 hours. After holding the treatment containers below that threshold for three days, DO was then slowly increased to baseline levels over the next ~3 hours. At one point during trial 5, DO levels rose slightly higher than 3 mg L^{-1}. However, most DO measurements across all trials during exposure were much lower. During the three-day Recovery phase, DO averaged 7.1 mg L^{-1}. DO levels in the control containers fluctuated between 6.3 mg L^{-1} and 7.9 mg L^{-1}. Salinity and temperature were also recorded, with an average salinity of 38.5 psu (Figure A1) and an average temperature of 22.1 ºC (Figure A2).

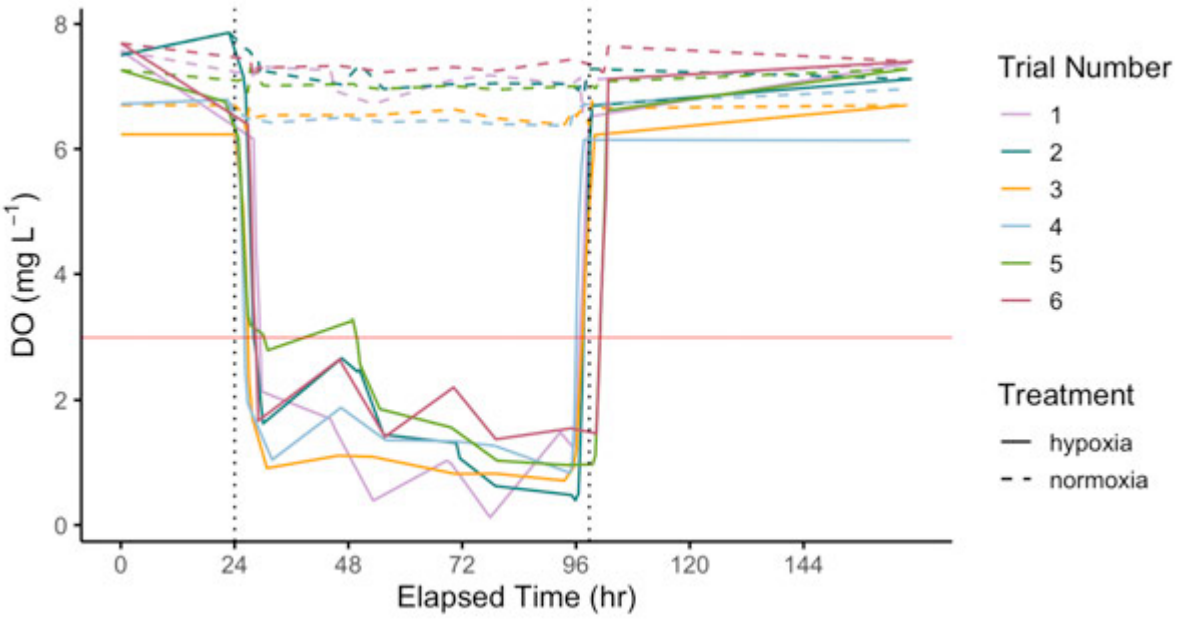

Figure 3. Plot of the change in dissolved oxygen (DO; mg L^{-1}) over time (elapsed hours) for the hypoxia trials. Solid lines represent the mean DO levels in containers where mussels were exposed to hypoxia. Dashed lines represent control (unmanipulated seawater) containers. Line colors correspond to different trials. The red horizontal line marks the 3 mg L^{-1} DO threshold at which conditions are considered stressful. Vertical dotted lines indicate the average onset of DO decline and subsequent recovery to baseline conditions.

Valve gape analysis

The proportion of open shells (valve > 5% open) did not differ significantly between the normoxia and hypoxia mussels in the Acclimation phase (Figure 4, Kruskal-Wallis (KW), $H_{(1)} = 0.14$, p = 0.71) and the Treatment phase (Figure 4, KW, $H_{(1)} = 1.92$, p = 0.17). Although not significantly different from the normoxia mussels, hypoxia mussels trended toward a higher proportion of open valves in the Recovery phase (Figure 4, KW, $H_{(1)} = 3.58$, p = 0.058). A Friedman test revealed that within the hypoxia treatment group, the proportion of open valves differed significantly across trial phases (Figure 4, $\chi^2_{(2)} = 14.6$, $p < 0.001$). Pairwise Wilcoxon signed-rank comparisons with Holm correction revealed that the proportion of open valves in the hypoxic Treatment phase was significantly lower than both the preceding Acclimation phase (p = 0.002) and the following Recovery phase (p = 0.01). In contrast, the Acclimation and Recovery phases did not differ (p = 0.64) within the hypoxia treatment group.

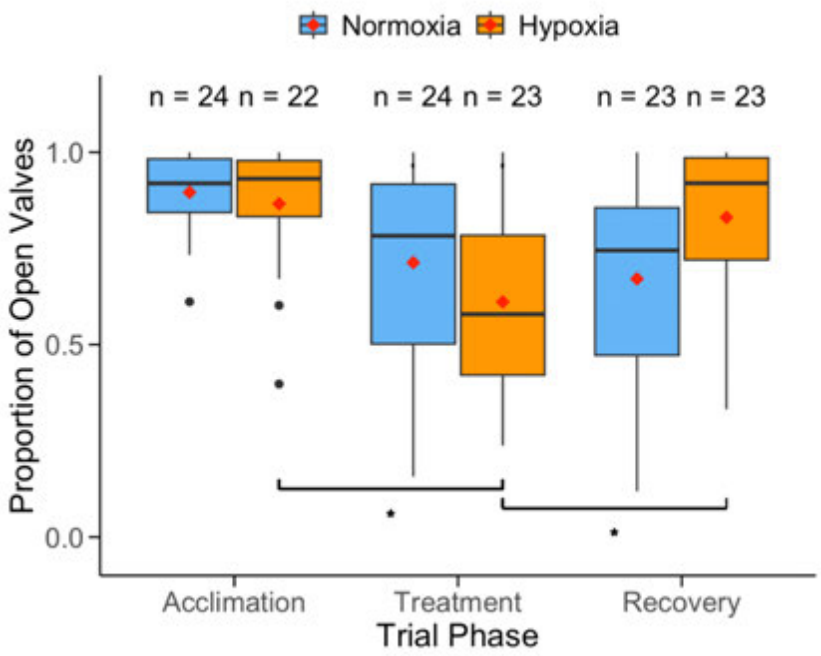

Figure 4. Proportion of open mussel valves separated by treatment group (normoxia or hypoxia) and trial phase (Acclimation, Treatment, and Recovery). Red diamonds represent means, and black bars represent medians. N = number of mussels. Significant differences as determined by pairwise Wilcoxon signed-rank comparisons with Holm correction, * = $p < 0.05$.

There was no significant difference in the proportion of open valves among the three locations when mussels were exposed to hypoxic conditions (Figure 5A, KW, $H_{(2)} = 0.52$, p = 0.77). However, the proportion of open valves was significantly different among locations in the normoxic treatment group (Figure 5B, KW, $H_{(2)} = 11.04$, p = 0.004), due to the lower proportion of open valves in SDB mussels compared to LPL (Dunn's post hoc, p = 0.009) and TRE mussels (Dunn's post hoc, p = 0.003) during the latter phases of the trials. Within the hypoxia treatment group, the proportion of open valves was not significantly different among mussels from different locations during the Acclimation (Figure 5A, KW, $H_{(2)} = 0.52$, p = 0.77), Treatment (Figure 5A, KW, $H_{(2)} = 0.07$, p = 0.97), and Recovery phases (Figure 5A, KW, $H_{(2)} = 1.15$, p = 0.56). Mussels from all three locations exhibited the same behavior of decreasing gaping during Treatment and increasing gaping during Recovery (Figure 6A). Mussels from the TRE exhibited a peak average gaping percentage of 83.2% during the Treatment phase, which is higher than the peak average gaping percentages of 63.2% for mussels from LPL and 72% for mussels from SDB (Figure 6A).

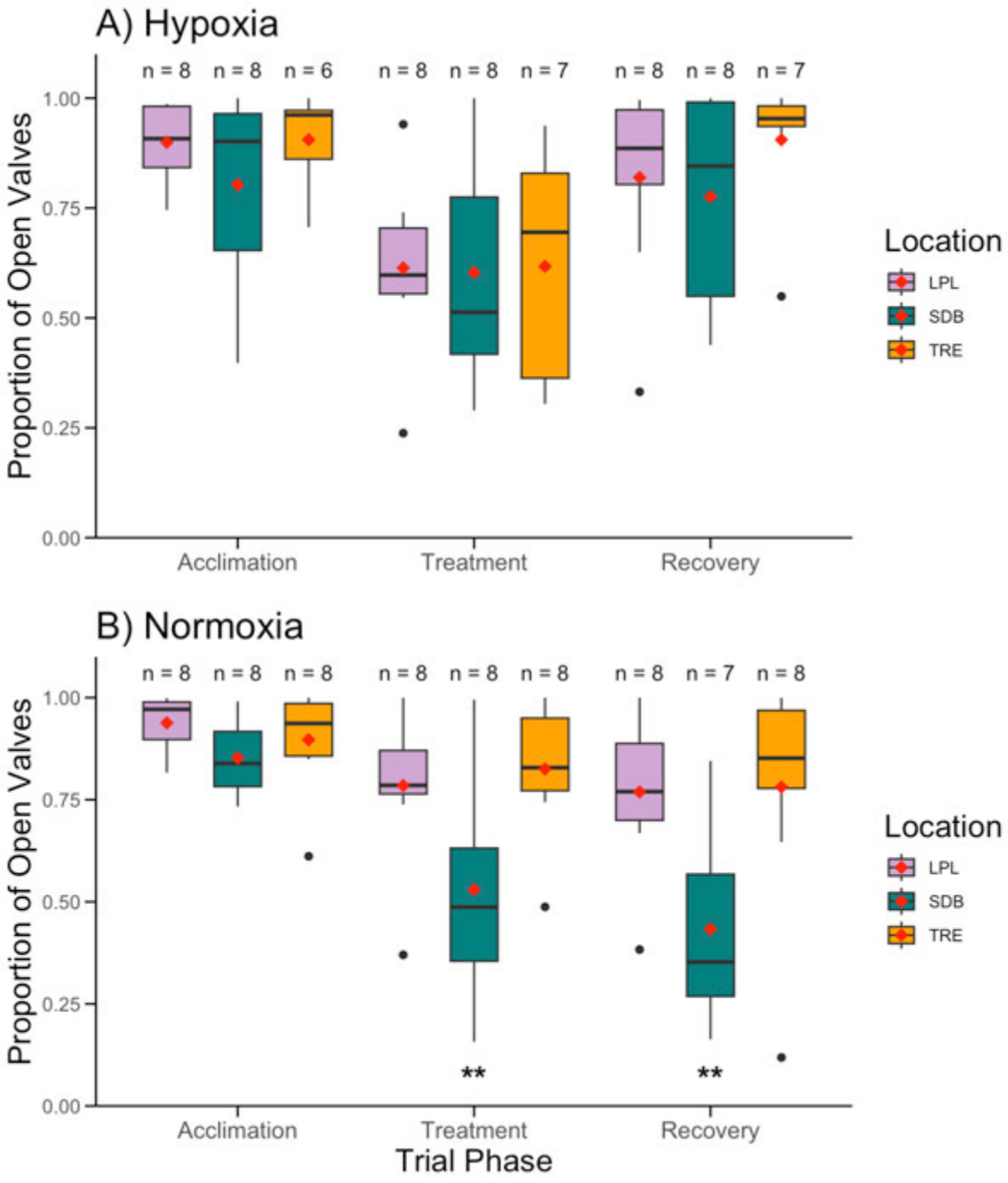

Figure 5. Proportion of open mussel valves during A) hypoxia or B) normoxia treatment separated by location (LPL, SDB, and TRE) and trial phase (Acclimation, Treatment, and Recovery). Red diamonds represent means, and black bars represent medians. N = number of mussels. Significant differences as determined by Dunn's post hoc comparisons, ** = $p < 0.01$.

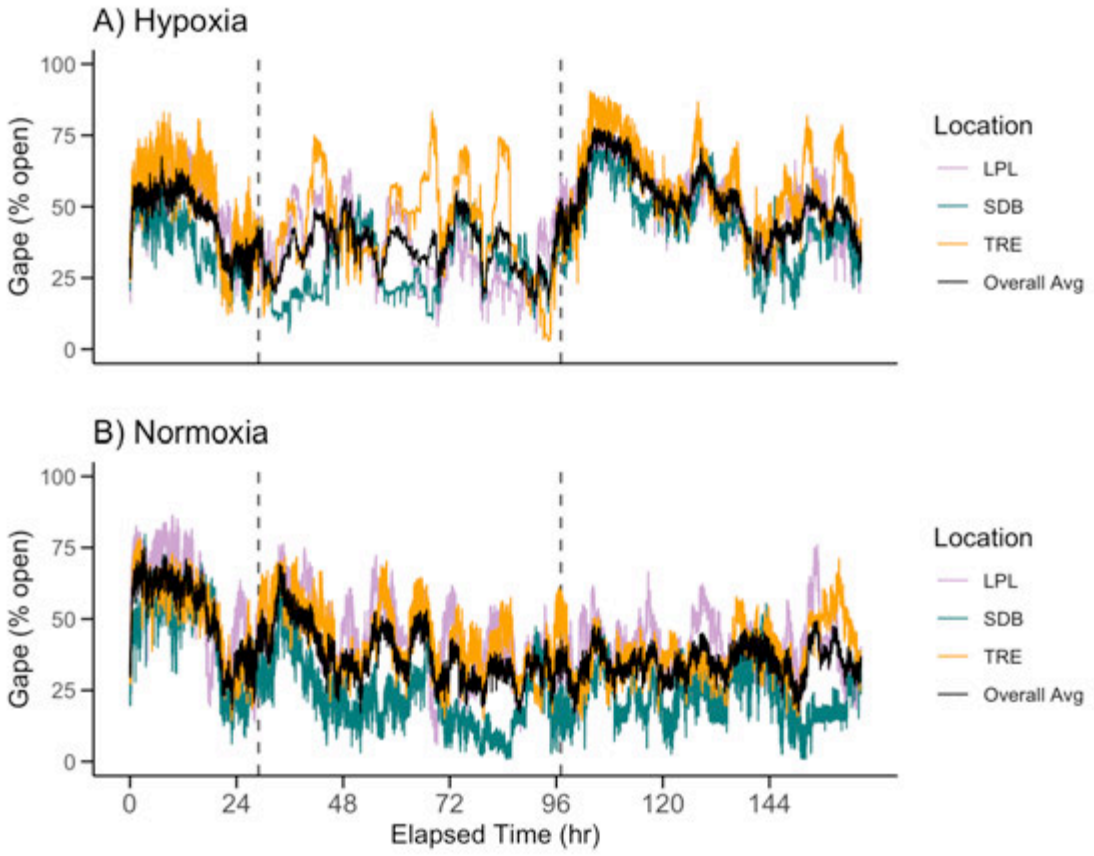

Figure 6. Plot of the average gape (%) of all A) hypoxia and B) normoxia mussels as the trial hours elapse. Colored lines represent location averages, the black line is the overall average, and the vertical dashed lines represent the average hour in which treatment began and ended.

Heart rate analysis

The average heart rate was significantly different between the hypoxia and normoxia treatment groups across the trial phases (Figure 7; Figure 8A, ANOVA, $F_{2,87.8} = 8.78$, $p < 0.001$). The average heart rate did not significantly differ between the hypoxia and normoxia treatment groups in the Acclimation phase (Figure 8A, Bonferroni, $p = 0.89$) or the Treatment phase (Figure 8A, Bonferroni, $p = 0.28$), but was significantly different in the Recovery phase, where a higher average heart rate was observed for the hypoxia mussels (Figure 8A, Bonferroni, $p < 0.001$). Mussels within the normoxia treatment group also had lower average heart rates as the trials progressed. In contrast, the average heart rate of hypoxia mussels did not decrease throughout the course of the trials. There was no

significant difference in the average heart rate among mussels from different locations, regardless of treatment (Figure 9, ANOVA, $F_{2,41.2} = 1.19$, $p = 0.32$).

Heart rate CV was significantly different between the normoxia and hypoxia treatment groups across the trial phases (Figure 8B, ANOVA, $F_{2,86.5} = 18.02$, $p < 0.001$). CV was not significantly different between hypoxia and normoxia mussels in the Acclimation phase (Figure 8B, Bonferroni, $p = 0.3$). There was a significant difference between the two treatment groups in the Treatment phase (Figure 8B, Bonferroni, $p = 0.003$), where mussels exposed to hypoxia had a higher CV, and the Recovery phase (Figure 8B, Bonferroni, $p = 0.002$), where mussels exposed to hypoxia had a lower CV. Within the hypoxia treatment group, CV was significantly higher during the Treatment phase compared to the Acclimation phase (Figure 8B, Bonferroni, $p < 0.001$) and the Recovery phase (Figure 8B, Bonferroni, $p < 0.001$). CV was also significantly higher in the Recovery phase than the Acclimation phase (Figure 8B, Bonferroni, $p < 0.001$). Location did not have a significant overall effect on the CV of hypoxia mussels across trial phases (Figure 10A, ANOVA, $F_{4,39.1} = 0.78$, $p = 0.55$). Although mussels from the TRE had a significantly lower CV during the Treatment phase compared to mussels from SDB (Figure 10A, Tukey's HSD, $p = 0.04$), pairwise comparisons did not reveal any other significant differences between locations within the hypoxia treatment group.

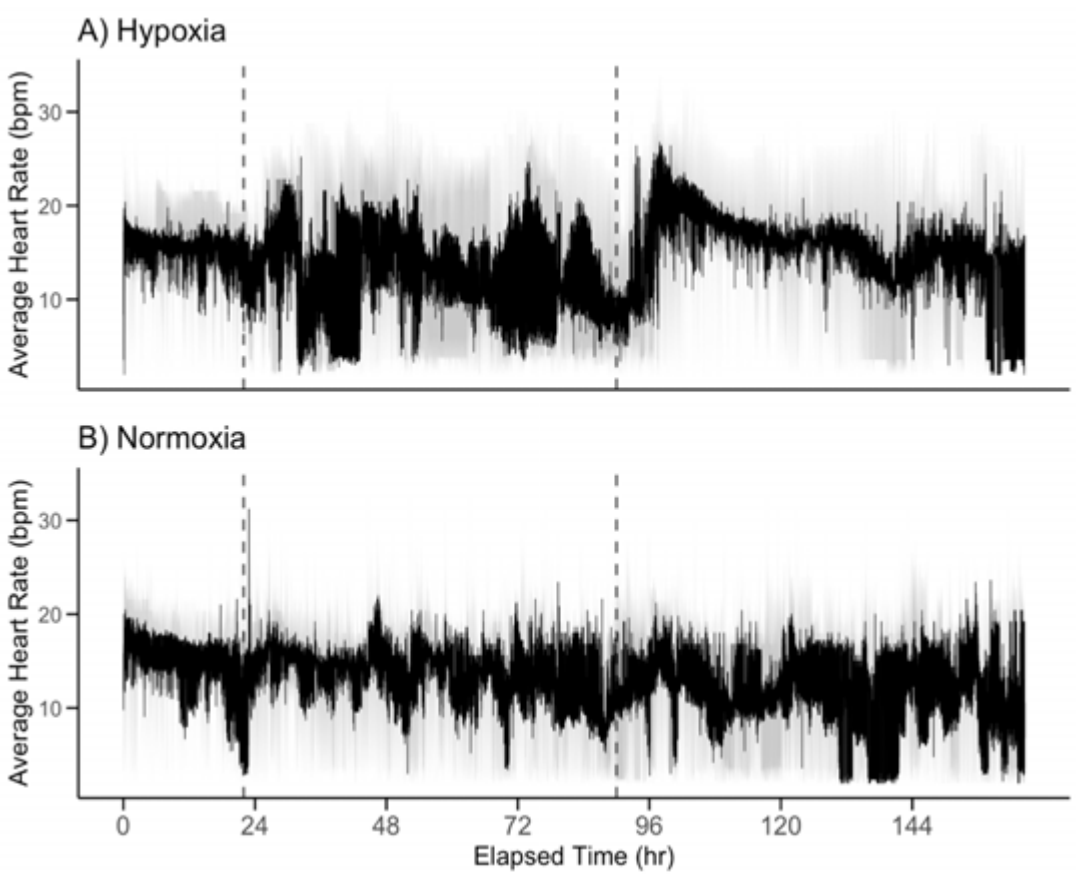

Figure 7. Plot of the average heart rate (bpm) of all A) hypoxia and B) normoxia mussels as trial hours elapse. The black line is the average heart rate, the grey line is the heart rate range, and the vertical dashed lines represent the average hour in which treatment began and ended.

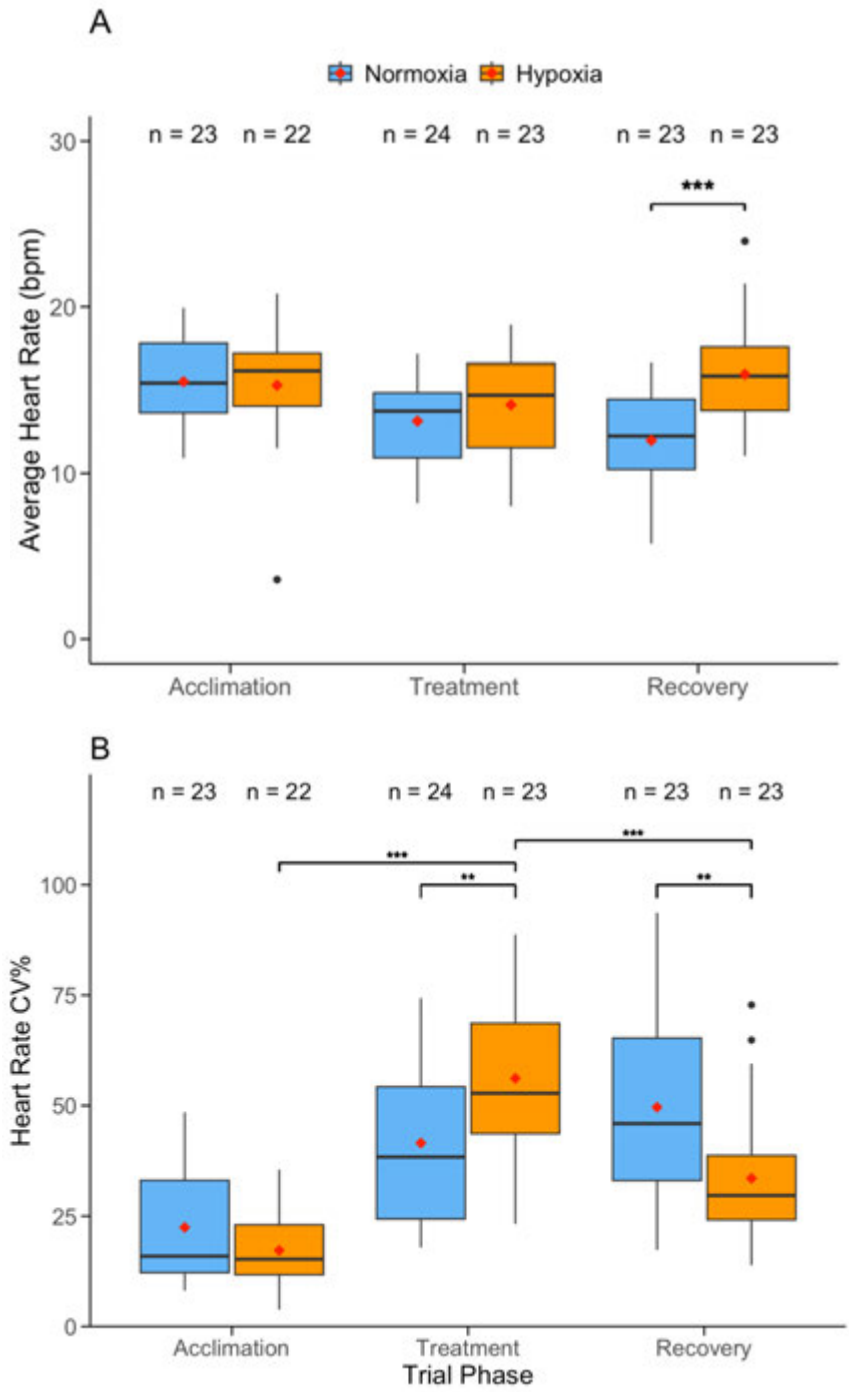

Figure 8. A) average heart rate (bpm) and B) heart rate CV of mussels separated by treatment group (normoxia or hypoxia) and trial phase (Acclimation, Treatment, and Recovery). Red diamonds represent means, and black bars represent medians. N = number of mussels. Significant differences as determined by post hoc pairwise comparisons adjusted using Bonferroni adjustment methods, ** = $p < 0.01$, *** = $p < 0.001$.

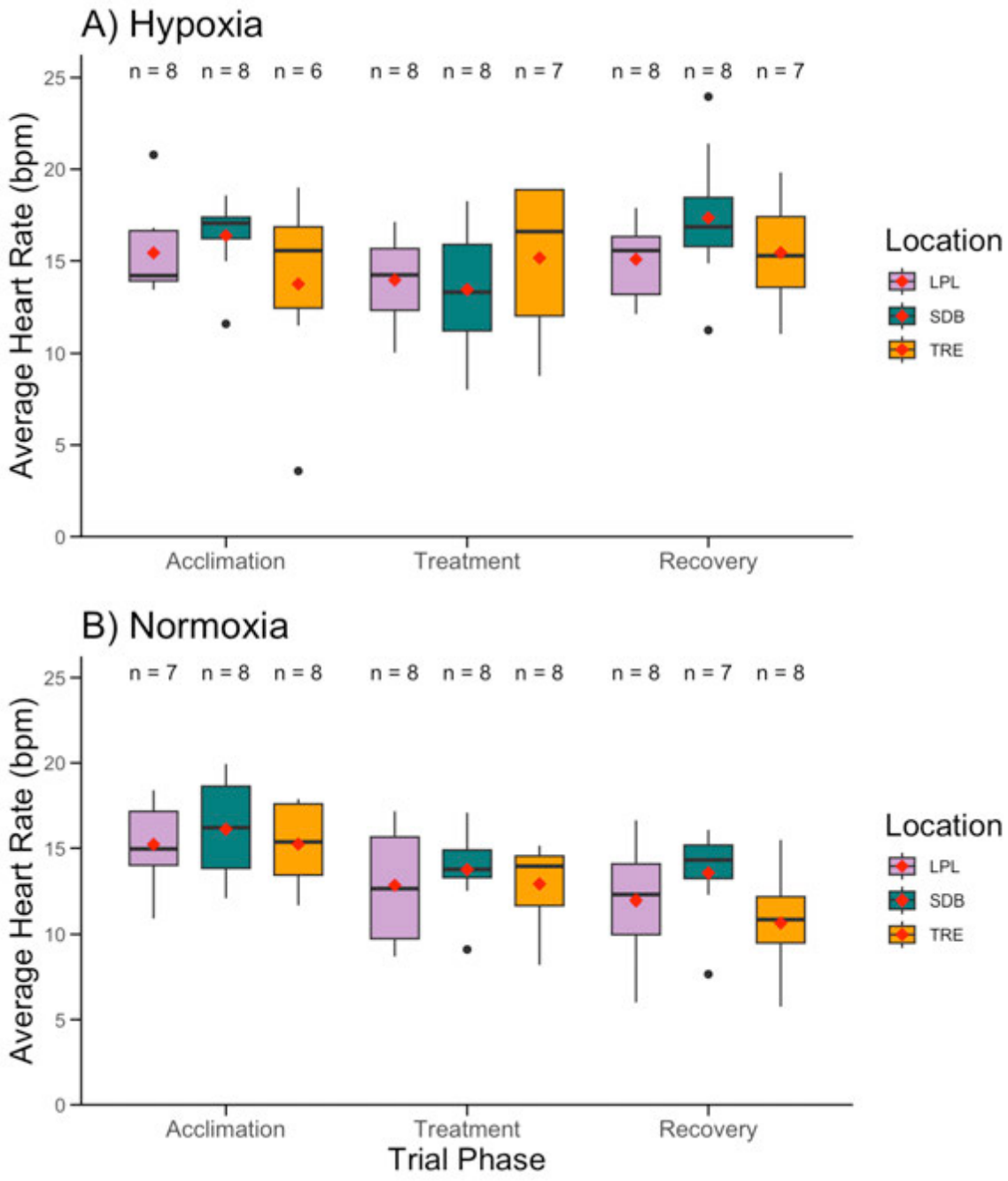

Figure 9. Average heart rate (bpm) of mussels in the A) hypoxia treatment group and the B) normoxia treatment group separated by trial phase (Acclimation, Treatment, and Recovery) and location (LPL, SDB, and TRE). Red diamonds represent means, and black bars represent medians. N = number of mussels.

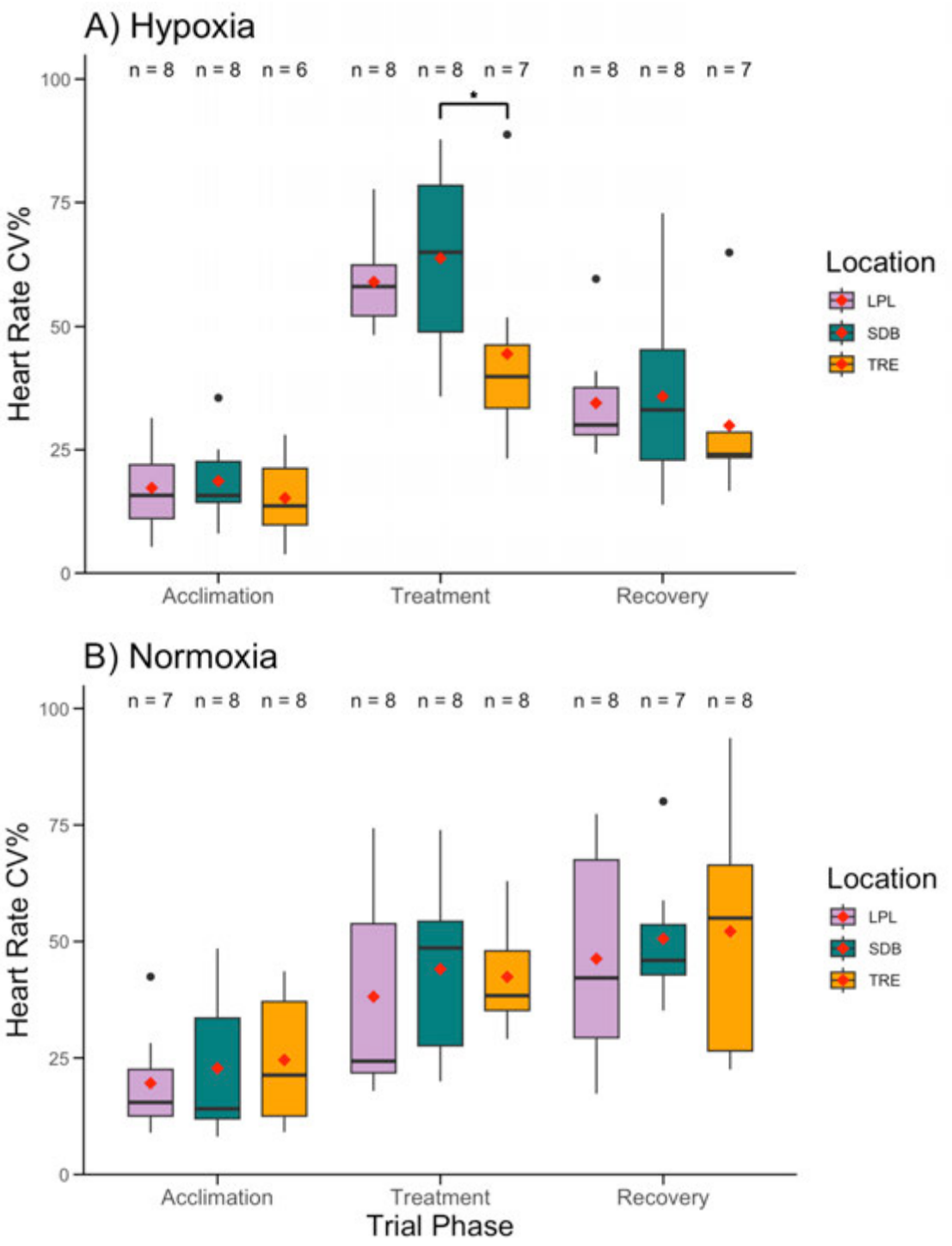

Figure 10. Heart rate CV of mussels in the A) hypoxia treatment group and the B) normoxia treatment group separated by trial phase (Acclimation, Treatment, and Recovery) and location (LPL, SDB, and TRE). Red diamonds represent means, and black bars represent medians. N = number of mussels. Significant differences as determined by post hoc pairwise comparisons adjusted using Bonferroni adjustment methods, * = $p < 0.05$.

LOW SALINITY TRIALS

Salinity (psu) was recorded throughout the six low salinity trials to characterize the exposure conditions (Figure 11). During the first 24 hours (the Acclimation phase), salinity in the individual containers across all trials averaged 38.3 psu. Salinity was then dropped to the 3 psu threshold over the course of ~3 hours. After holding the treatment containers below that threshold for three days, salinity was then slowly increased to baseline levels over the next ~3 hours. Salinity levels during the three-day Recovery phase averaged 38.5 psu. Salinity levels in the control containers fluctuated between 37.2 psu and 38.9 psu. DO and temperature were also recorded, with DO averaging 8.5 mg L^{-1} (Figure A3) and temperature averaging 17 ºC (Figure A4) throughout the duration of the trials. DO showed a slight increase during salinity reduction; however, the change remained within non-stressful ranges and is unlikely to have acted as a confounding variable (Figure A3).

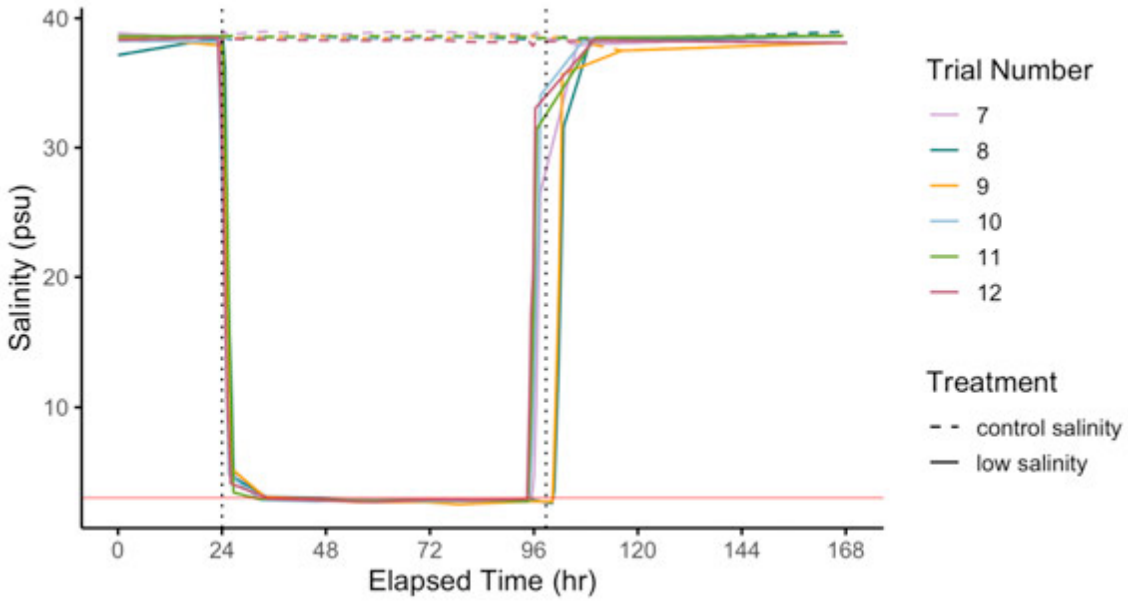

Figure 11. Change in salinity (psu) over time (elapsed hours) for the low salinity trials. Solid lines represent the mean salinity levels in containers where mussels were exposed to low salinity. Dashed lines represent control (unmanipulated seawater) containers. Line colors correspond to different trials. The red horizontal line marks the 3 psu threshold at which conditions are considered stressful. Vertical dotted lines indicate the average onset of salinity decline and subsequent recovery to baseline conditions.

Valve gape analysis

The proportion of open valves was not significantly different between the two treatment groups during the Acclimation (Figure 12, KW, $H_{(1)} = 0.18$, $p = 0.67$) and Recovery phases (Figure 12, KW, $H_{(1)} = 1.05$, $p = 0.31$), but was significantly different during the Treatment phase (Figure 12, KW, $H_{(1)} = 30.77$, $p < 0.001$). A Friedman test revealed that within the low salinity treatment group, the proportion of open valves differed significantly among all trial phases (Figure 12, $\chi^2_{(2)} = 19.5$, $p < 0.001$). The proportion of open valves was significantly lower during the Treatment phase compared to both the Acclimation phase ($p = 0.001$) and the Recovery phase ($p = 0.001$). There was no significant difference between the Acclimation and Recovery phases ($p = 0.11$). A Friedman test of the control mussels also revealed an overall significant difference in the proportion of open valves between trial phases (Figure 12, $\chi^2_{(2)} = 10.43$, $p = 0.005$), where mussels closed their valves more as time elapsed.

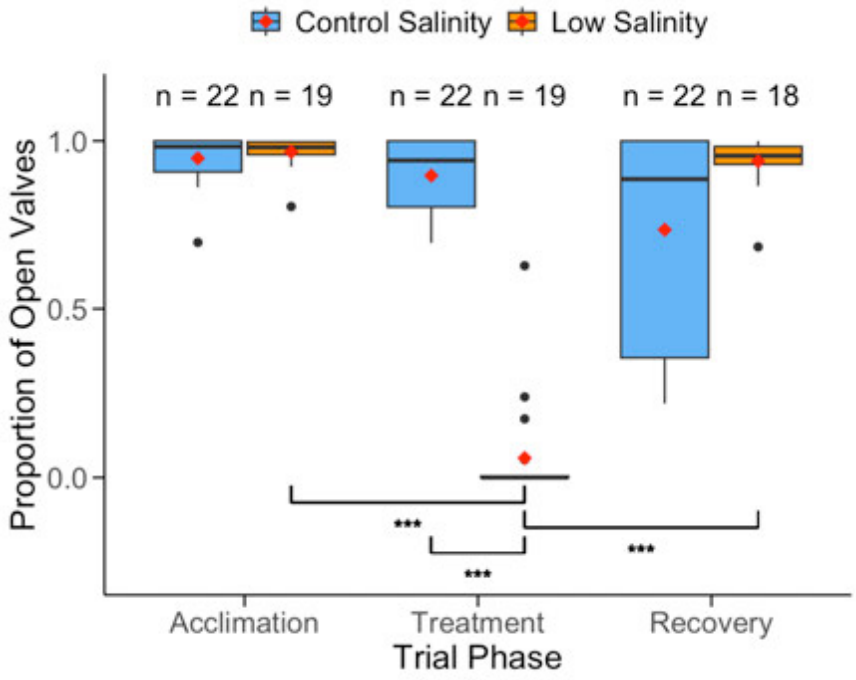

Figure 12. Proportion of open mussel valves separated by treatment group (control salinity or low salinity) and trial phase (Acclimation, Treatment, and Recovery). Red diamonds represent means, and black bars represent medians. N = number of mussels. Significant differences as determined by Dunn's and Wilcoxon signed rank tests, *** = $p \leq 0.001$.

There was no significant difference in the proportion of open valves among the three locations when mussels were exposed to low salinity conditions (Figure 13A, KW, $H_{(2)} = 0.31$, $p = 0.86$). However, there was a significant difference in the proportion of open valves among the three locations when mussels were exposed to control salinity conditions (Figure 13B, KW, $H_{(2)} = 6.62$, $p = 0.04$). This was due to the lower proportion of open valves exhibited by mussels from the TRE compared to LPL (Dunn's post hoc, $p = 0.05$) and SDB (Dunn's post hoc, $p = 0.02$) during the Recovery phase. Within the low salinity treatment group, location did not have a significant effect on the proportion of open valves during the Acclimation (Figure 13A, KW, $H_{(2)} = 0.41$, $p = 0.81$), Treatment (Figure 13A, KW, $H_{(2)} = 1.49$, $p = 0.48$), or Recovery phases (Figure 13A, KW, $H_{(2)} = 0.3$, $p = 0.86$). Low salinity mussels from all locations exhibited the same behavior of closing valves during Treatment and reopening them during Recovery (Figure 14A).

Heart rate analysis

The average heart rate (bpm) was significantly different between the low salinity and control salinity mussels across trial phases (Figure 15; Figure 16A, ANOVA, $F_{2,81.2} = 142.48$, $p < 0.001$). The average heart rate (bpm) was marginally significantly different between treatment groups in the Acclimation phase (Figure 16A, Bonferroni, $p = 0.05$); however, this difference is likely due to individual-level variation. In the Treatment phase, mussels that were exposed to low salinity had significantly lower average heart rates than the control mussels (Figure 16A, Bonferroni, $p < 0.001$). Furthermore, in the Recovery phase, mussels exposed to low salinity had significantly higher average heart rates than their control counterparts (Figure 16A, Bonferroni, $p < 0.001$). Within the low salinity treatment group, mussels in the Treatment phase had significantly lower average heart rates than the Acclimation (Figure 16A, Bonferroni, $p < 0.001$) or Recovery phases (Figure 16A, Bonferroni, $p < 0.001$). Similar to the normoxia mussels in the low DO trials, the average heart rate in the control group steadily declined throughout the trials. There was no significant difference in the average heart rate among mussels from different locations (Figure 17, ANOVA, $F_{2,37.2} = 0.53$, $p = 0.59$). Low salinity mussels from all locations exhibited the same response of decreasing heart rate during Treatment and increasing heart rate during Recovery (Figure 15A).

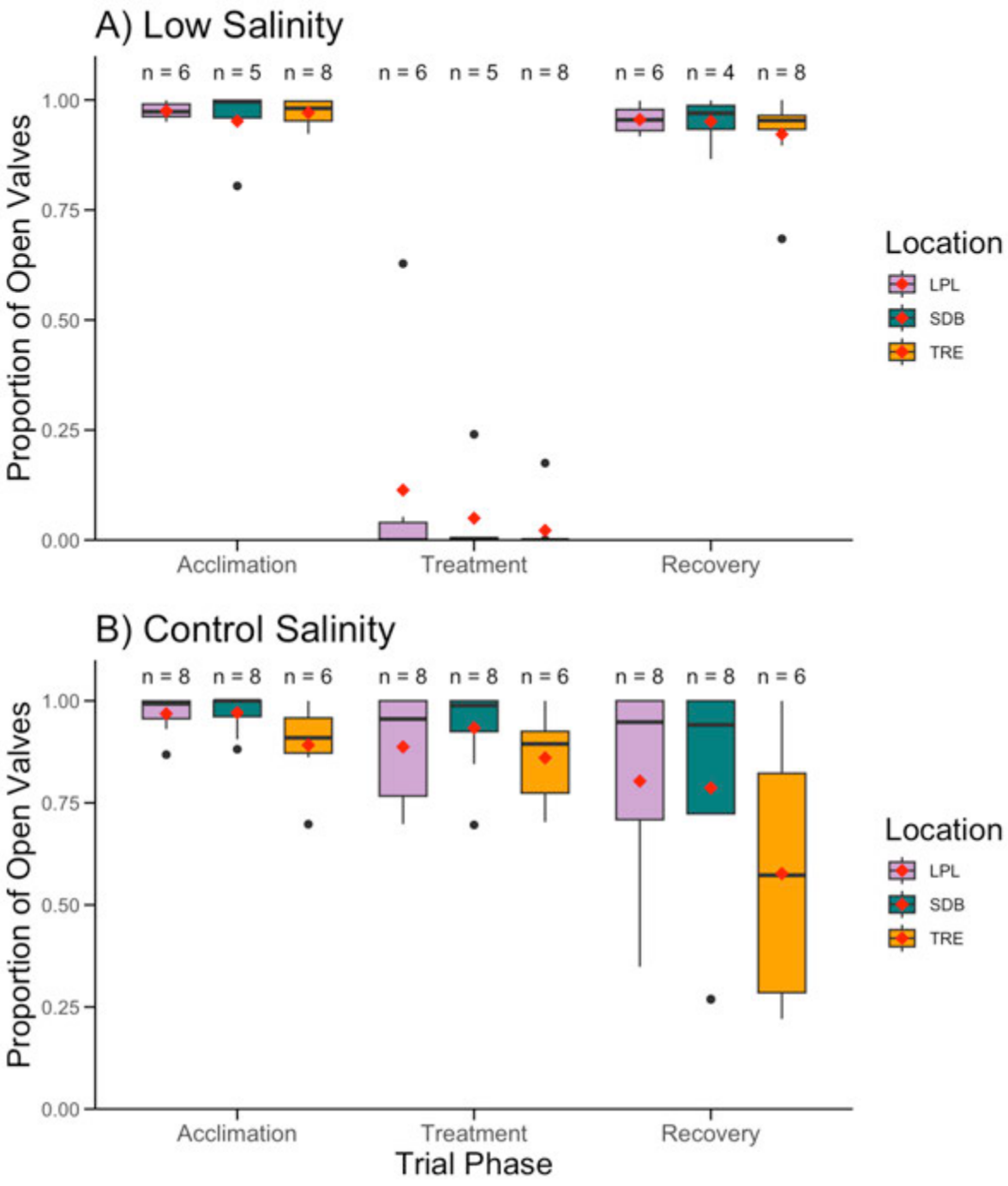

Figure 13. Proportion of open valves during A) low salinity or B) control salinity treatment separated by trial phase (Acclimation, Treatment, and Recovery) and location (LPL, SDB, and TRE). Red diamonds represent means, and black bars represent medians. N = number of mussels.

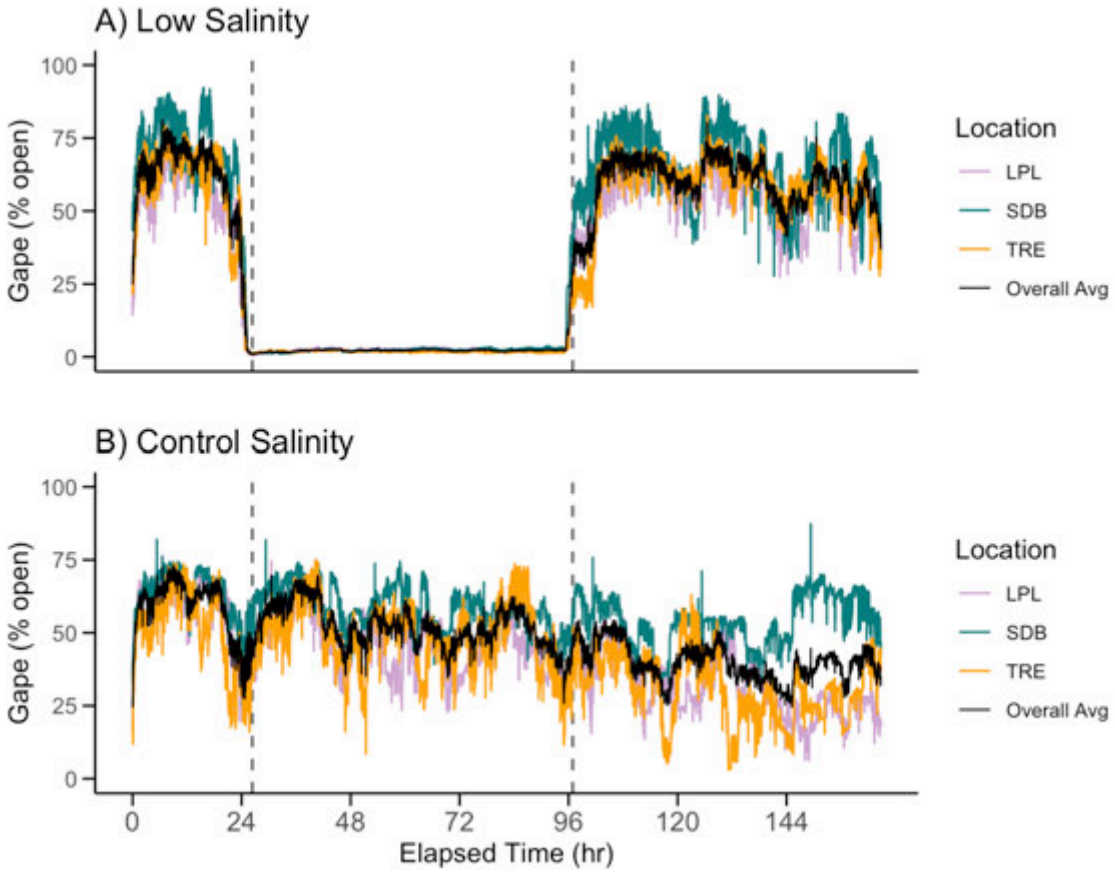

Figure 14. Average gape (%) of all A) low salinity and B) control salinity mussels as the trial hours elapse. Colored lines represent location averages, the black line is the overall average, and the vertical dashed lines represent the average hour in which treatment began and ended.

CV was significantly different between the low salinity and control salinity mussels across trial phases (Figure 16B, ANOVA, $F_{2,81.5} = 55.41$, $p < 0.001$). CV was not significantly different between the low salinity and the control treatment groups in the Acclimation (Figure 16B, Bonferroni, $p = 0.53$) or the Recovery phases (Figure 16B, Bonferroni, $p = 0.28$). However, there was a significant difference between the two treatment groups in the Treatment phase, where mussels exposed to low salinity had a much higher heart rate CV (Figure 16B, Bonferroni, $p < 0.001$). Within the low salinity treatment group, CV was significantly higher in the Treatment phase compared to the Acclimation phase (Figure 16B, Bonferroni, $p < 0.001$) and the Recovery phase (Figure 16B, Bonferroni, $p < 0.001$). There was a marginally significant difference in the heart rate CV among mussels

from different locations exposed to low salinity (Figure 18A, ANOVA, $F_{2,53} = 3.02$, $p = 0.06$). That difference was driven by mussels from the TRE exhibiting a significantly higher CV compared to mussels from LPL (Figure 18A, Bonferroni, $p < 0.001$). Overall, mussels from all locations exhibited the same response: an increase in heart rate variability during Treatment and a decrease during Recovery.

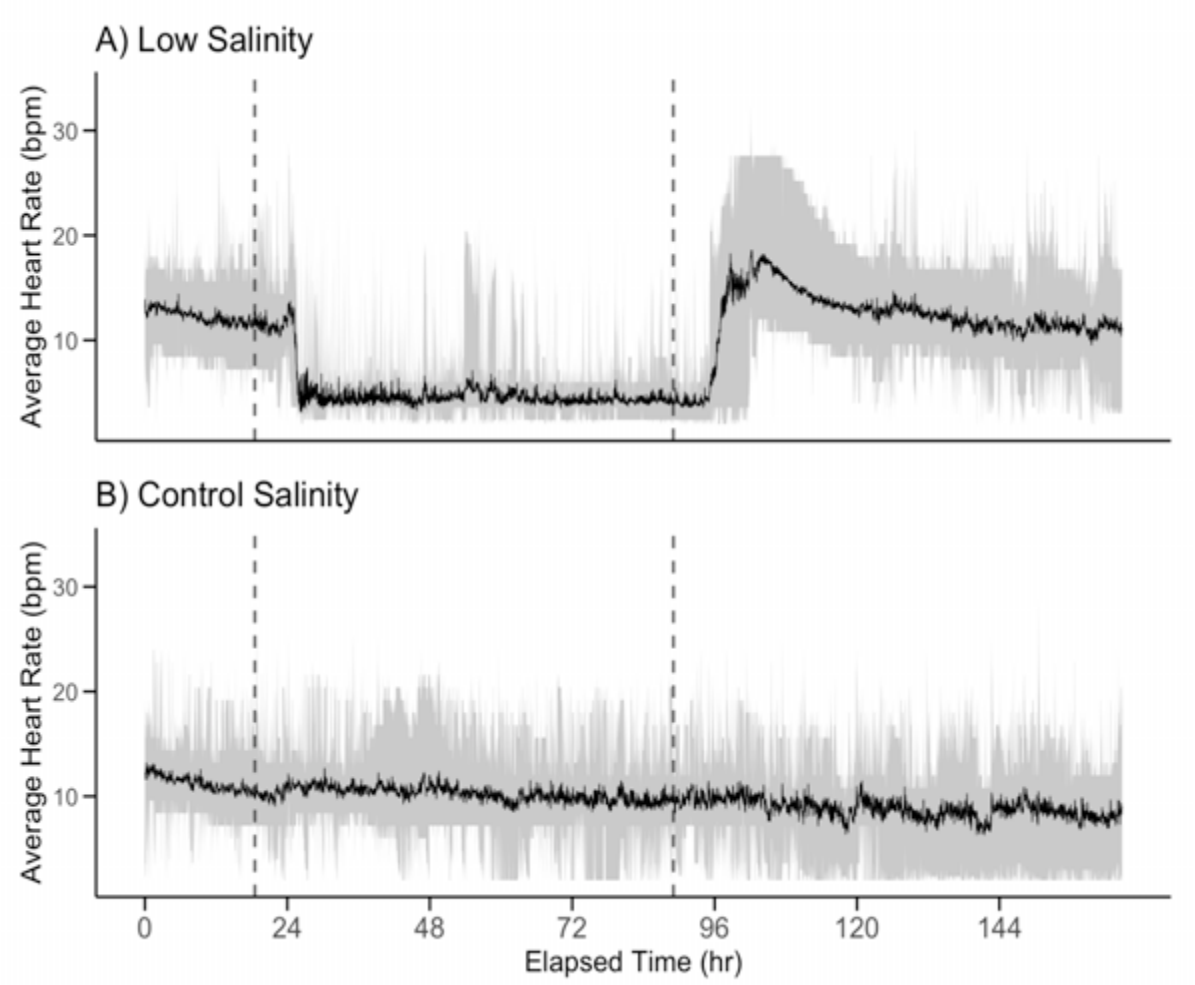

Figure 15. Average heart rate (bpm) of all A) low salinity and B) control salinity mussels as trial hours elapse. The black line is the average heart rate, the grey line is the heart rate range, and the vertical dashed lines represent the average hour in which treatment began and ended.

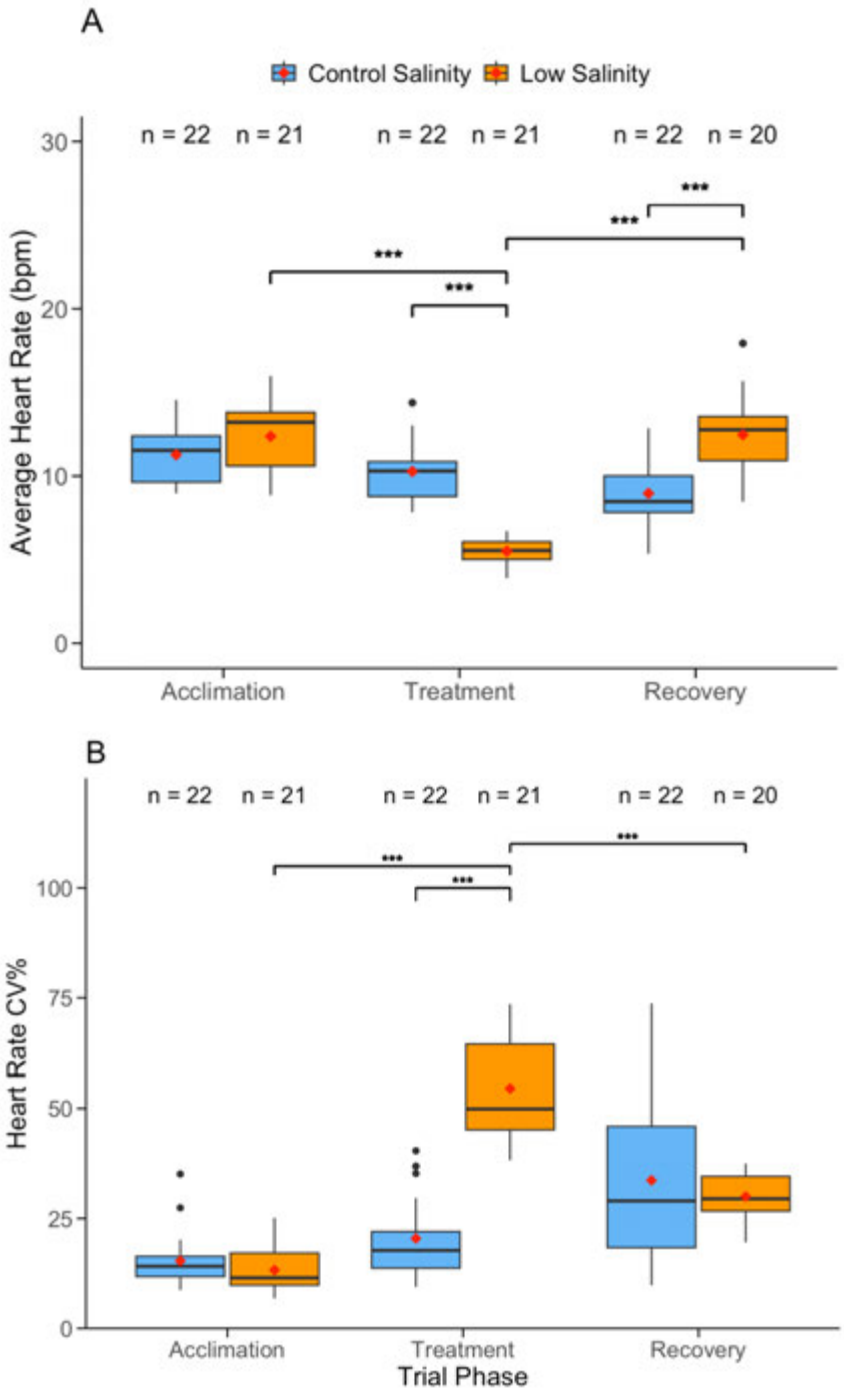

Figure 16. A) average heart rate (bpm) and B) heart rate CV of mussels separated by treatment group (control salinity or low salinity) and trial phase (Acclimation, Treatment, and Recovery). Red diamonds represent means, and black bars represent medians. N = number of mussels. Significant differences as determined by post hoc pairwise comparisons with Bonferroni adjustment methods, *** = $p < 0.001$.

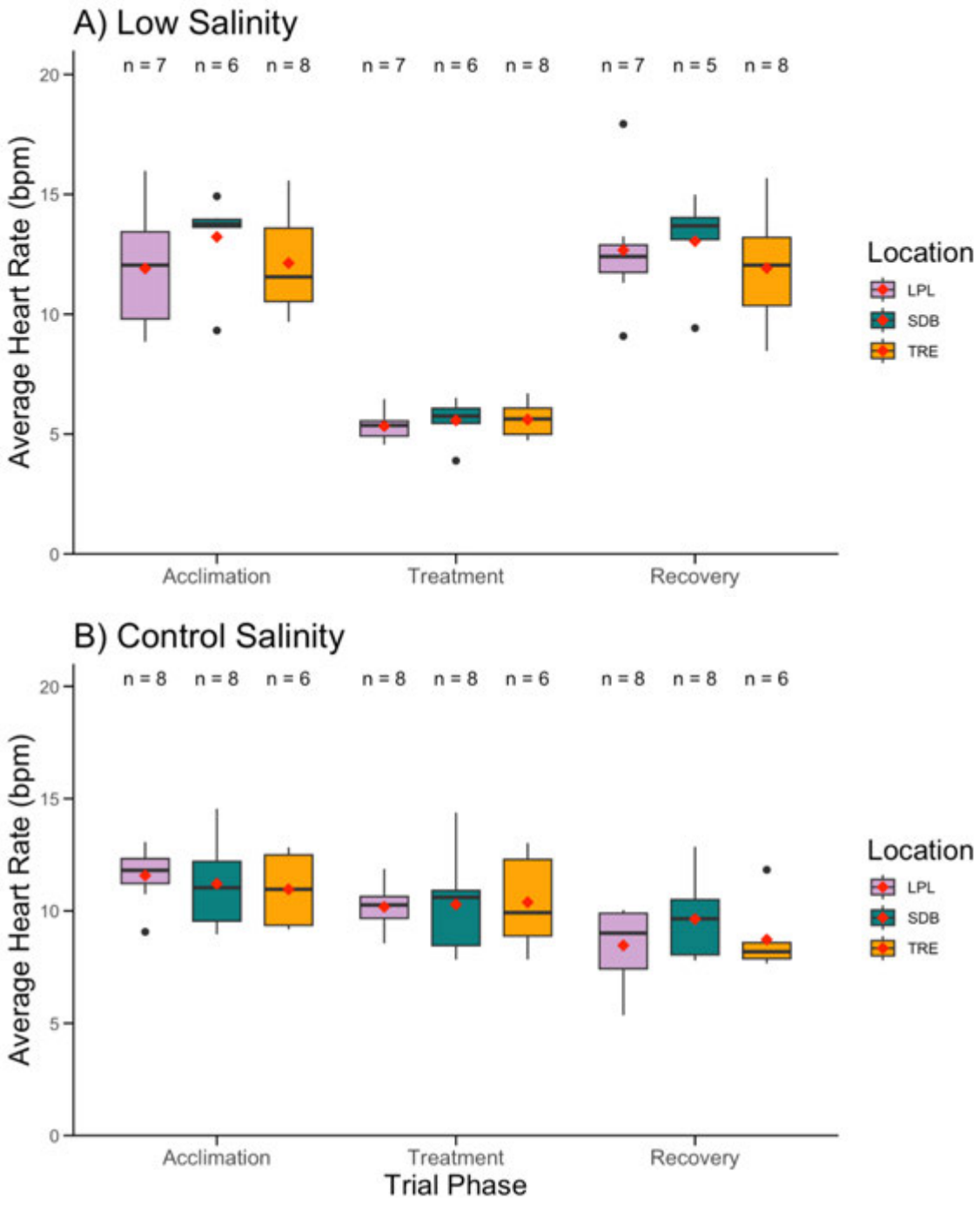

Figure 17. Average heart rate (bpm) of mussels in the A) low salinity treatment group and the B) control salinity treatment group separated by trial phase (Acclimation, Treatment, and Recovery) and location (LPL, SDB, and TRE). Red diamonds represent means, and black bars represent medians. N = number of mussels.

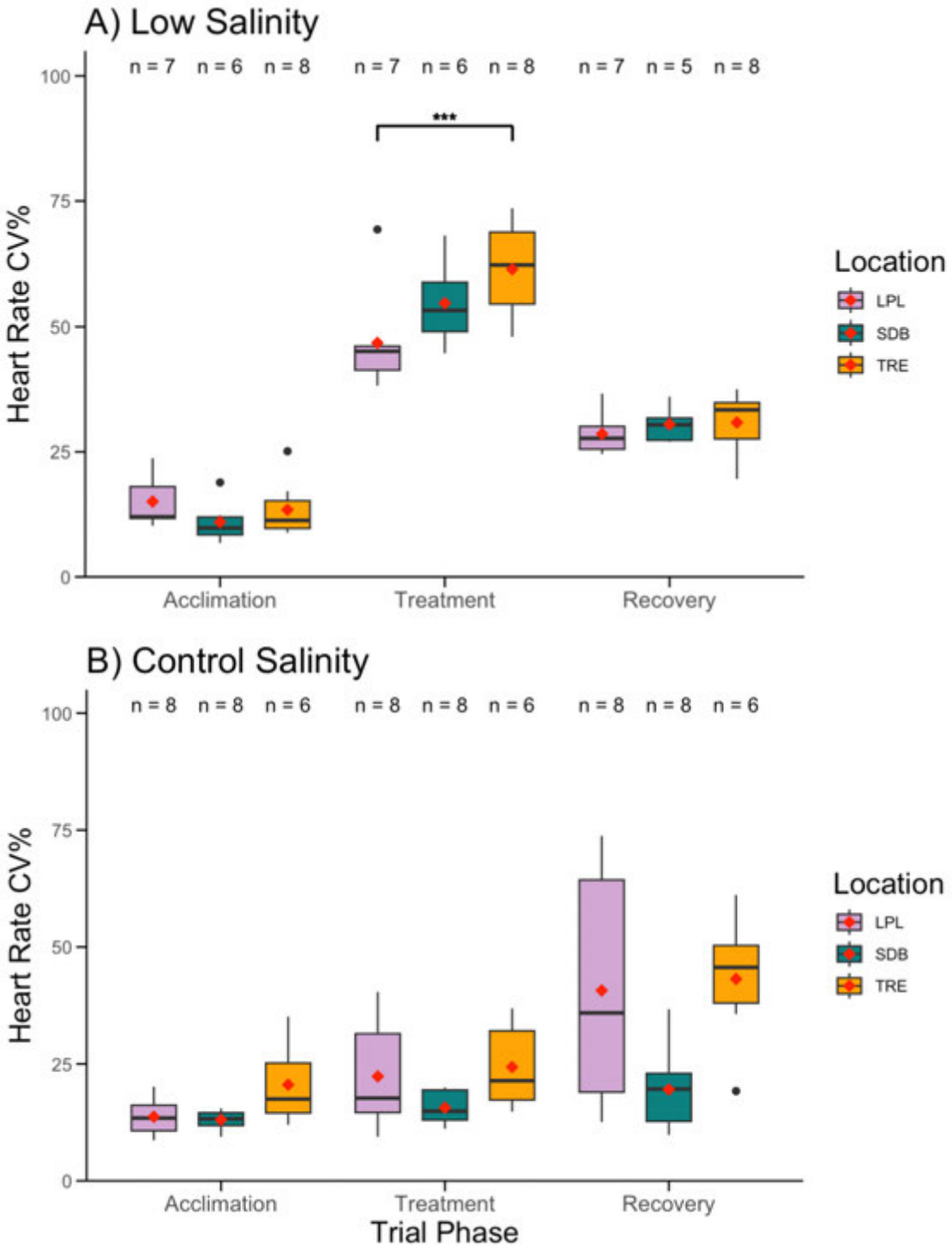

Figure 18. Heart rate CV of mussels in the A) low salinity treatment group and the B) control salinity treatment group separated by trial phase (Acclimation, Treatment, and Recovery) and location (LPL, SDB, and TRE). Red diamonds represent means, and black bars represent medians. N = number of mussels. Significant differences as determined by post hoc pairwise comparisons with Bonferroni adjustment methods, *** = $p < 0.001$.

FIELD DEPLOYMENTS

Tijuana River Estuary

Between February 26 and April 29, 2025, mussels deployed in the TRE experienced dynamic abiotic conditions that influenced their gaping behavior and heart rates. DO near the benthos fluctuated daily between 0 and 10 mg L^{-1} (Figure 19C), while surface DO did not exceed 8 mg L^{-1} and occasionally remained at 0 mg L^{-1} for several consecutive days (Figure 20B). Salinity patterns also differed between depths: conditions near the benthos generally remained between 20 and 30 psu (Figure 19D), with sharp declines to 0 psu following precipitation events (Figure 19H), whereas conditions near the surface frequently dropped below 20 psu throughout the duration of the deployment (Figure 20C). Precipitation events similarly decreased salinity at the surface to 0 psu (Figure 20G). Temperatures were relatively stable, averaging 15.2 °C and ranging from ~12 to 24 °C at the bottom (Figure 19E), and averaging 16.1 ºC and ranging from ~12 to 26 °C at the surface (Figure 20D). Turbidity was highly variable, averaging 84.7 FNU/NTU and occasionally peaking above 800 FNU/NTU (Figure 19F; Figure 20E). The water level fluctuated predictably with tidal cycles, ranging from 0.6 to 1.9 m (Figure 19G; Figure 20F). Surface mussels experienced a negative growth rate of -0.001 mm/day, while bottom mussels grew at a rate of 0.008 mm/day throughout the deployment period (Table A1). Two of the eight bottom mussels survived the full duration of the deployment. All eight surface mussels were dead by March 24, 2025.

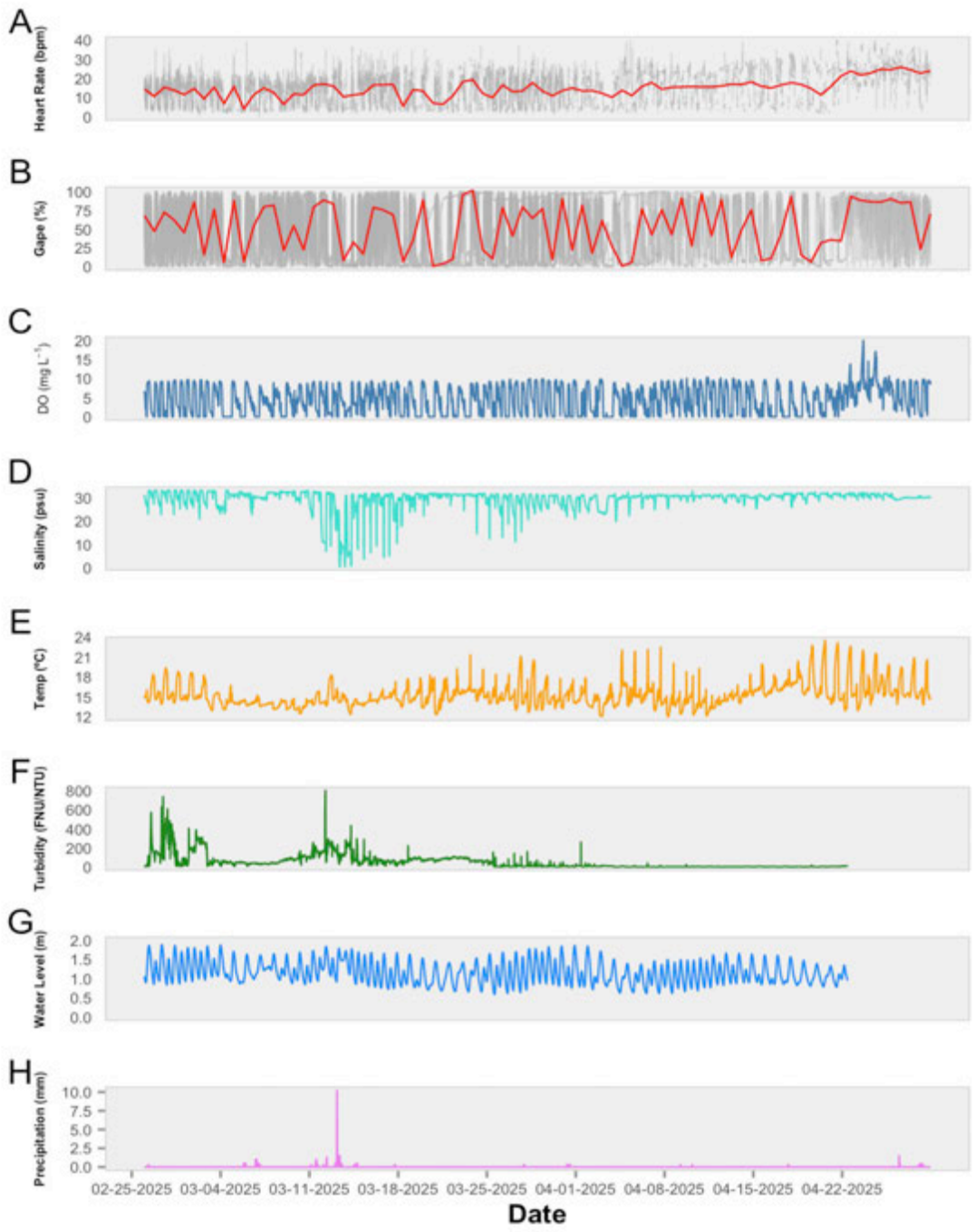

Figure 19. A) heart rate (bpm), B) gape %, C) dissolved oxygen (DO; mg L^{-1}), D) salinity (psu), E) temperature (ºC), F) turbidity (FNU/NTU), G) water level (m), and H) precipitation (mm) for bottom mussels at the TRE between February 26 and April 29, 2025. Grey lines represent gape and heart rate data for individual mussels. Red lines represent LOESS trend lines. DO and temperature data were retrieved from the bottom MiniDOT, and salinity data were retrieved from the bottom CTD. Turbidity and water level data were retrieved from the Boca Rio SWMP sensor (TJRBRWQ). Precipitation data were retrieved from the tidal linkage SWMP sensor (TJRTLMET).

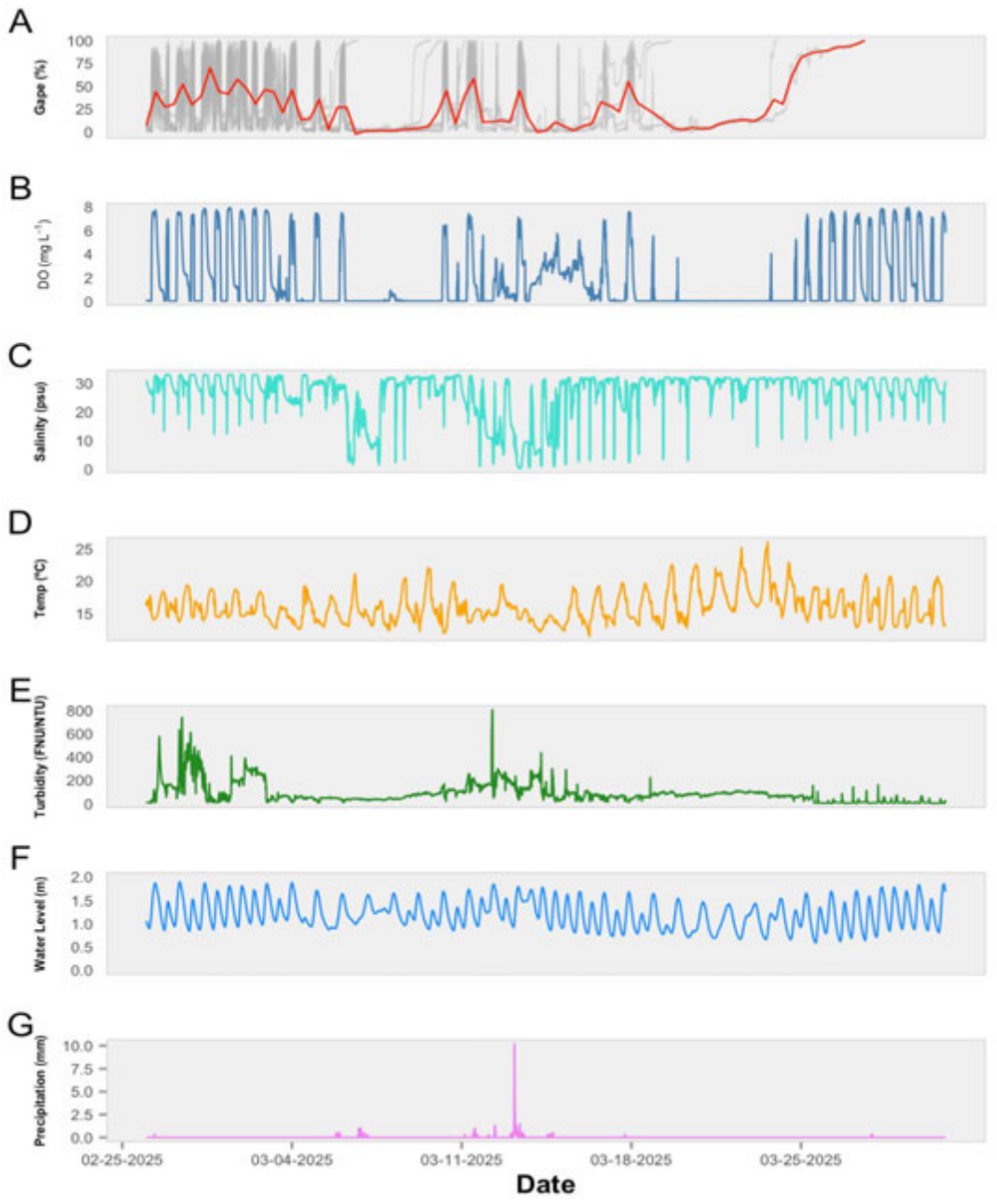

Figure 20. A) gape opening %, B) dissolved oxygen (mg L^{-1}), C) salinity (psu), D) temperature (°C), E) turbidity (FNU/NTU), F) water level (m), and G) precipitation (mm) for surface mussels at the TRE between February 26 and March 31, 2025. Grey lines represent gape and heart rate data for individual mussels. A gape line terminating at 100% represents mortality of that mussel. Red lines represent LOESS trend lines. DO and temperature data were retrieved from the surface MiniDOT, and salinity data were retrieved from the surface CTD. Turbidity and water level data were retrieved from the Boca Rio SWMP sensor (TJRBRWQ). Precipitation data were retrieved from the tidal linkage SWMP sensor (TJRTLMET). Mussel heart rate data were unavailable for this deployment due to equipment failure.

For bottom mussels at the TRE, using repeated measures correlation analysis methods with heart rate as the response variable revealed a strong, positive association with gape (Figure 21A, $r_{rm} = 0.69$, CI [0.68, 0.7], slope = 0.14, $p < 0.001$), a strong positive association with DO (Figure 21B, $r_{rm} = 0.57$, CI [0.56, 0.58], slope = 1.15, $p < 0.001$), a negligible positive association with salinity (Figure 21C, $r_{rm} = 0.03$, CI [0.02, 0.04], slope = 0.05, $p < 0.001$), a negligible positive association with temperature (Figure 21D, $r_{rm} = 0.015$, CI [-0.004, 0.03], slope = 0.06, $p = 0.03$), and a negligible negative association with turbidity (Figure 21E, $r_{rm} = -0.06$, CI [-0.08, -0.05], slope = -0.005, $p < 0.001$) within individuals. Using gape as the response variable revealed a strong positive association with DO (Figure 22A, $r_{rm} = 0.66$, CI [0.66, 0.67], slope = 7.06, $p < 0.001$), a positive, but much weaker association with salinity (Figure 22B, $r_{rm} = 0.09$, CI [0.08, 0.1], slope = 0.68, $p < 0.001$), a moderately weak negative association with temperature (Figure 22C, $r_{rm} = -0.23$, CI [-0.24, -0.22], slope = -5.28, $p < 0.001$), and a negligible negative association with turbidity (Figure 22D, $r_{rm} = -0.07$, CI [-0.08, -0.05], slope = -0.03, $p < 0.001$) within individuals. Due to the large number of observations (gape: $n > 15{,}000$; heart rate: $n > 25{,}000$), even weak associations yielded statistically significant p-values. Therefore, the interpretation was focused on effect size/direction and confidence intervals rather than significance alone.

The pairwise correlations between bottom mussel response and DO or salinity are further complemented by an alternative visualization of mussel responses across the joint distribution of DO and salinity (Figure 23A-B). This plot was included to examine the combined influence of DO and salinity and to highlight the range of conditions encountered in the field. Both the heart rate and gape responses of bottom mussels were more strongly influenced by DO than by salinity at the TRE.

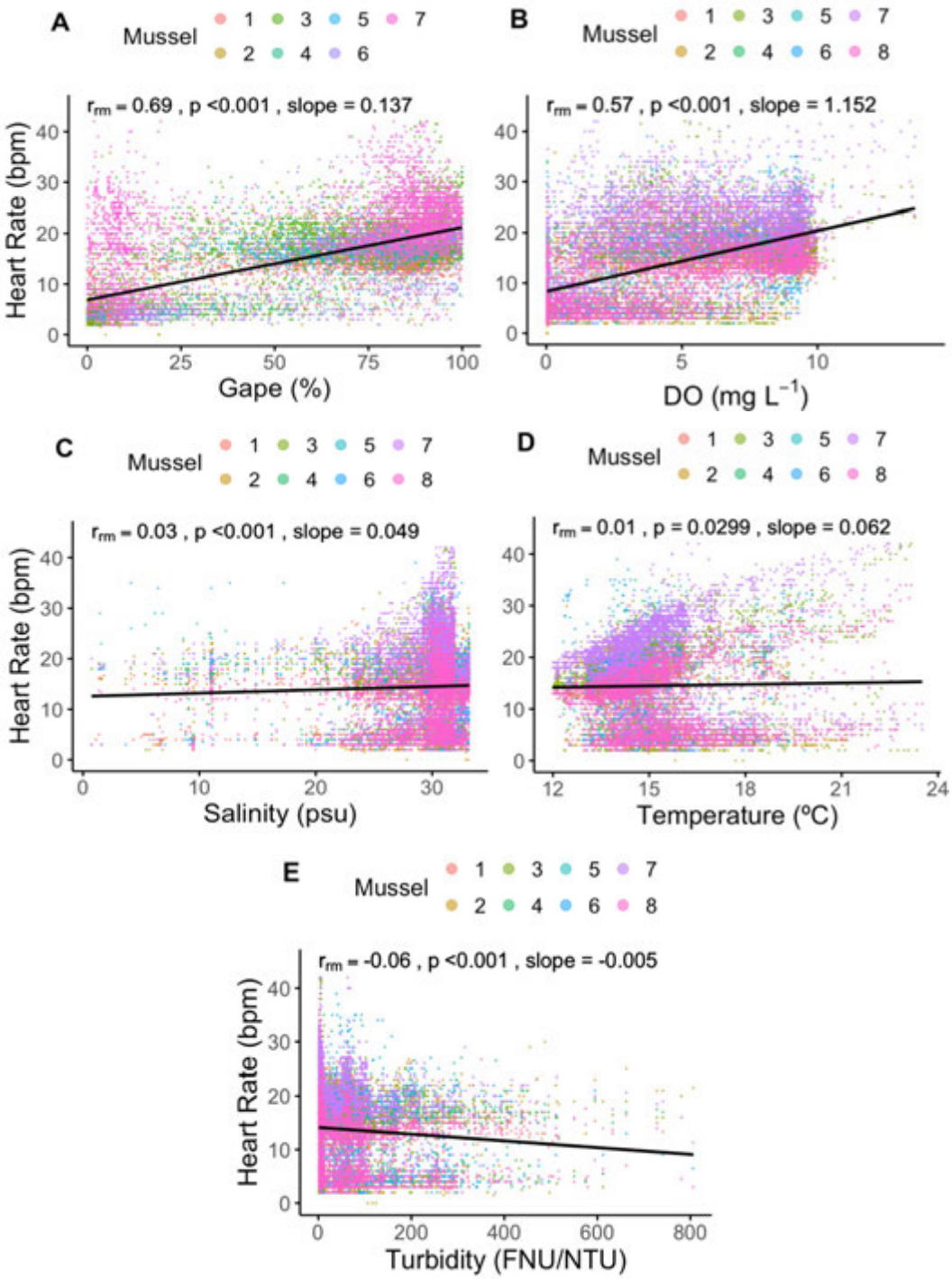

Figure 21. Repeated measures correlation between the heart rate (bpm) of bottom TRE mussels and A) gape opening %, B) dissolved oxygen (DO; mg L^{-1}), C) salinity (psu), D) temperature (°C), and E) turbidity (FNU/NTU). Observations were averaged in 15-minute intervals between February 26 and April 29, 2025. Points are colored by individual mussel, and the black line represents the shared linear slope across all mussels. The repeated measures coefficient (r_{rm}), p-value, and slope are reported at the top of each graph.

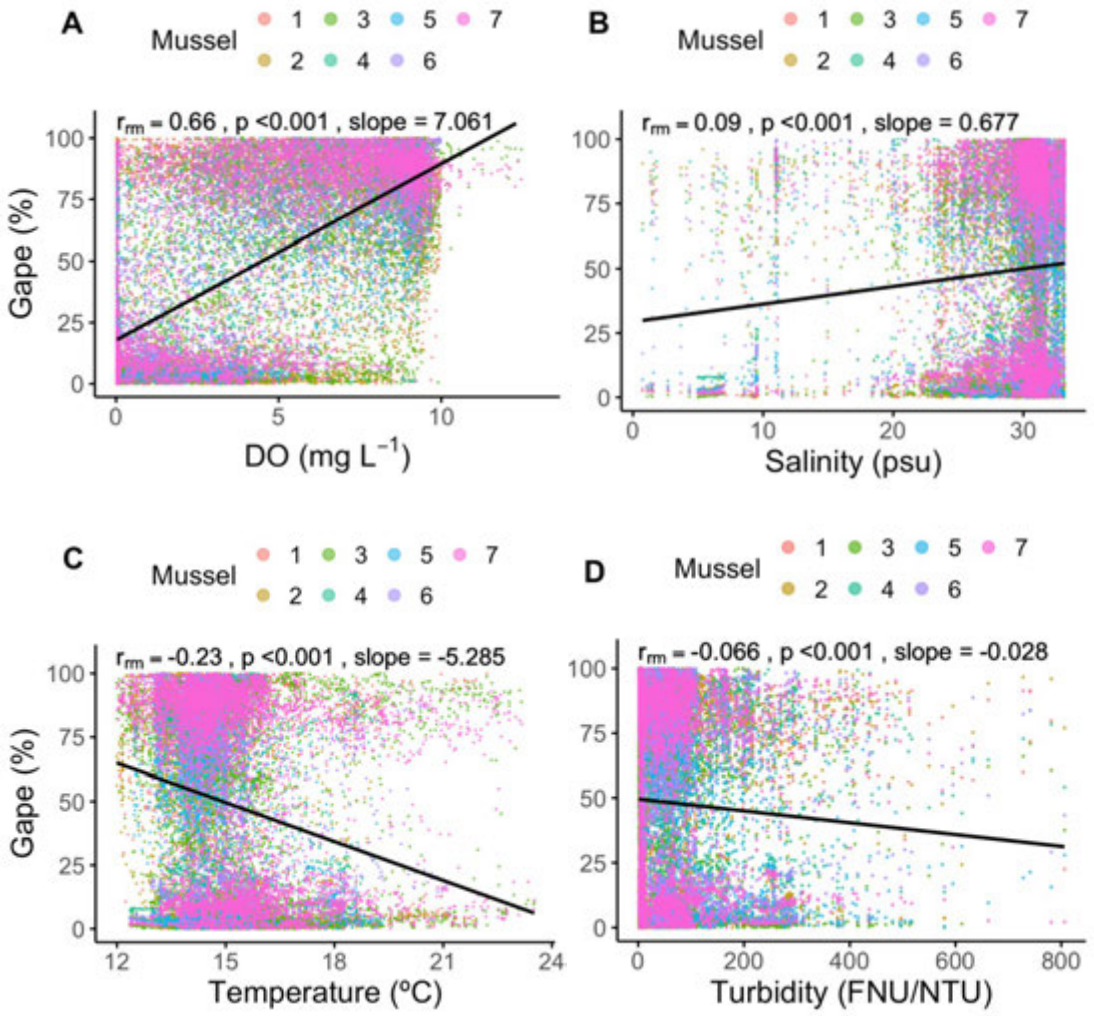

Figure 22. Repeated measures correlation between gape opening % of bottom TRE mussels and A) dissolved oxygen (DO; mg L^{-1}), B) salinity (psu), C) temperature (°C), and D) turbidity (FNU/NTU). Observations were averaged in 15-minute intervals between February 26 and April 29, 2025. Points are colored by individual mussel, and the black line represents the shared linear slope across all mussels. The repeated measures coefficient (r_{rm}), p-value, and slope are reported at the top of each graph.

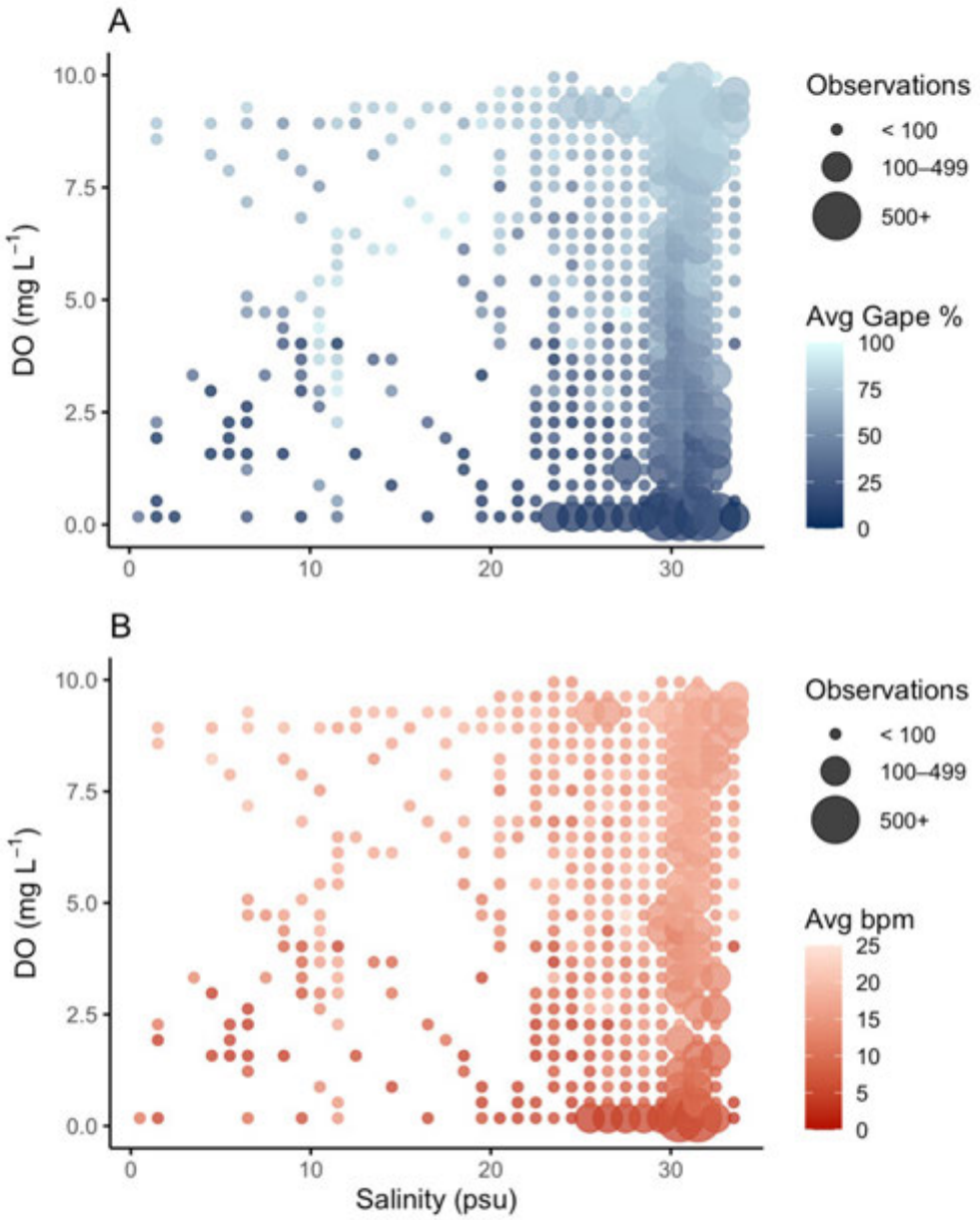

Figure 23. The relationship between salinity (psu), dissolved oxygen (DO; mg L^{-1}), and the A) average gape % across bottom mussels at the TRE and B) average heart rate (bpm) of bottom mussels at the TRE. Observations were averaged in 15-minute intervals between February 26 and April 29, 2025. Each point represents aggregated observations at 1-unit increments of salinity and 0.35-unit increments of DO concentration. Point size corresponds to the number of observations in each bin, and point color reflects the average gape % or bpm.

For surface mussels at the TRE, repeated measures correlations with gape as the response variable revealed a strong positive association with DO (Figure 24A, $r_{rm} = 0.68$, CI

[0.67, 0.69], slope = 8.45, $p < 0.001$), a positive, but much weaker association with salinity (Figure 24B, $r_{rm} = 0.17$, CI [0.16, 0.19], slope = 0.69, $p < 0.001$), a weak negative association with temperature (Figure 24C, $r_{rm} = -0.14$, CI [-0.15, -0.12], slope = -2.08, $p < 0.001$), and a negligible positive association with turbidity (Figure 24D, $r_{rm} = 0.08$, CI [0.06, 0.1], slope = 0.02, $p < 0.001$) within individuals. Due to the large number of observations (n > 13,000), interpretation was focused on effect size/direction and confidence intervals rather than significance alone.

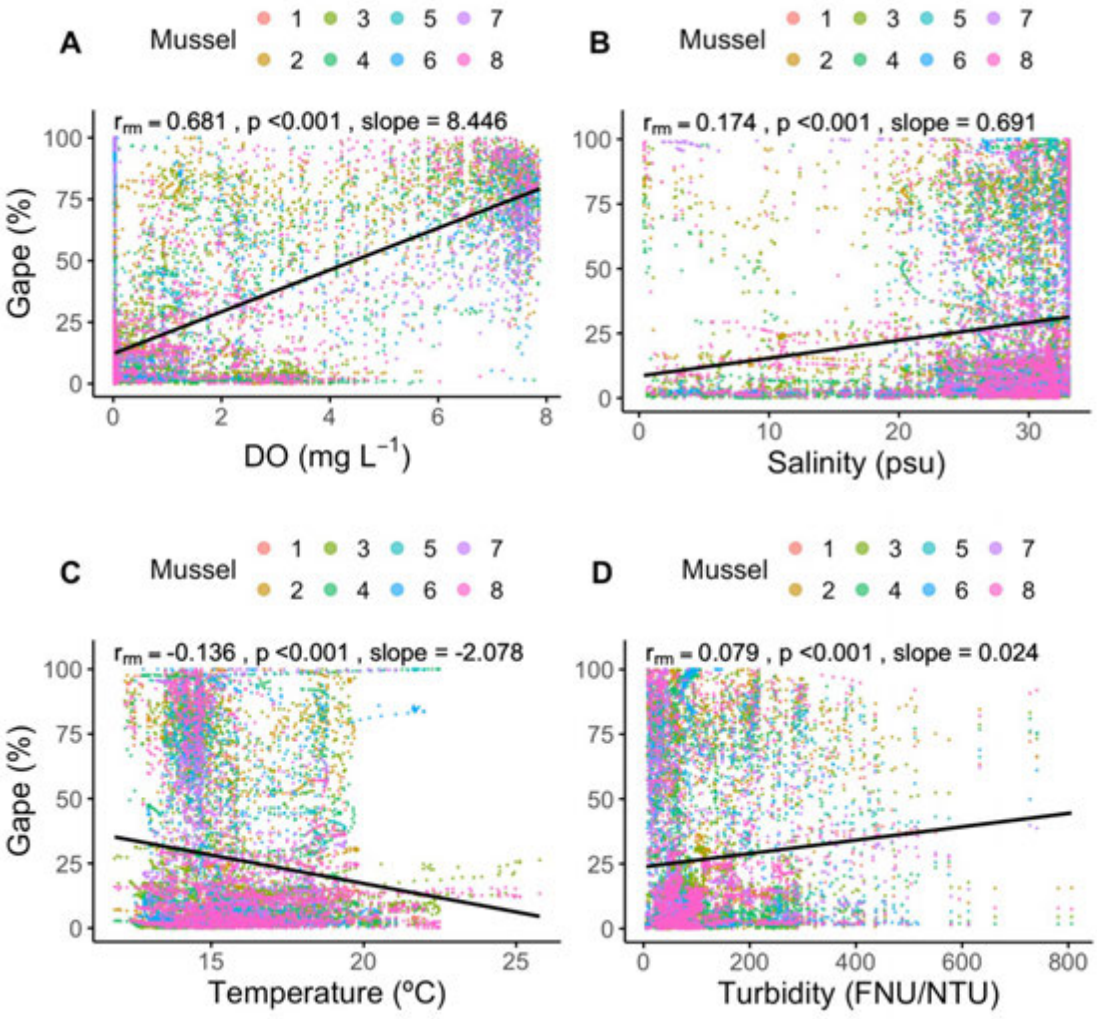

Figure 24. Repeated measures correlation between the gape opening % of surface TRE mussels and A) dissolved oxygen (DO; mg L^{-1}), B) salinity (psu), C) temperature (°C), and D) turbidity (FNU/NTU). Observations were averaged in 15-minute intervals between February and April 29, 2025. Points are colored by individual mussel, and the black line represents the shared linear slope across all mussels. The repeated measures coefficient (r_{rm}), p-value, and slope are reported at the top of each graph.

The pairwise correlations between surface mussel response and DO or salinity are further complemented by Figure 25. Gape responses of surface mussels were more strongly influenced by DO than by salinity at the TRE.

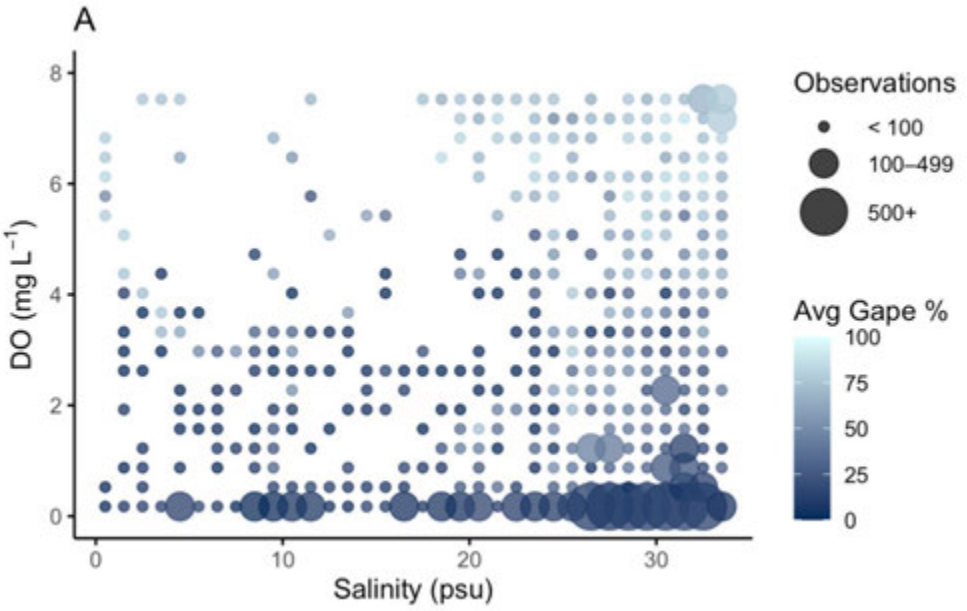

Figure 25. The relationship between salinity (psu), dissolved oxygen (DO; mg L^{-1}), and the average gape % across surface mussels from the TRE. Observations were averaged in 15-minute intervals between February 26 and March 24, 2025. Each point represents aggregated observations at 1-unit increments of salinity and 0.35-unit increments of DO concentration. Point size corresponds to the number of observations in each bin, and point color reflects the average gape %.

Generalized linear mixed effect models with a binomial error distribution revealed that mussels deployed near the benthos at the TRE significantly changed their gaping behavior in response to DO ($\chi^2_{(1)} = 3340.4$, $p < 0.001$) and salinity ($\chi^2_{(1)} = 245.4$, $p < 0.001$), where mussels opened more frequently with higher levels of DO and salinity. Turbidity ($\chi^2_{(1)} = 0.58$, $p = 0.45$) and temperature ($\chi^2_{(1)} = 0.7$, $p = 0.4$) were not significant predictors. The model explained 37% of the variance through fixed effects alone (marginal R^2) and 53.9% of the variance when accounting for both fixed and random effects (conditional R^2). For mussels on the surface of the water column at the TRE, DO had the strongest impact on gape behavior ($\chi^2_{(1)} = 1233.2$, $p < 0.001$), where mussels opened more frequently with higher DO. Mussels also opened more frequently with higher salinities ($\chi^2_{(1)} = 437.5$, $p < 0.001$). Turbidity ($\chi^2_{(1)} = 222.5$, $p < 0.001$) and temperature ($\chi^2_{(1)} = 142.8$, $p < 0.001$) also

significantly impacted gape behavior, although the effects were not as pronounced as those of DO and salinity. The model explained 34.6% of the variance through fixed effects and 46.4% of the variance when accounting for both fixed and random effects.

Los Peñasquitos Lagoon

Between October 8, 2024, and May 9, 2025, mussels at LPL experienced relatively stable but occasionally extreme abiotic conditions. DO near the benthos averaged 6.6 mg L^{-1}, ranging from 0.03 to 14.8 mg L^{-1} (Figure 26C), while surface DO averaged 7.2 mg L^{-1}, with values between 0.7 and 12.6 mg L^{-1} (Figure 27C). Due to a malfunctioning surface CTD, salinity was only measured near the benthos, where it ranged between 0.6 and 33.5 psu and averaged around 31.4 psu (Figure 26D; Figure 27D). Salinity only decreased substantially during precipitation events (Figure 26G; Figure 27G). Temperatures near the benthos ranged from 11.9 to 23.5 °C and averaged 15.2 °C (Figure 26E). At the surface, temperatures ranged from 7.7 to 23.5 °C and averaged 15.5 °C (Figure 27E). Turbidity averaged ~3 FNU/NTU and reached a peak of 380 FNU/NTU (Figure 26F; Figure 27F). The water level ranged from 0.7 m to 2.2 m and tracked mostly with the tides, although low tides were truncated for much of the deployment, likely due to a sill forming at the mouth of the estuary, which limits the lower extent of the low tide (Figure 26G; Figure 27G). Surface mussels grew at a rate of 0.03 mm day^{-1}. Growth rates are unknown for the bottom mussels, as they were dead upon recovery, and the timing of their mortality was unclear.

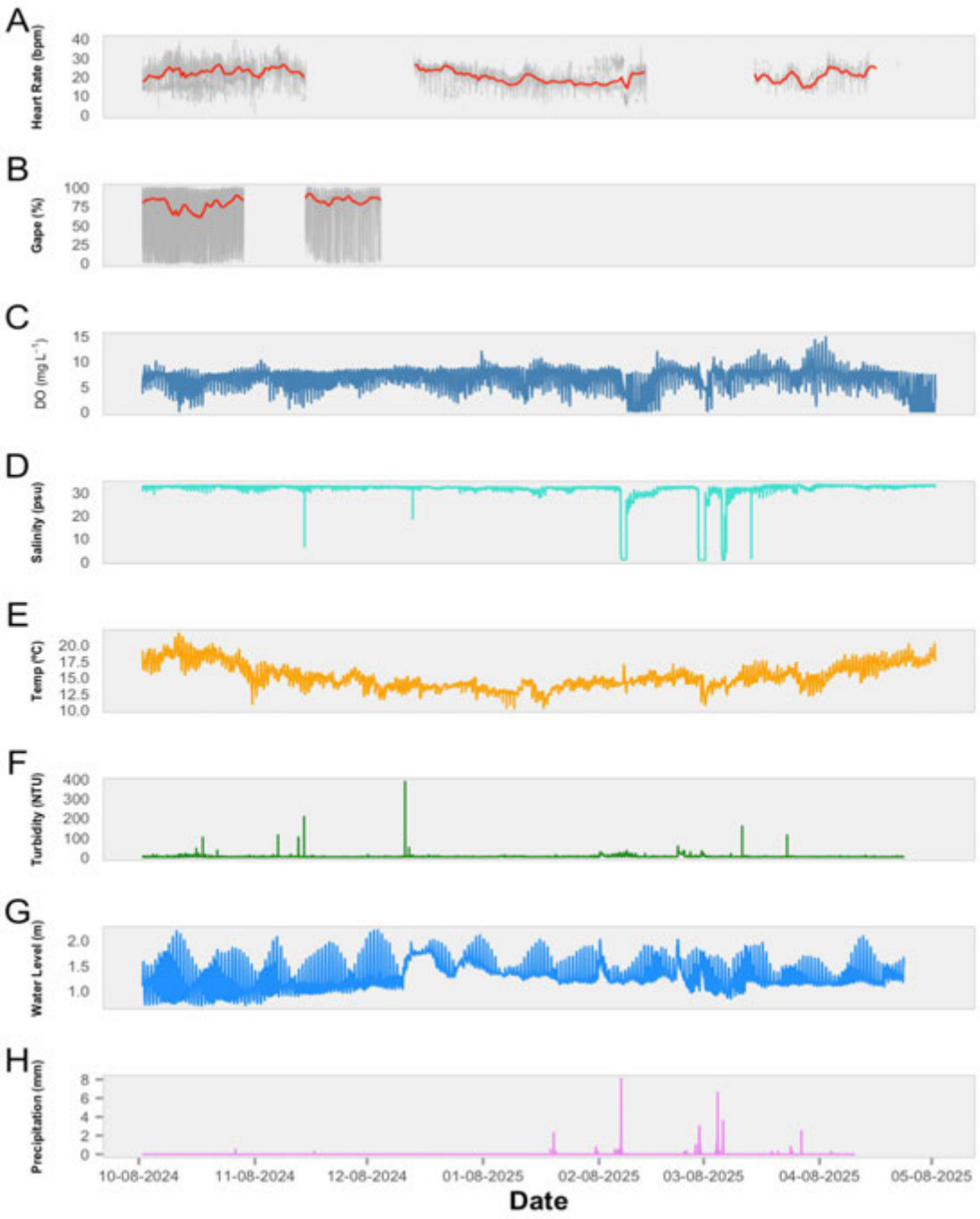

Figure 26. A) heart rate (bpm), B) gape opening %, C) dissolved oxygen (DO; mg L^{-1}), D) salinity (psu), E) temperature (ºC), F) turbidity (NTU), G) water level (m), and H) precipitation (mm) for bottom mussels at LPL between October 8, 2024, and May 9, 2025. Grey lines represent gape and heart rate data for individual mussels. Red lines represent LOESS trends. DO and temperature data were retrieved from the bottom MiniDOT. Salinity data were retrieved from the bottom CTD. Turbidity and water level data were retrieved from the nearby SWMP water quality station (LPLNW). Precipitation data were retrieved from the Miramar Airport weather station (KNKX).

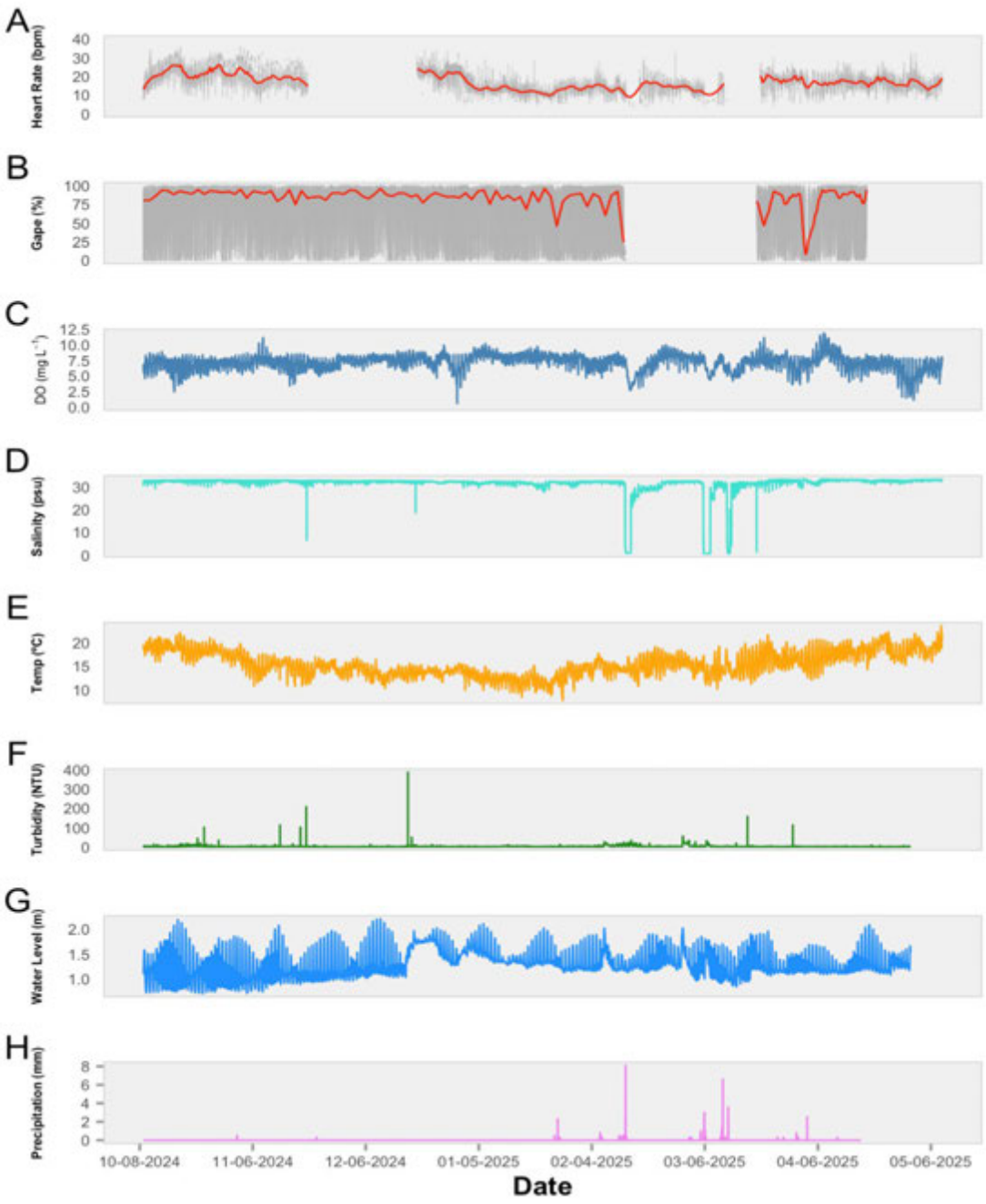

Figure 27. A) heart rate (bpm), B) gape opening %, C) dissolved oxygen (DO; mg L^{-1}), D) salinity (psu), E) temperature (ºC), F) turbidity (NTU), G) water level (m), and H) precipitation (mm) for surface mussels at LPL between October 8, 2024, and May 9, 2025. Grey lines are raw gape and heart rate data for individual mussels. Red lines represent LOESS trend lines. DO and temperature data were retrieved from the surface MiniDOT. Salinity data were retrieved from the bottom CTD because the surface CTD was malfunctioning. Turbidity and water level data were taken from the nearby SWMP water quality station (LPLNW). Precipitation data were retrieved from the Miramar Airport weather station (KNKX).

For bottom mussels at LPL, repeated measures correlations with heart rate as the response variable revealed a moderately positive association with gape (Figure 28A, r_{rm} = 0.38, 95% CI [0.35, 0.41], slope = 0.07, $p < 0.001$), a very weak negative association with DO (Figure 28B, r_{rm} = -0.09, 95% CI [-0.11, -0.08], slope = -0.24, $p < 0.001$), a weak positive association with salinity (Figure 28C, r_{rm} = 0.19, 95% CI [0.18, 0.21], slope = 0.35, $p < 0.001$), and a moderately positive association with temperature (Figure 28D, r_{rm} = 0.41, 95% CI [0.39, 0.42], slope = 0.89, $p < 0.001$) within individuals. Using gape as the response variable revealed a moderate positive association with DO (Figure 29A, r_{rm} = 0.43, 95% CI [0.41, 0.44], slope = 6.75, $p < 0.001$), a positive, but much weaker association with salinity (Figure 29B, r_{rm} = 0.14, 95% CI [0.12, 0.16], slope = 8.24, $p < 0.001$), and a weak negative association with temperature (Figure 29C, r_{rm} = -0.14, 95% CI [-0.16, -0.13], slope = -2.11, $p < 0.001$) within individuals. Due to the large number of overall observations (gape: $n > 10,000$; heart rate: $n > 24,000$), interpretation was focused on effect size/direction and confidence intervals rather than significance alone.

The pairwise correlations between bottom mussel response and DO or salinity are further complemented by Figure 30A-B. Bottom mussels at LPL did not experience the same range of conditions as those at the TRE, and mussel responses remained largely unaffected by those conditions.

For surface mussels at LPL, repeated measures correlations with heart rate as the response variable revealed a positive association with gape, although it was a much weaker association than expected (Figure 31A, r_{rm} = 0.2, 95% CI [0.18, 0.21], slope = 0.05, $p < 0.001$), a weak negative association with DO (Figure 31B, r_{rm} = -0.1, 95% CI [-0.11, -0.09], slope = -0.34, $p < 0.001$), a weak positive association with salinity (Figure 31C, r_{rm} = 0.24, 95% CI [0.23, 0.25], slope = 0.54, $p < 0.001$), and a moderately positive association with temperature (Figure 31D, r_{rm} = 0.45, 95% CI [0.45, 0.46], slope = 0.74, $p < 0.001$) within individuals. Using gape as the response variable revealed a weak positive association with DO (Figure 32A, r_{rm} = 0.1, 95% CI [0.09, 0.11], slope = 2.16, $p < 0.001$), a weak positive association with salinity (Figure 32B, r_{rm} = 0.08, 95% CI [0.07, 0.09], slope = 2.67, $p < 0.001$), and a weak positive association with temperature (Figure 32C, r_{rm} = 0.1, 95% CI [0.09, 0.11], slope = 0.86, $p < 0.001$) within individuals. Due to the large number of overall

observations (gape: n > 60,000; heart rate: n > 34,000), interpretation was focused on effect size/direction and confidence intervals rather than significance alone.

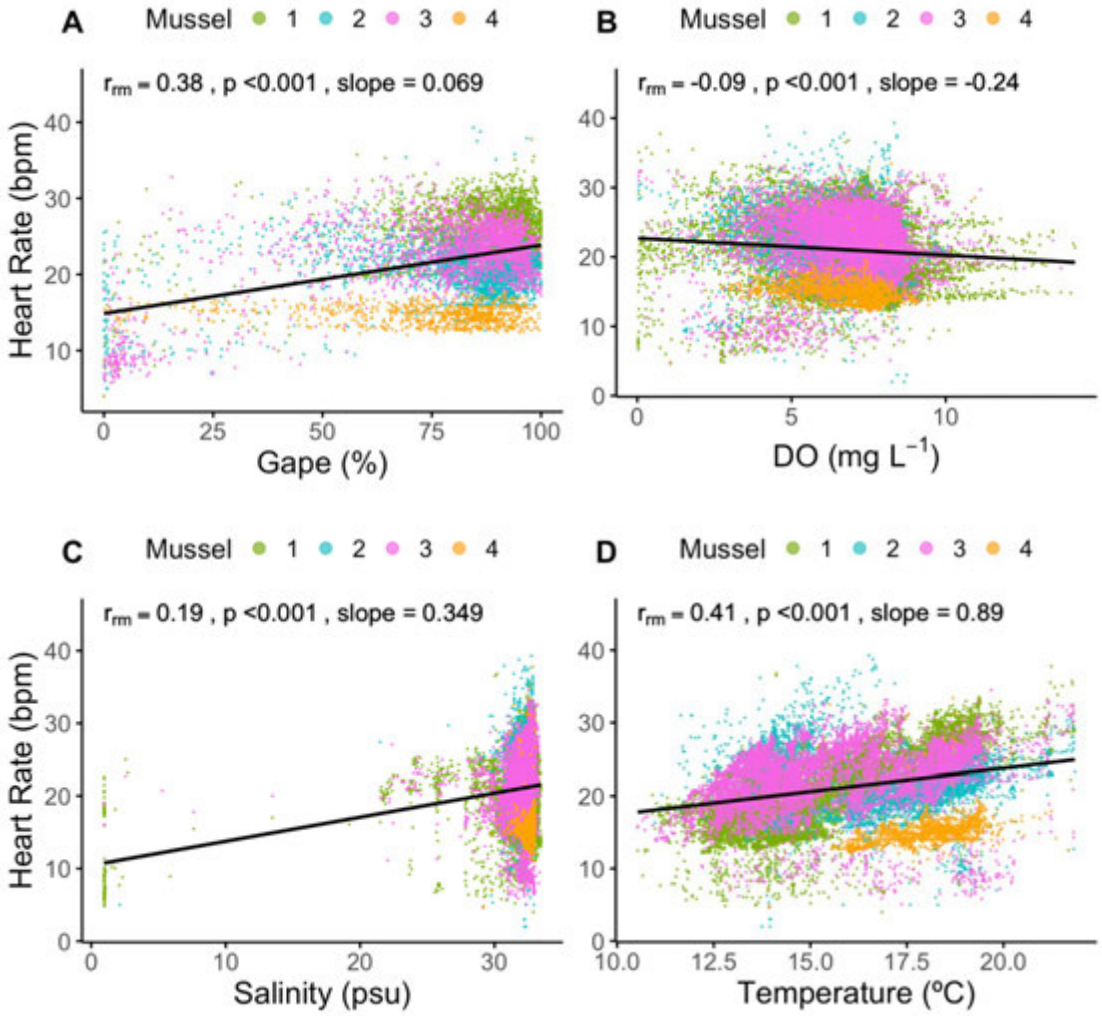

Figure 28. Repeated measures correlation between the heart rate (bpm) of bottom LPL mussels and A) gape opening %, B) dissolved oxygen (DO; mg L^{-1}), C) salinity (psu), and D) temperature (ºC). Observations were averaged in 15-minute intervals from October 8, 2024, to May 9, 2025. Points are colored by individual mussel, and the black line represents the shared linear slope across all mussels. The repeated measures coefficient (r_{rm}), p-value, and slope are reported at the top of each graph.

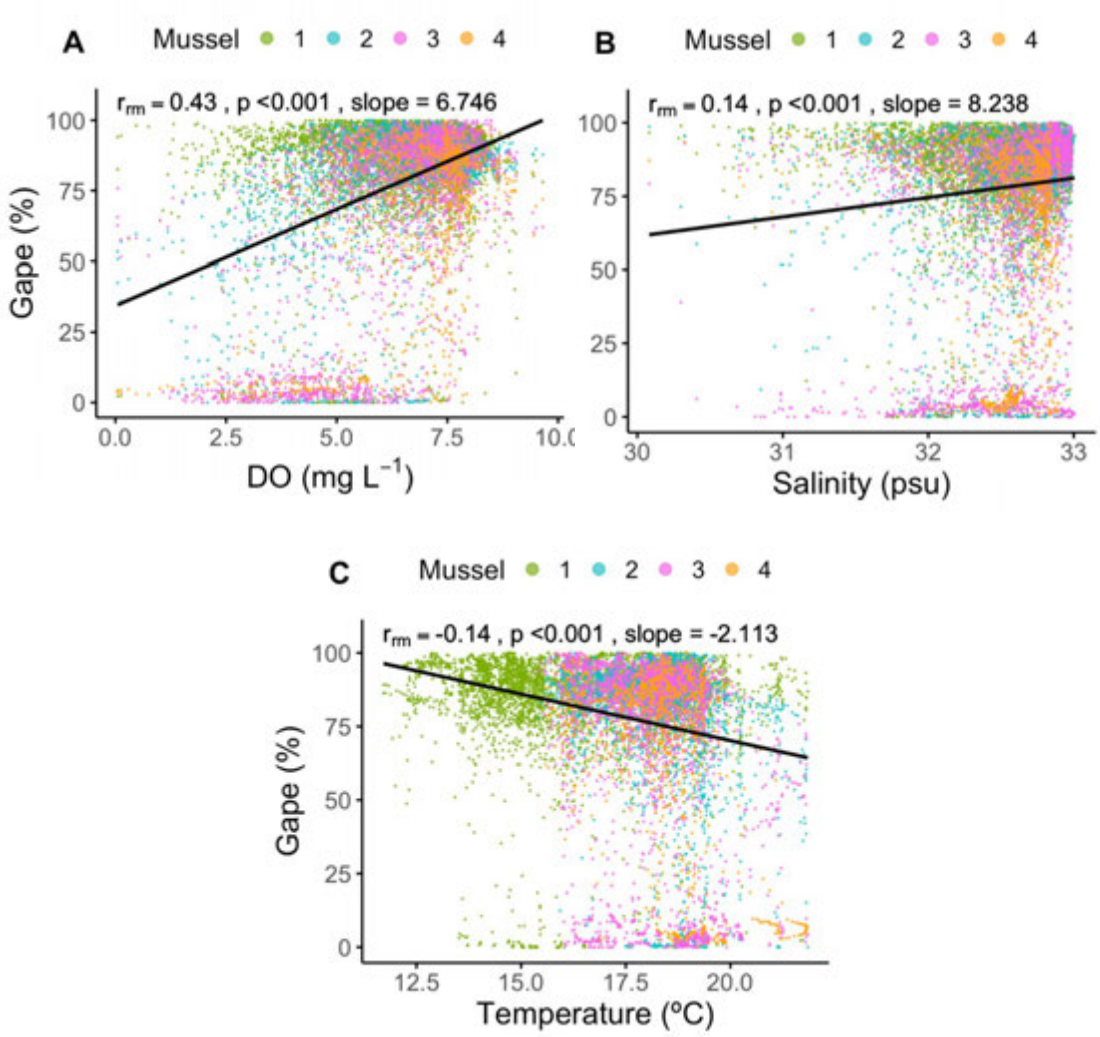

Figure 29. Repeated measures correlation between the gape % of bottom LPL mussels and A) dissolved oxygen (DO; mg L^{-1}), B) salinity (psu), and C) temperature (ºC). Observations were averaged in 15-minute intervals from October 8, 2024, to May 9, 2025. Points are colored by individual mussel, and the black line represents the shared linear slope across all mussels. The repeated measures coefficient (r_{rm}), p-value, and slope are reported at the top of each graph.

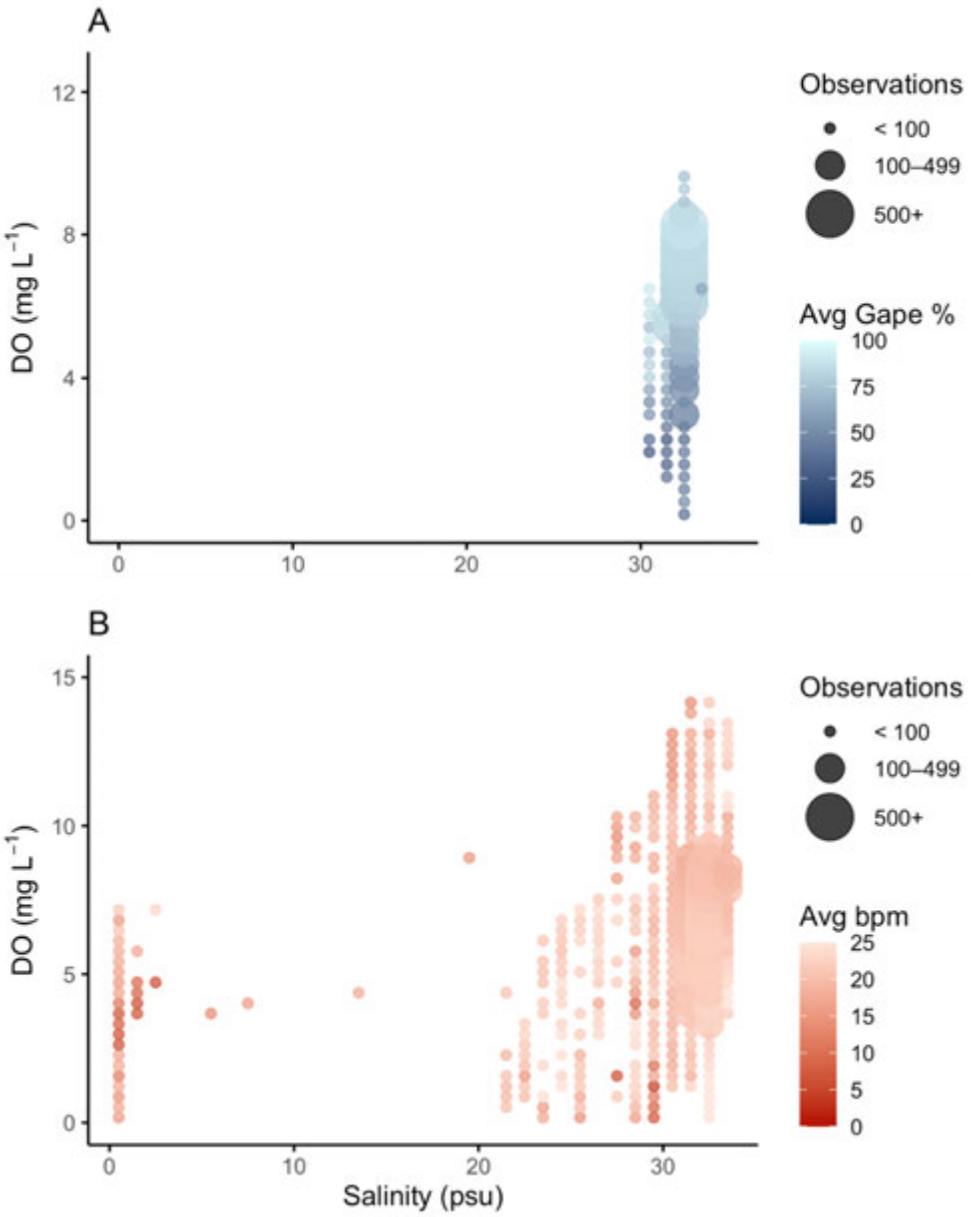

Figure 30. The relationship between salinity (psu), dissolved oxygen (DO; mg L^{-1}), and A) the average gape % across bottom mussels from LPL and B) the average heart rate (bpm) of bottom mussels from LPL. Observations were averaged in 15-minute intervals from October 8, 2024, to May 9, 2025. Each point represents aggregated observations at 1-unit increments of salinity and 0.35-unit increments of DO concentration. Point size corresponds to the number of observations in each bin, and point color reflects the average gape % or bpm.

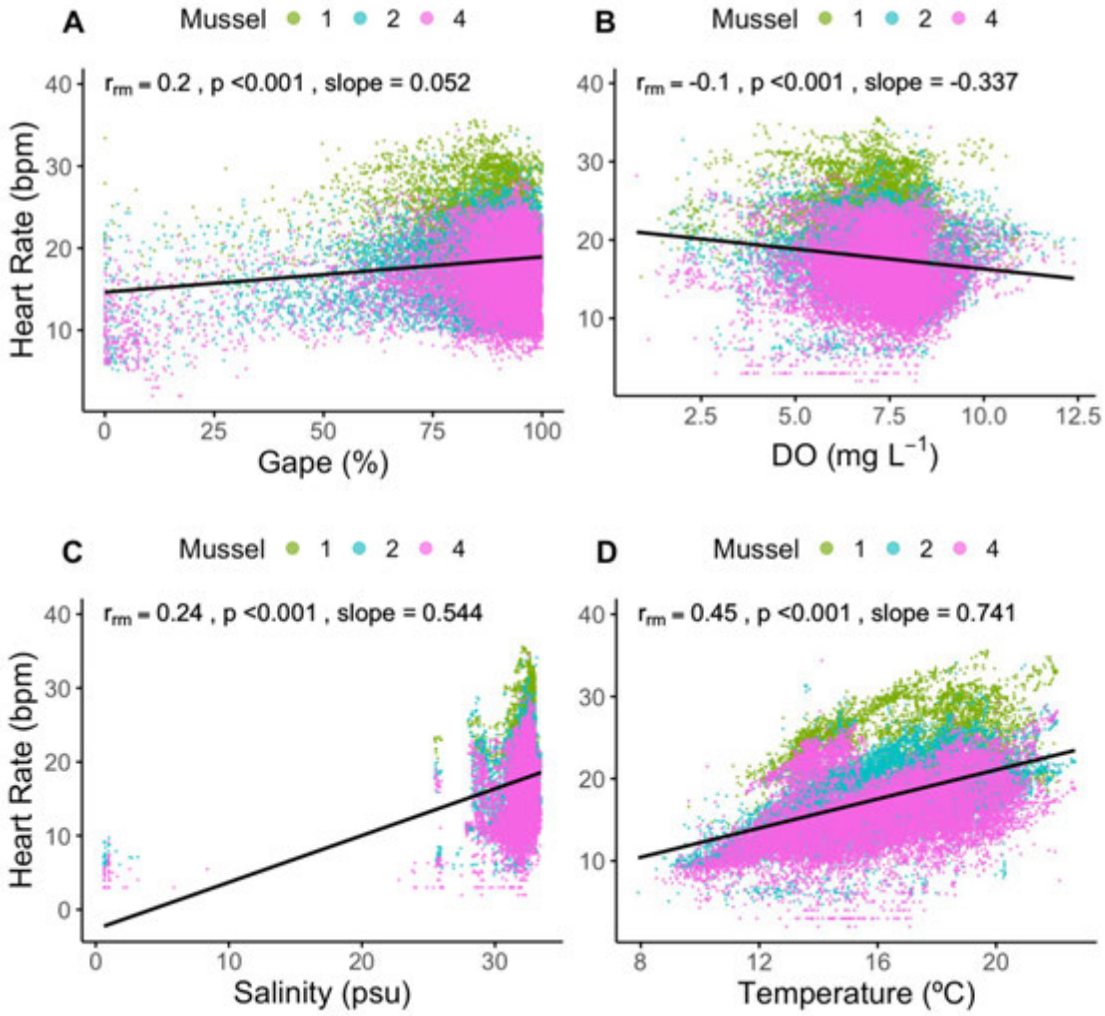

Figure 31. Repeated measures correlation between the heart rate (bpm) of surface LPL mussels and A) gape opening %, B) dissolved oxygen (DO; mg L^{-1}), C) salinity (psu), and D) temperature (ºC). Observations were averaged in 15-minute intervals from October 8, 2024, to May 9, 2025. Points are colored by individual mussel, and the black line represents the shared linear slope across all mussels. The repeated measures coefficient (r_{rm}), p-value, and slope are reported at the top of each graph.

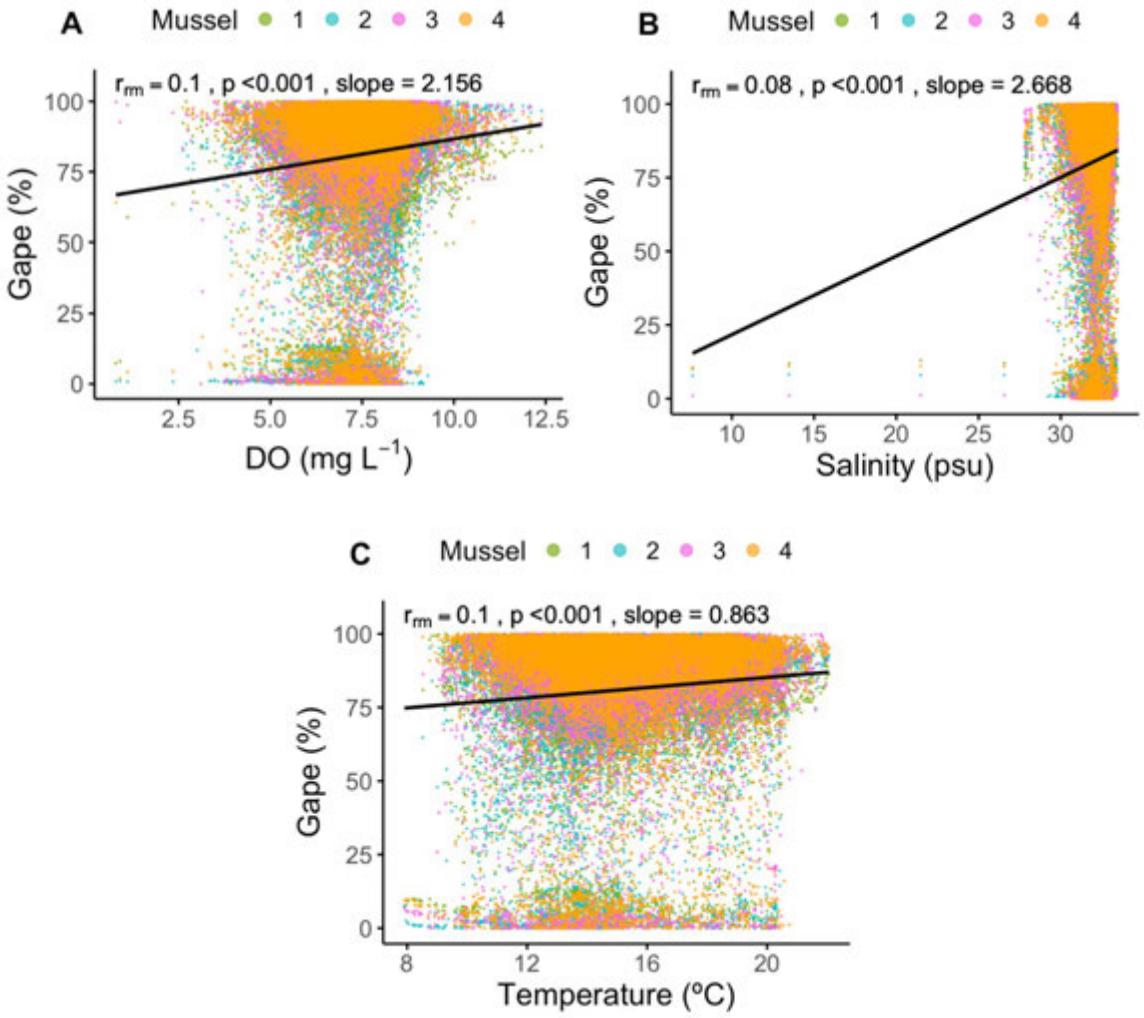

Figure 32. Repeated measures correlation between the gape % of surface LPL mussels and A) dissolved oxygen (DO; mg L^{-1}), B) salinity (psu), and C) temperature (°C). Observations were averaged in 15-minute intervals from October 8, 2024, to May 9, 2025. Points are colored by individual mussel, and the black line represents the shared linear slope across all mussels. The repeated measures coefficient (r_{rm}), p-value, and slope are reported at the top of each graph.

The pairwise correlations between surface mussel response and DO or salinity are further complemented by Figure 33A-B. Surface mussels at LPL did not experience the same range of conditions as those at the TRE, and mussel responses remained largely unaffected by those conditions—aside from a handful of low gape and low heart rate observations coinciding with lower DO and salinity.

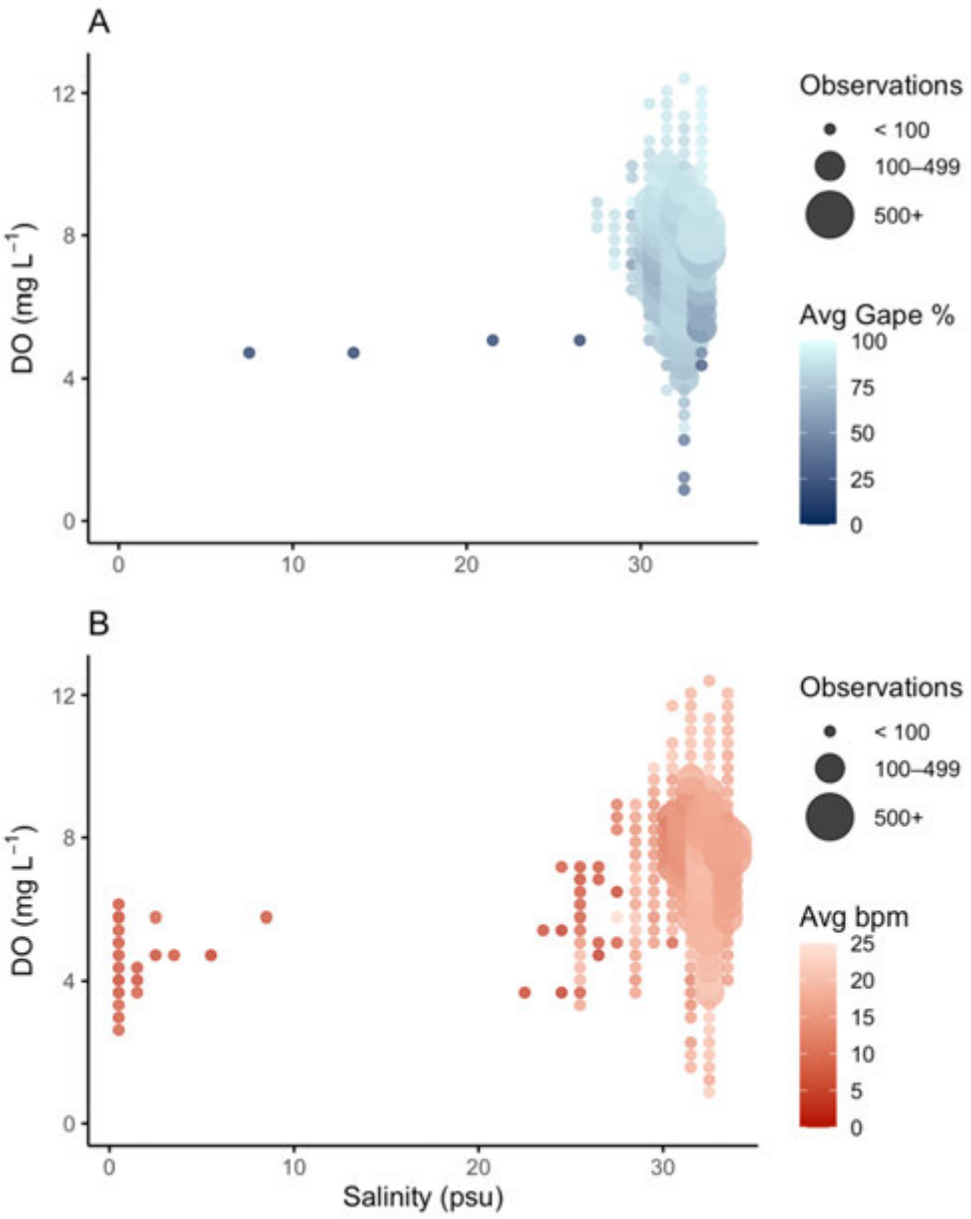

Figure 33. The relationship between salinity (psu), dissolved oxygen (DO; mg L^{-1}), and the A) average gape % across surface mussels from LPL and B) average heart rate (bpm) of surface mussels from LPL. Observations were averaged in 15-minute intervals from October 8, 2024, to May 9, 2025. Each point represents aggregated observations at 1-unit increments of salinity and 0.35-unit increments of DO concentration. Point size corresponds to the number of observations in each bin, and point color reflects the average gape % or bpm.

Generalized linear mixed effect models with a binomial error distribution revealed that for mussels near the benthos at LPL, DO ($\chi^2_{(1)} = 532$, $p < 0.001$), temperature ($\chi^2_{(1)} =$

38.7, $p < 0.001$), and turbidity ($\chi^2_{(1)} = 7.6$, $p = 0.006$) significantly influenced gape behavior, while salinity was not a significant predictor ($\chi^2_{(1)} = 0.32$, $p = 0.57$). The fixed effects explain 24.5% of the variance in gape state, and adding random effects explains 39.7%. DO also had a strong, positive effect on gaping behavior for mussels near the surface at LPL ($\chi^2_{(1)} = 545.3$, $p < 0.001$), followed by temperature ($\chi^2_{(1)} = 305.4$, $p < 0.001$), and salinity ($\chi^2_{(1)} = 57.8$, $p < 0.001$). Turbidity was not a significant predictor ($\chi^2_{(1)} = 2.8$, $p = 0.09$). The fixed effects explained 11.7% of the variance in gape state and 14.4% when accounting for both fixed and random effects.

San Diego Bay

Relative to the TRE and LPL, conditions fluctuated much less at SDB. Between May 8 and October 18, 2024, DO near the benthos averaged 6.8 mg L^{-1}, ranging from 4.7 to 9 mg L^{-1} (Figure 34C). Surface DO, measured from February 16 to December 19, 2024, showed a similar pattern, averaging 6.6 mg L^{-1} and ranging from 3 to 8.8 mg L^{-1} (Figure 35C). Due to the malfunctioning of the surface CTD, only bottom salinity was recorded between May and November 2024, typically fluctuating between 32 and 34 psu (Figure 34D; Figure 35D). However, a surface CTD deployed at this site the previous year (April to December 2023) recorded salinities from 30.8 to 33.9 psu, suggesting that surface salinity during our deployment was not substantially different. Temperatures near the benthos ranged from 17.5 to 25 °C and averaged 21.5 °C (Figure 34E). Temperatures at the surface ranged from 14.9 to 25 °C and averaged 19.6 °C (Figure 35E). Chlorophyll fluorescence was recorded from July to October 2024 near the benthos, averaging 5.7 µg L^{-1} and ranging from 0 to 122.3 µg L^{-1} (Figure 34F). At the surface, chlorophyll fluorescence was measured from July to November 2024, averaging 5.9 µg L^{-1} and ranging from 0 to 92 µg L^{-1} (Figure 35F). Zeros reflect values below the instrument's detection limit. Precipitation was generally low, peaking at 20.6 mm on January 22, 2024 (Figure 35H). Water levels fluctuated with the tides, ranging from -0.5 m to 2.4 m (Figure 34G; Figure 35G). Turbidity was not measured. Surface mussels grew at a rate of 0.02 mm/day, and bottom mussels grew at a rate of 0.03 mm/day throughout the deployment period (Table A1).

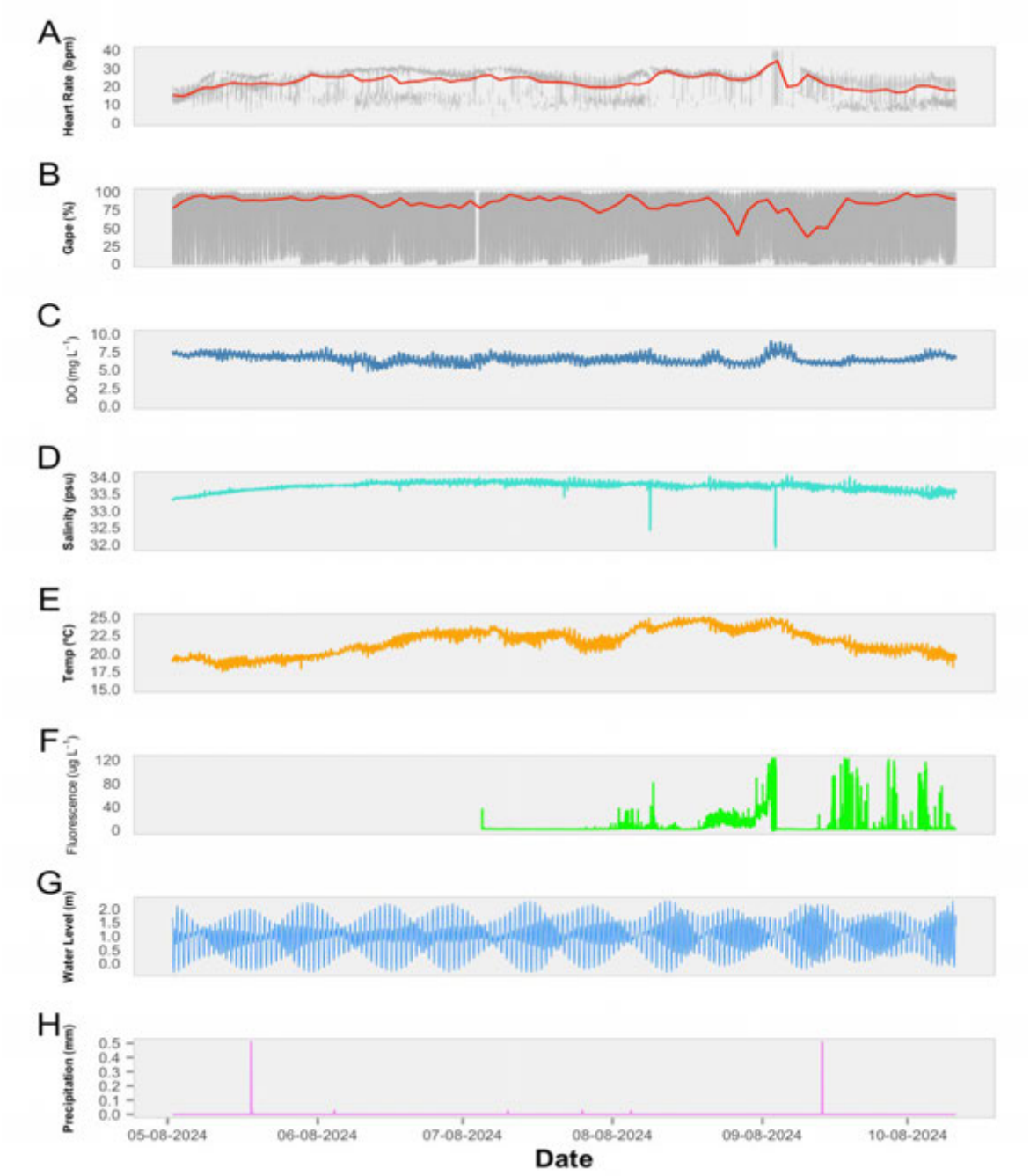

Figure 34. A) heart rate (bpm), B) gape opening %, C) dissolved oxygen (DO; mg L^{-1}), D) salinity (psu), E) temperature (ºC), F) fluorescence (ug L^{-1}), G) water level (m) and H) precipitation (mm) for bottom mussels at SDB between May 8 and October 18, 2024. Grey lines are raw gape and heart rate data for individual mussels. Red lines represent LOESS trend lines. DO and temperature data were retrieved from the bottom MiniDOT, and salinity data were retrieved from the bottom CTD. Chlorophyll data were retrieved from the bottom fluorometer. Water level data were retrieved from the NOAA tides and currents station in San Diego (ID: 9410170). Precipitation data were retrieved from the San Diego International Airport weather station (KSAN).

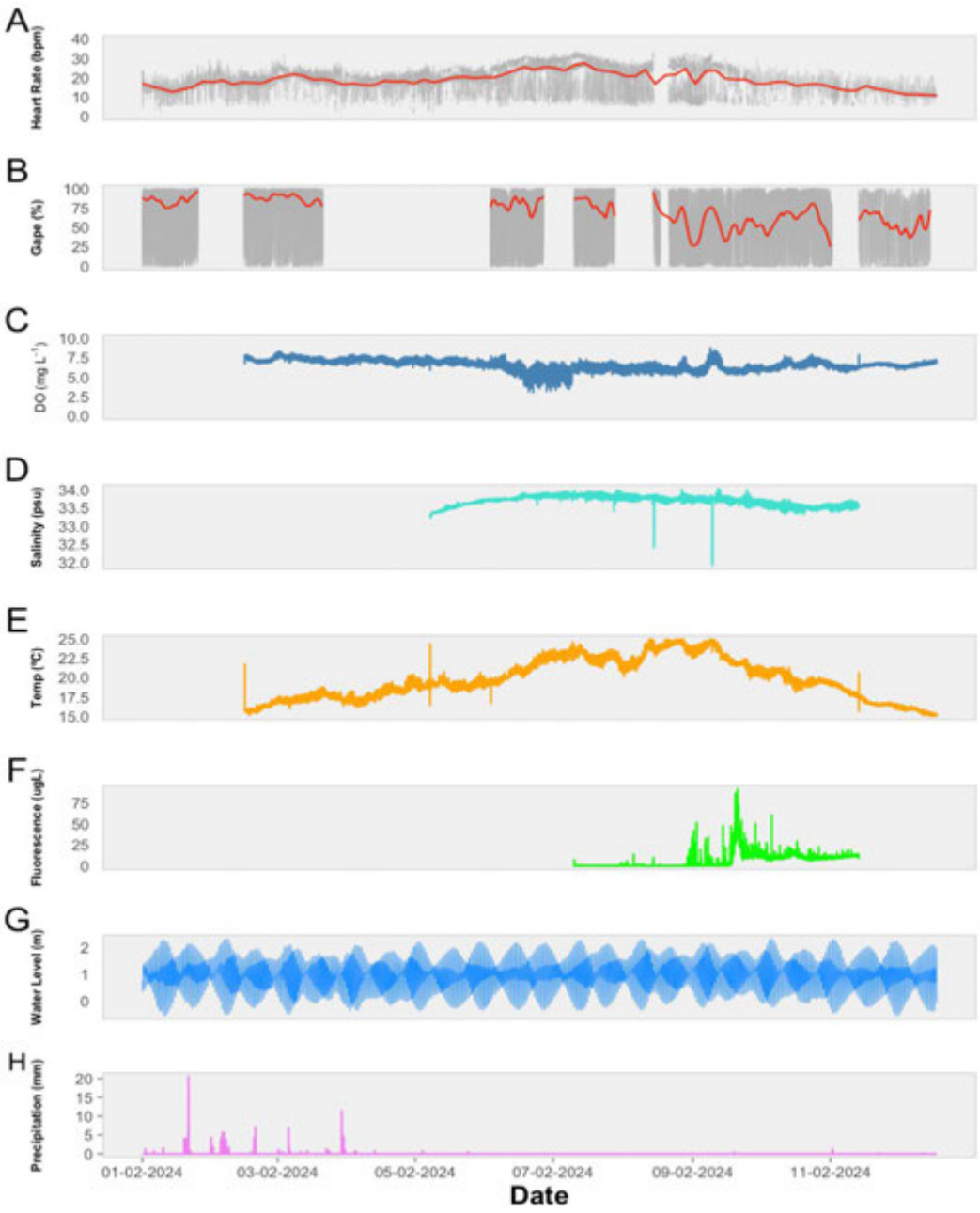

Figure 35. A) heart rate (bpm), B) gape opening %, C) dissolved oxygen (DO; mg L^{-1}), D) salinity (psu), E) temperature (ºC), F) fluorescence (ug L^{-1}), G) water level (m) and H) precipitation (mm) for surface mussels at SDB between January 2 and December 19, 2024. Grey lines are raw gape and heart rate data for individual mussels. Red lines represent LOESS trend lines. DO and temperature data were retrieved from the surface MiniDOT, while salinity data were retrieved from the bottom CTD due to a failed surface CTD. Chlorophyll data were retrieved from the surface fluorometer. Water level data were retrieved from the NOAA tides and currents station in San Diego (ID: 9410170). Precipitation data were retrieved from the San Diego International Airport weather station (KSAN).

For bottom mussels at SDB, repeated measures correlations with heart rate as the response variable revealed a moderately positive association with gape (Figure 36A, r_{rm} = 0.34, 95% CI [0.33, 0.36], slope = 0.07, $p < 0.001$), no association with DO (Figure 36B, r_{rm} = -0.005, 95% CI [-0.02, 0.01], slope = -0.04, p = 0.47), a moderate positive association with salinity (Figure 36C, r_{rm} = 0.3, 95% CI [0.28, 0.31], slope = 9.11, $p < 0.001$), and a moderate positive association with temperature (Figure 36D, r_{rm} = 0.29, 95% CI [0.27, 0.3], slope = 0.78, $p < 0.001$) within individuals. Using gape as the response variable revealed a moderate positive association with DO (Figure 37A, r_{rm} = 0.34, 95% CI [0.33, 0.34], slope = 16.28, $p < 0.001$), a negligible negative association with salinity (Figure 37B, r_{rm} = -0.08, 95% CI [-0.08, -0.07], slope = 15. 54, $p < 0.001$), and a weak negative association with temperature (Figure 37C, r_{rm} = -0.17, 95% CI [-0.18, -0.16], slope = -2.53, $p < 0.001$) within individuals. Due to the large number of observations (gape: $n > 60,000$; heart rate: $n > 21,000$), the interpretation focused on effect size and direction, as well as confidence intervals, rather than significance alone.

The pairwise correlations between bottom mussel response and DO or salinity are further complemented by Figure 38A-B. Bottom mussels at SDB experienced a very narrow range of conditions, and mussel responses remained largely unaffected.

For surface mussels at SDB, repeated measures correlations with heart rate as the response variable revealed a positive association with gape (Figure 39A, r_{rm} = 0.46, 95% CI [0.45, 0.47], slope = 0.1, $p < 0.001$), a weak negative association with DO (Figure 39B, r_{rm} = -0.2, 95% CI [-0.21, -0.19], slope = -1.95, $p < 0.001$), a positive association with salinity (Figure 39C, r_{rm} = 0.39, 95% CI [0.38, 0.4], slope = 19.5, $p < 0.001$), and a strong positive association with temperature (Figure 39D, r_{rm} = 0.53, 95% CI [0.52, 0.54], slope = 1.24, $p < 0.001$) within individuals. Using gape as the response variable revealed a positive association with DO (Figure 40A, r_{rm} = 0.27, 95% CI [0.27, 0.28], slope = 13.76, $p < 0.001$), a negligible positive association with salinity (Figure 40B, r_{rm} = 0.04, 95% CI [0.03, 0.06], slope = 12.21, $p < 0.001$), and a negligible negative association with temperature (Figure 40C, r_{rm} = -0.07, 95% CI [-0.08, -0.06], slope = -0.88, $p < 0.001$) within individuals. Due to the large number of overall observations (gape: $n > 42,000$; heart rate: $n > 37,000$), interpretation was focused on effect size/direction and confidence intervals rather than significance alone.

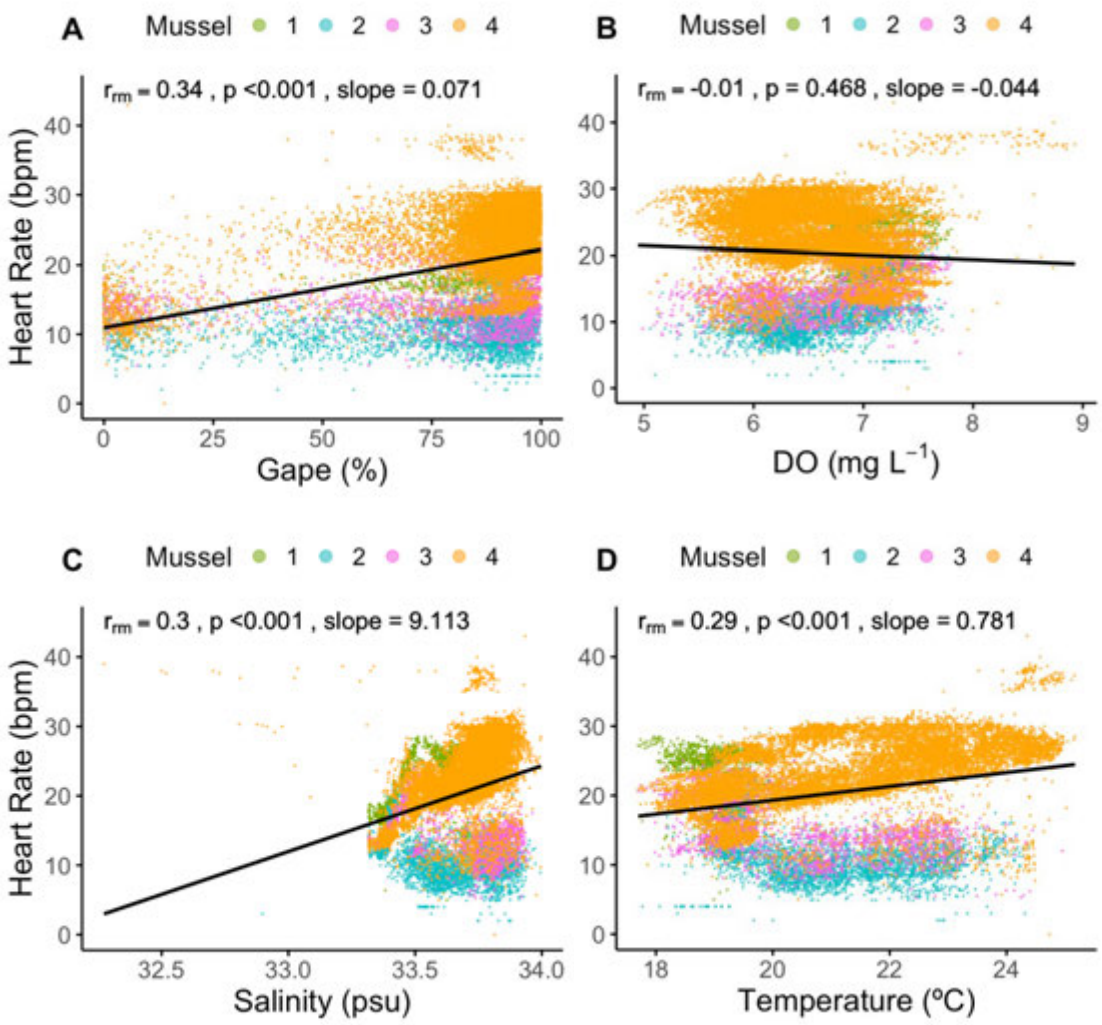

Figure 36. Repeated measures correlation between the heart rate (bpm) of bottom SDB mussels and A) gape opening %, B) dissolved oxygen (DO; mg L^{-1}), C) salinity (psu), and D) temperature (ºC). Observations were averaged in 15-minute intervals from May 8 to October 18, 2024. Points are colored by individual mussel, and the black line represents the shared linear slope across all mussels. The repeated measures coefficient (r_{rm}), p-value, and slope are reported at the top of each graph.

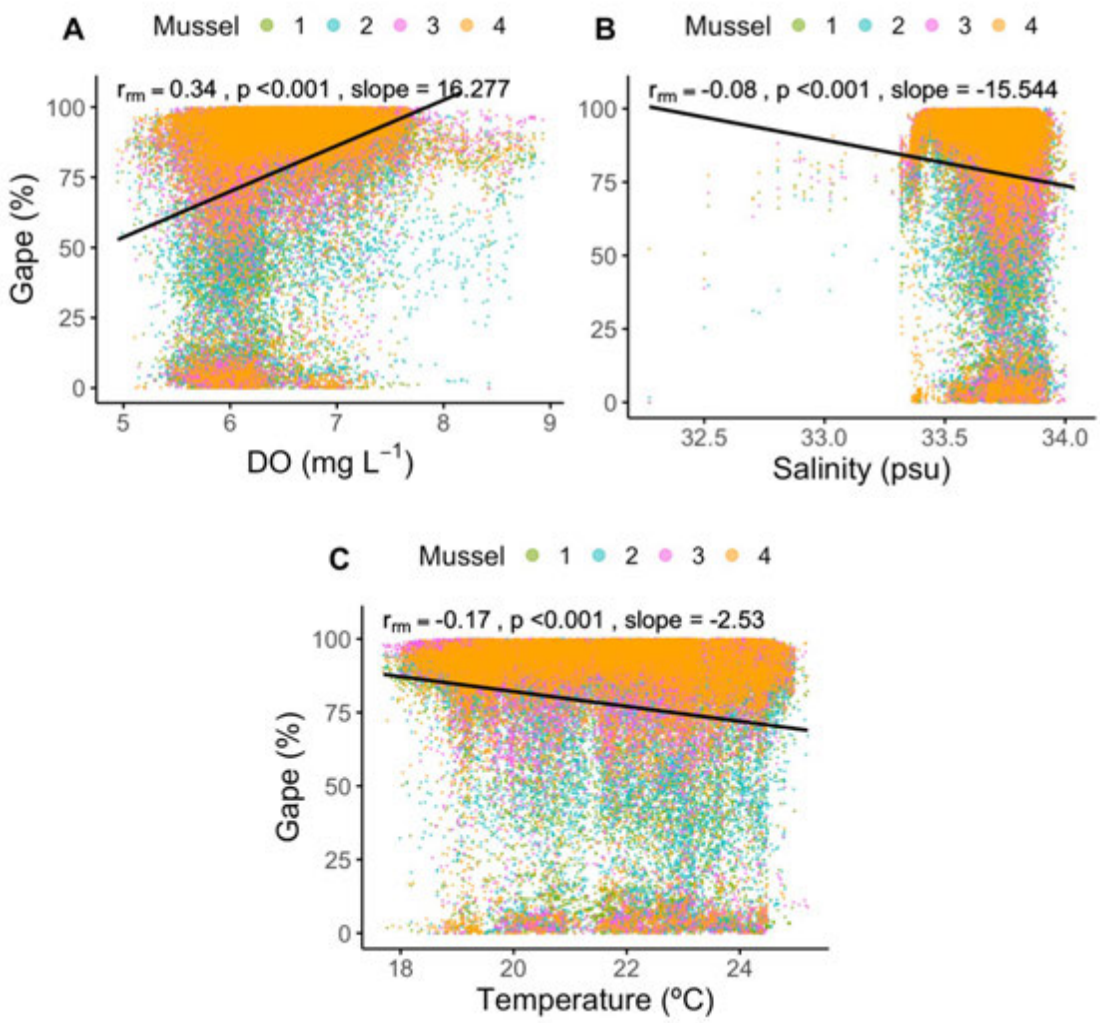

Figure 37. Repeated measures correlation between the gape % of bottom SDB mussels and A) dissolved oxygen (DO; mg L^{-1}), B) salinity (psu), and C) temperature (°C). Observations were averaged in 15-minute intervals from May 8 to October 18, 2024. Points are colored by individual mussel, and the black line represents the shared linear slope across all mussels. The repeated measures coefficient (r_{rm}), p-value, and slope are reported at the top of each graph.

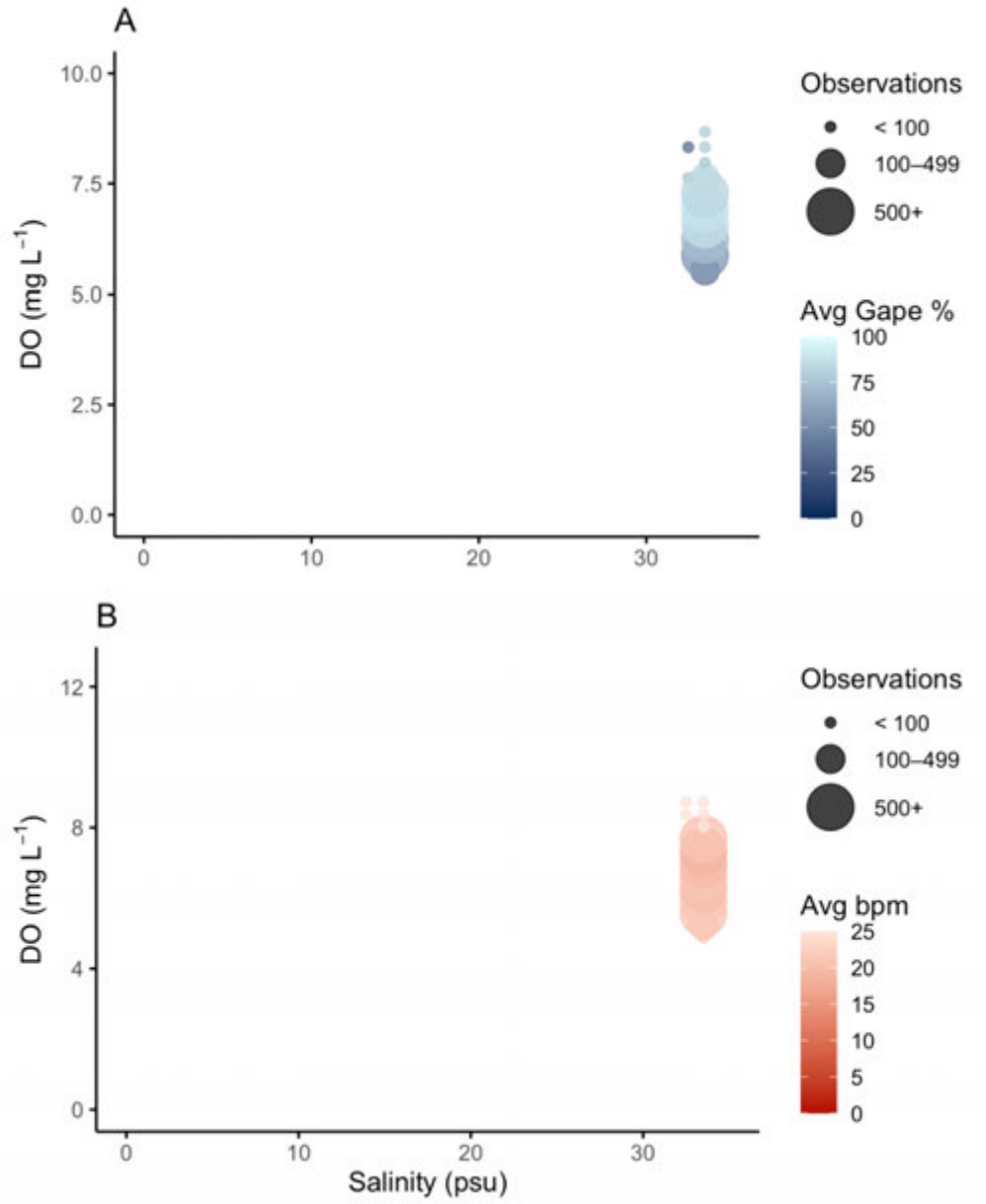

Figure 38. The relationship between salinity (psu), dissolved oxygen (DO; mg L^{-1}), and the A) average gape % across bottom mussels from SDB and B) average heart rate (bpm) of bottom mussels from SDB. Observations were averaged in 15-minute intervals from May 8 to October 18, 2024. Each point represents aggregated observations at 1-unit increments of salinity and 0.35-unit increments of DO concentration. Point size corresponds to the number of observations in each bin, and point color reflects the average gape % or bpm.

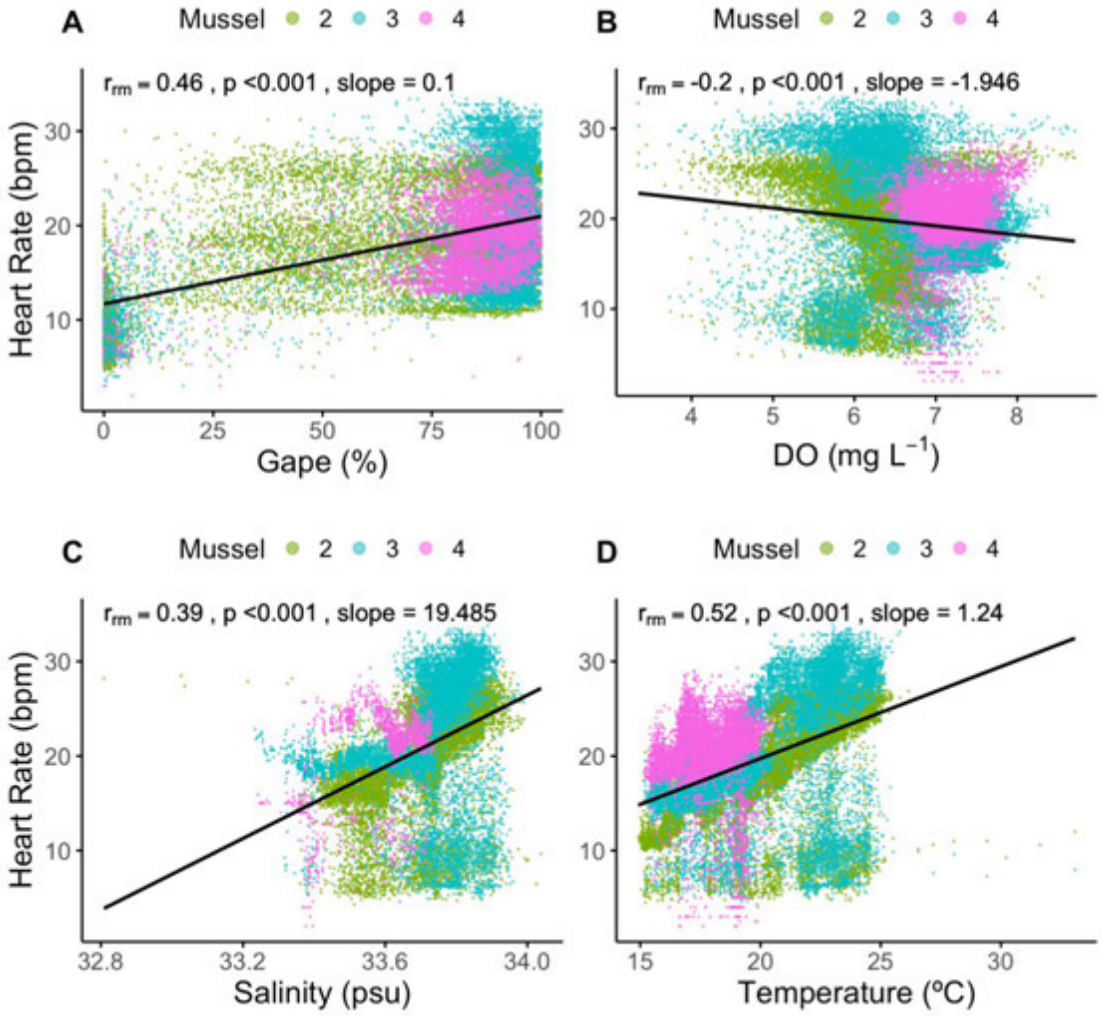

Figure 39. Repeated measures correlation between the heart rate (bpm) of surface SDB mussels and A) gape opening %, B) dissolved oxygen (DO; mg L^{-1}), C) salinity (psu), and D) temperature (ºC). Observations were averaged in 15-minute intervals from May 8 to December 19, 2024. Points are colored by individual mussel, and the black line represents the shared linear slope across all mussels. The repeated measures coefficient (r_{rm}), p-value, and slope are reported at the top of each graph.

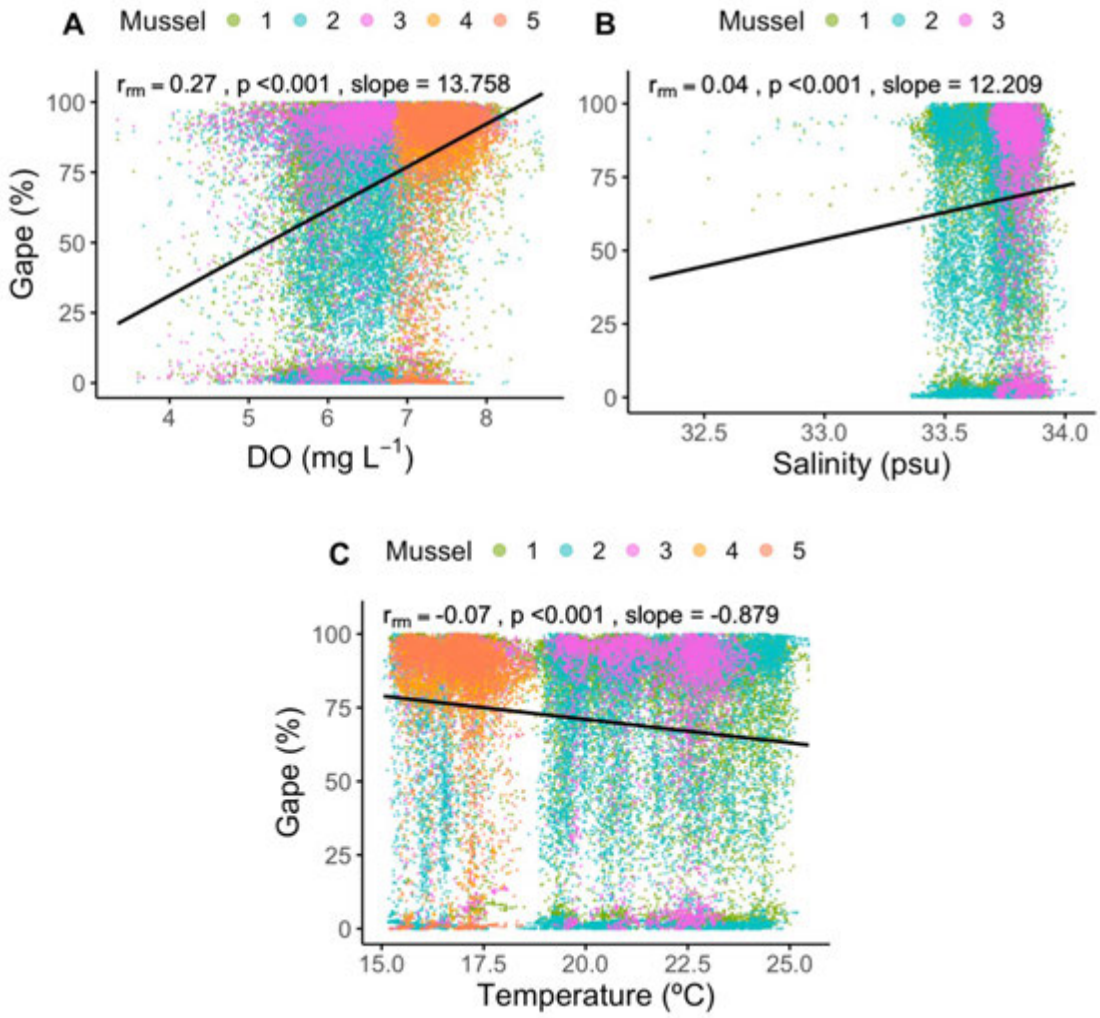

Figure 40. Repeated measures correlation between the gape % of surface SDB mussels and A) dissolved oxygen (DO; mg L^{-1}), B) salinity (psu), and C) temperature (ºC). Observations were averaged in 15-minute intervals from May 8 to December 19, 2024. Points are colored by individual mussel, and the black line represents the shared linear slope across all mussels. The repeated measures coefficient (r_{rm}), p-value, and slope are reported at the top of each graph.

The pairwise correlations between surface mussel response and DO or salinity are further complemented by Figure 41A-B. Surface mussels at SDB experienced a very narrow range of conditions, and mussel responses remained largely unaffected.

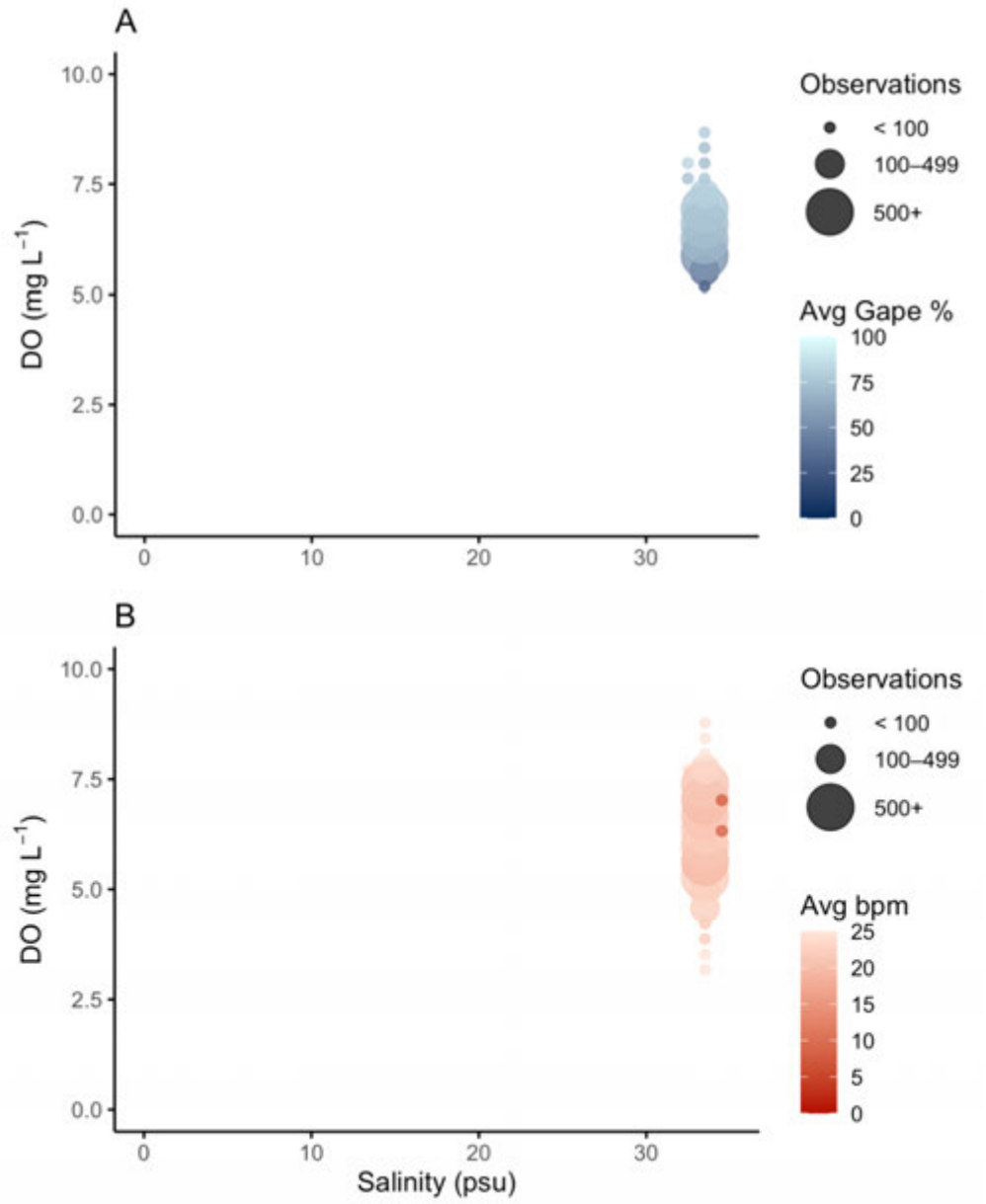

Figure 41. The relationship between salinity (psu), dissolved oxygen (DO; mg L^{-1}), and the A) average gape % surface mussels from SDB and B) average heart rate (bpm) of surface mussels from SDB. Observations were averaged in 15-minute intervals from May 8 to December 19, 2024. Each point represents aggregated observations at 1-unit increments of salinity and 0.35-unit increments of DO concentration. Point size corresponds to the number of observations in each bin, and point color reflects the average gape % or bpm. Salinity data were taken from the bottom CTD sensor due to a failed surface sensor and are therefore only an estimate of surface salinity.

For mussels near the benthos at SDB, generalized linear mixed effect models with a binomial error distribution revealed that gape behavior was strongly influenced by DO ($\chi^2_{(1)} =$

360.3, $p < 0.001$), followed by salinity ($\chi^2_{(1)} = 29.7$, $p < 0.001$) and chlorophyll fluorescence ($\chi^2_{(1)} = 6.2$, $p = 0.01$). Temperature ($\chi^2_{(1)} = 1.05$, $p = 0.3$) was not a significant predictor. The model explained 35.7% of the variance through fixed effects and 40% when accounting for both fixed and random effects. All predictors of gape behavior were significant for mussels at the surface of SDB, with DO having the strongest effect ($\chi^2_{(1)} = 393.1$, $p < 0.001$), followed by temperature ($\chi^2_{(1)} = 53.7$, $p < 0.001$), salinity ($\chi^2_{(1)} = 26.7$, $p < 0.001$), and chlorophyll fluorescence ($\chi^2_{(1)} = 10.4$, $p = 0.001$). The model explained 33.3% of the variance through fixed effects, and 40.5% of the total variance when also accounting for random effects.

DISCUSSION

The goal of my study was to provide insight into the physiological and behavioral responses of mussels to hypoxia and low salinity stress in both controlled laboratory settings and in the field in order to inform ongoing monitoring efforts using bivalve biosentinels in San Diego estuaries. Both heart rate and valve gaping responses differed for mussels exposed to hypoxia or low salinity compared to mussels maintained in unmanipulated seawater. However, there were minimal differences among mussels collected from the three estuary locations. In the field, variation in mussel response was closely tied to environmental conditions at each deployment site. The results of my study can help guide the interpretation of biosensor data and support estuary management in the San Diego region.

HYPOXIA EXPOSURE IMPACTS GAPING BEHAVIOR

During the lab trials, *M. galloprovincialis* individuals did not differ in gaping behavior between the treatment groups across the three trial phases, although mussels exposed to aqueous hypoxia trended toward increased gaping behavior during the Recovery phase (Figure 4). The lack of difference is likely due to the gradual closure of the normoxia mussels as the trial progressed. This behavior is primarily driven by the disproportionate closure of SDB normoxia mussels compared to LPL and TRE normoxia mussels (Figure 5B). Gurr et al. (2021) ran into a similar issue and concluded that initial handling stress and decreased food availability may be to blame. Although the mussels were fed a shellfish diet throughout the trial, it is possible that the flow of seawater through the individual containers was washing the food away, resulting in a decreased feeding rate—and thus an increased valve closure rate—as the trials progressed.

Despite the decline in performance of the SDB normoxia mussels throughout the trials, a lack of similar response in the hypoxia mussels indicates sensitivity to low DO conditions (Gurr et al., 2021). Furthermore, a treatment effect was still observed in the hypoxia mussels. For the individuals in the hypoxia treatment group, the proportion of open

valves decreased during the Treatment phase (Figure 4). However, the mussels still exhibited valve activity—unlike mussels exposed to aerial hypoxia (Altieri, 2006). Continued valve activity under aqueous hypoxia has also been observed for other bivalves such as the blue mussel *M. edulis*, the bay scallop *Argopecten irradians*, and the hard clam *Mercenaria mercenaria* (Peterson et al., 2025; Stevens and Gobler, 2018). Unfortunately, due to continuous, non-synchronous valve activity, a threshold value of DO or a time point at which *M. galloprovincialis* individuals from San Diego estuaries simultaneously close or open their valves could not be determined. Peterson et al. (2025) observed that a portion of *M. edulis* individuals exhibited open valves for the first 55 minutes of exposure to <1.0 mg L^{-1}, after which they completely closed their valves. However, similar to my study, other individuals did not show the same response, indicating substantial variability at the individual level.

DO levels never dropped below 1.0 mg L^{-1} during the trials. Since the manipulated seawater was hypoxic and not anoxic (0 mg L^{-1}), valve opening may have been an attempt to filter any available oxygen out of the water column (Peterson et al., 2025). Gaping activity increased immediately following the return to normoxic conditions (Figure 6A). This is consistent with other studies that have exposed bivalves to hypoxia, although those studies only expose bivalves to diel-cycling hypoxia (Porter and Beritburg, 2016; Porter and Porter, 2018). Hypoxic and anoxic conditions in urban estuaries are increasing in severity and frequency. This is especially evident at the TRE, where anoxic conditions can occur for a day or more (Figure 19C; Figure 20B). It is therefore crucial to understand how mussel physiology and behavior change over time during prolonged exposure to hypoxia.

HYPOXIA EXPOSURE INCREASES HEART RATE VARIABILITY

The average heart rate of *M. galloprovincialis* individuals only differed between hypoxia and normoxia mussels during the Recovery phase, where the average heart rate for hypoxia mussels was higher than normoxia mussels (Figure 8A). However, this is likely a result of the steady decline in average heart rate for normoxia mussels throughout the trials, as the average heart rate for hypoxia mussels did not change over time (Figure 8A). Further analysis revealed that the average heart rate was not capturing the true changes in cardiac activity during hypoxia exposure. Since heart rate variability is a proxy for physiological

performance, calculating the coefficient of variation (CV) in heart rate allows for the analysis of how heart rate variability—and thus performance—changes over time. The CV in heart rate was higher during exposure to hypoxia compared to the other trial phases and compared to the normoxia treatment group during the Treatment phase (Figure 8B). The heart rate of the hypoxia mussels during treatment fluctuated between 0 and 34 bpm. In comparison, normal fluctuations typically range between 5 and 20 bpm (Figure 7). These fluctuations align with observed "burst activity" interspersed with bradycardia during exposure to aqueous hypoxia in the blue mussel *M. edulis* and the subtropical mussel *Perna viridis* (Nicholson, 2002; Peterson et al., 2025). Periodically increasing heart rate may be a compensatory response to quickly redistribute hemolymph and maintain tissue oxygen perfusion during hypoxic conditions (Nicholson, 2002; Reiber and McMahon, 1998). CV then significantly decreased for hypoxia mussels during the Recovery phase compared to both normoxia mussels in the Recovery phase and hypoxia mussels in the Treatment phase (Figure 8B). This is likely because hypoxia mussels were sustaining higher average heart rates during this time in order to recover from oxygen debt (Figure 8A).

Heart rate appeared to fluctuate more across the board during the hypoxia trials than during the low salinity trials (Figure 7). This variability may have been influenced by several factors, most notably sensor placement, which was likely less precise in the hypoxia trials than in the subsequent salinity trials. As a result, the algorithms may have struggled to consistently detect heartbeats, leading to more measurements being categorized as "NA". This could have resulted in a reduced number of valid observations and, consequently, greater variability in the data. Individual variation in heart rate may have also introduced some noise. Nevertheless, the effect of hypoxia on mussel heart rate remains distinguishable from that of the control group.

LOW SALINITY EXPOSURE IMPACTS GAPING BEHAVIOR

Low salinity exposure appeared to have an even more pronounced impact on valve gaping behavior than hypoxia. The proportion of open valves for mussels exposed to low salinity was reduced to nearly 0% during treatment (Figure 12). This is a protective response that isolates the mantle cavity and maintains hemolymph ion composition (Davenport, 1979; Shumway, 1977). This response was evident even with the steady decline of gaping behavior

observed in the control mussels. Unlike the hypoxia trials, the driver of this decline in control mussel gaping activity came from mussels from the TRE (Figure 13B). Similar to the hypoxia trials, this result could have been due to handling stress or low food availability. The overwhelming response to low salinity was expected, as very low salinity levels negatively impact performance metrics (Addis et al., 2021; Andrews et al., 1959; Braby and Somero, 2006; Shurova, 2001). However, the timing of valve closure was unexpected. Nearly all mussels closed fully at the very beginning of the decline in salinity (Figure 14A), before salinity reached stressful levels. This premature closure is likely a result of human interference. The containers used in the trials were small, and frequently submerging the YSI to take water quality measurements likely disturbed the mussels, causing them to close. Because of this, I was unable to decipher the osmotic threshold at which *M. galloprovincialis* individuals from San Diego estuaries close their valves. In the absence of human interference, I would have expected valves to close at ~20 psu (Addis et al., 2021). However, it is possible that valve-closure could occur at even lower salinities. Vasquez et al. (2022) found that *M. galloprovincialis* individuals from the Marina del Rey harbor in Los Angeles, CA, increased their metabolic rates at 20 psu, which is lower than other studies that found similar metabolic increases at 29.8 psu (Lockwood and Somero, 2011; Tomanek et al., 2012). Vasquez et al. (2022) proposed that the lower threshold may be due to the more frequent and intense fluctuations in salinity that can occur at the study site due to urban runoff. Since SDB, LPL, and the TRE are also prone to freshwater influxes from urban runoff after rain events, the mussels collected from those sites could similarly be more tolerant of salinity shifts and thus have a lower osmotic stress threshold.

LOW SALINITY EXPOSURE DECREASES AVERAGE HEART RATE AND INCREASES HEART RATE VARIABILITY

The average heart rate of mussels exposed to low salinity declined during the Treatment phase and spiked during the Recovery phase (Figure 15A; Figure 16A). This was coupled with a substantial increase in the CV of low salinity mussels during the Treatment phase compared to the Acclimation and Recovery phases as well as compared to the CV of the control salinity mussels during the Treatment phase (Figure 16B). The larger heart rate CV during the low salinity Treatment phase is driven in large part by the sharp decline in

heart rate that occurs during the initial decline in salinity (Figure 15A), followed by a more consistent period of (low) heart rate during the remainder of the low salinity period (Figure 15A; Figure 16A). Removing observations from the start of the Treatment period in the low salinity group prior to the sharp decline in heart rate lowered the average CV from 55% to 32%, bringing that value closer to the CV of the control mussels during the Treatment phase (21%) and closer to the average CV during the Recovery phase of both control and low salinity mussels (34% and 29% respectively). The sustained lower heart rate and low CV during the bulk of the low salinity Treatment period is unsurprising when coupled with complete valve closure over the same timeframe (Figure 14A). The delayed response in heart rate at the onset of treatment is a common observation when exposing bivalves to prolonged stress. When exposing *M. edulis* individuals to high levels of copper, Curtis et al. (2000) found that mussels only began to exhibit abnormal heart rate responses 2-3 hours after initial exposure. In my study, mussels took an average of 7 hours to decrease and sustain low heart rates. Therefore, short-term exposure to stress is unlikely to result in substantial changes to physiological response. As climate change and human impacts continue to increase the frequency, severity, and duration of stressful events, understanding physiological responses to long-term stress is crucial for developing appropriate monitoring efforts.

INDUCED STRESS CAUSES A SWITCH FROM AEROBIC TO ANAEROBIC METABOLISM

Upon aerial exposure, mussels living in the intertidal zone close their valves and are able to quickly switch from aerobic metabolism to anaerobic metabolism. This mechanism is also frequently used when mussels detect issues with the water in which they are submerged, such as during times of increased thermal stress (Tomanek and Zuzow, 2010). Since closed valves are often accompanied by decreased heart rates, both measurements can be a good indication that anaerobic metabolism has been initiated. Anaerobic metabolism utilizes existing stores of glycogen to produce succinate and alanine for energy use (Isani et al., 1995). Mussels can benefit from switching to anaerobic respiration in the short term; however, long-term exposure can lead to decreases in growth, energy storage, and reproduction (Sokolova et al., 2012). I found that exposure to low salinity (< 3 psu) caused mussels to close for nearly the entire 3 days of treatment (Figure 14A), indicating that they

likely performed anaerobic metabolism during that time. Immediately following the initial decline in salinity, there was a small spike in average heart rate (Figure 15A), which may indicate an attempt to briefly continue aerobic respiration while the valves are closed (Brand and Roberts, 1973). After aerobic respiration is no longer feasible, heart rate drops, and anaerobic metabolism kicks in. No mortality was observed during the experiments, suggesting that mussels can sustain anaerobic respiration for extended periods of low salinity. In contrast to the low salinity mussels, the mussels exposed to hypoxia (≤ 3.0 mg L^{-1}) continued to open throughout the hypoxic treatment period (Figure 6A). Since aerobic metabolism is nearly 18 times more efficient than anaerobic metabolism in mussels (Gosling, 2008), the continued gaping behavior and resulting cardiac burst activity (Figure 7A) may have allowed for partial aerobic metabolism even in low oxygen conditions (Gurr et al., 2021; Nicholson, 2002).

The timing of the experiments may have also contributed to the mussels exposed to low salinity closing and performing anaerobic metabolism more readily. The hypoxia trials were conducted during summer and fall, while the low salinity trials were conducted during fall and winter. Bivalves store extra glycogen in their tissues during the fall and winter to compensate for the lower food availability during the winter (Davis et al., 2023). If the mussels I used had stored extra glycogen before the low salinity trials, they may have been better prepared to perform sustained anaerobic metabolism than the mussels in the hypoxia trials. Furthermore, increased glycogen storage coincides with the rainy season in San Diego, when low-salinity events are more common, meaning mussels are physiologically more primed to withstand multi-day valve closure during this period. Future studies should replicate these treatments across seasons to disentangle the role of glycogen storage in shaping responses.

HEART RATE SPIKES AT THE ONSET OF THE RECOVERY PHASE

Regardless of stressor type, all mussels exhibited the same response of brief, intense cardiac activity immediately following the alleviation of stress (Figure 7A; Figure 15A). Since the mussels exposed to stress were likely undergoing anaerobic metabolism during treatment—either due to prolonged valve closure or lack of oxygen in the water—a return to

control conditions allows for the mussels to switch back to aerobic metabolism. Once the mussels open back up, the spike in heart rate signifies an attempt to reduce oxygen debt and reestablish a normal physiological status (Bakhmet et al., 2005). Additionally, the lower intestine of *M. galloprovincialis* passes through the heart, and in related mussel species, it has been speculated that reduced heart rate may lead to an accumulation of waste in the intestine, which may then be evacuated by the sudden tachycardia that occurs during shell re-opening (Nicholson, 2002). Brief, intense heart rates may play a role in eliminating waste once stressful conditions are removed. Shortly after the spike, heart rates steadily declined back to normal levels. This response is evident even when mussels have been exposed to continuous low salinity for upwards of 7 days (Bakhmet et al., 2005), although periods of low salinity in the field typically last only 1-3 days.

MUSSEL RESPONSES DURING LAB EXPERIMENTS WERE LARGELY CONSISTENT ACROSS LOCATIONS

Contrary to expectations, mussels collected from the three different locations (LPL, SDB, and TRE) and exposed to hypoxia or low salinity did not have differing gaping behavior (Figure 5A; Figure 13A) or average heart rates (Figure 9A; Figure 17A) during the treatment phase. This likely reflects the fact that *M. galloprovincialis* has a multi-week pelagic larval stage that facilitates high levels of gene flow along the San Diego coastline for upwards of 30 km (Becker et al., 2007). As a result, populations across these estuaries are probably well-mixed, limiting the potential for local adaptation or strong site-specific selection.

For the hypoxia trials, the only difference among the locations was a higher average CV in heart rate for hypoxia mussels from SDB relative to those from the TRE during treatment (Figure 10A). Many studies have linked historic exposure to hypoxia to higher physiological performance during subsequent exposures (Altieri, 2006; Davis et al., 2023; Gurr et al., 2021; Meng et al., 2018). Given this trend, it might be expected that mussels from the TRE—an estuary that experiences more frequent hypoxic events—would perform better than mussels from SDB when exposed to hypoxia in controlled laboratory conditions.

In contrast, for the salinity trials, a slightly higher average CV in heart rate for hypoxia mussels from the TRE relative to those from LPL during treatment was the only

difference among the locations (Figure 18A). In any case, the minimal presence of differences suggests that even if *M. galloprovincialis* individuals grow in estuaries that have different stress regimes, their cardiac and gape responses will still be quite similar under controlled laboratory stress simulations—at least for severe hypoxia and low salinity. More moderate stress levels may reveal subtle differences in stress response that could have been hidden by the nearly ubiquitous response to severe stress. For example, Hamer et al. (2008) found that *M. galloprovincialis* individuals acclimated for 14 days under salinity levels of either 28 or 18 psu increased oxygen consumption by up to 65% during similar salinity conditions compared to mussels that had not been acclimated. Since salinity levels during my experiments were as low as 3 psu, it is likely that the subtle differences in stress response among mussels from different locations were obscured.

DIVERGENCE IN MUSSEL RESPONSES IN THE FIELD

Biosentinel mussels deployed in the three estuaries experienced a range of environmental conditions. The heart rate and valve-gaping measurements collected throughout the deployment periods provide insight into how mussels respond to both baseline and stressful conditions.

San Diego Bay

Biosentinel mussels at the surface of SDB were deployed the longest, capturing nearly a full year of environmental conditions and physiological response data (Figure 35). In combination with the bottom mussels that collected data from May 8 to October 18, 2024 (Figure 34), SDB biosentinels offer a valuable reference point for mussel response to relatively benign conditions. Throughout the deployment period, neither DO nor salinity levels deviated to the extent that they were considered stressful (Addis et al., 2021; Vaquer-Sunyer and Duarte, 2008). There was a gradual rise in temperature in the summer months, but the overall range of temperatures was also not considered stressful (Lockwood and Somero, 2011). Chlorophyll *a* fluorescence began to be measured on July 11, 2024, and had only a minimal influence on mussel responses.

For mussels at the surface of SDB, gape was the most positively associated with DO (Figure 40A), while heart rate was more positively associated with salinity and temperature

(Figure 39C-D). For mussels near the benthos, DO remained the most positively associated with gape (Figure 37A), while salinity showed the strongest positive association with heart rate (Figure 36C). DO was the strongest predictor of gape behavior at both depths. The association between DO and gape behavior may reflect the natural coupling of environmental and physiological rhythms under non-stressful conditions. In estuaries, DO commonly fluctuates on a diel cycle, rising during daylight hours due to photosynthetic activity and declining at night with respiration (D'Avanzo and Kremer, 1994). Mussels, in turn, may exhibit circadian patterns of gaping that align with oxygen availability (Ameyaw-Akumfi and Naylor, 1987; Comeau et al., 2018). In the context of SDB's small fluctuations in DO, the observed relationship between DO and gape is likely not a stress-driven response but instead a reflection of synchronized cycles in environmental conditions and behavioral activity.

Furthermore, across both depths, gape and heart rate were only moderately correlated (Figure 36A; Figure 39A), suggesting a degree of physiological decoupling. This decoupling is also likely due to the relatively benign environmental conditions. In the absence of acute stressors, the observed significant relationships may reflect subtle, non-stress-driven variations in mussel physiology. This is further exemplified by Figure 38 and Figure 41, where mussel gape and heart rate responses were clustered very tightly along non-stressful DO concentrations and salinities. Curtis et al. (2000) also observed a moderate positive correlation between gape and heart rate in *M. edulis* individuals exposed to unmanipulated seawater. They surmised that the lower correlation coefficient is partly due to many short valve-closure events that did not coincide with a change in heart rate. Additionally, since conditions are typically not considered stressful at SDB, mussels are not cued to close their valves or change their heart rates as a group. In the absence of stress, individual variability in heart rate and gape behavior is much more noticeable.

Los Peñasquitos Lagoon

Stressful events were also relatively absent at LPL. Unfortunately, despite the deployment covering winter and spring—the time of year when mouth closure is most likely to occur—data logging was patchy and failed to capture responses during potentially stressful events. At the surface, DO and temperature remained similar to conditions at SDB. Salinity dropped during precipitation events, but the data loggers failed to capture any responses

following those events (Figure 27). Data loggers also failed to capture responses to stress for mussels near the benthos. Hypoxic conditions occurred more frequently than at the surface; however, since hypoxia tended to occur during precipitation events, no mussel responses were recorded (Figure 26). It is likely that the lack of sunlight during rain events contributed to data logger failure, as battery power relied on solar panels.

Despite a lack of response to stressful conditions, successfully logged responses showed that at the surface, gape was only weakly associated with environmental variables (Figure 32) while heart rate was mostly positively associated with temperature (Figure 31D). Near the benthos, gape was moderately positively associated with DO (Figure 29A), while heart rate was also mostly positively associated with temperature (Figure 28D). DO again emerged as the strongest predictor of gape behavior at both depths, though temperature had a notable effect size at the surface. These associations may also reflect baseline physiological rhythms rather than acute environmental responses. This is further illustrated by Figure 30 and Figure 33, where mussel gape and heart rate responses were mostly clustered at non-stressful DO concentrations and salinities. Similar to observations at SDB, it is likely that under stable, non-stressful conditions, both DO and gape fluctuate on natural diel cycles. Also similar to SDB, heart rate and gape were not closely associated with each other (Figure 28A; Figure 31A), indicating that consistent low-level variation at the individual level contributes more to the observed patterns in the absence of stress.

Tijuana River Estuary

Although the deployment at the TRE was far shorter than at LPL or SDB, conditions at the TRE were by far the most stressful. Hypoxic and anoxic conditions occurred daily, sometimes extending for multiple days at the surface of the water column (Figure 20B). Salinity also consistently dropped at the surface (Figure 20C), likely due to chronic sewage runoff (Scrivner et al., 2025). Turbidity reached much higher levels than those measured at LPL (Figure 19F; Figure 20E). However, temperatures at both depths remained non-stressful throughout the deployment period (Figure 19E; Figure 20D).

DO was strongly and positively associated with gape and heart rate at both depths (Figure 21B; Figure 22A; Figure 24A) and was by far the strongest predictor of gape behavior. Within individuals at the surface, gape increased by 8.4% for each 1 mg L^{-1}

increase in DO. At the bottom, gape increased by 7.1% and heart rate increased by 1.2 bpm for each 1 mg L^{-1} increase in DO. While DO near the benthos did seem to fluctuate on a diel cycle (Figure 19C), the conditions at the surface of the TRE often suppressed this natural rhythm (Figure 20B). Mussels at the surface were exposed to anoxia for extended periods, overriding their normal behavioral rhythms and forcing more extreme and sustained physiological responses. As a result, the influence of DO on gape behavior at the TRE likely reflects the interruption of natural physiological processes due to mitigating harm from prolonged oxygen limitation rather than the more subtle, cyclical patterns observed at SDB and LPL.

Surprisingly, salinity was not as tightly linked with gape and heart rate as DO (Figure 21C; Figure 22B; Figure 24B). As illustrated in Figure 23 and Figure 25, average gape % and heart rate increased most strongly with higher DO concentrations, regardless of salinity. Although salinity spanned a wide range, mussel responses were consistently aligned with oxygen gradients, reinforcing that DO was the more immediate driver of physiological performance. This may be because the frequent and severe drops in DO at the TRE overwhelmed the mussels' ability to respond to other environmental cues. Even in the more benign conditions at SDB and LPL, DO tended to be more strongly linked to gape and heart rate than salinity, suggesting that oxygen availability is a more immediate and sensitive driver of mussel behavior and physiology across a range of environmental contexts.

DIFFERENCES IN MUSSEL RESPONSES BETWEEN LABORATORY AND FIELD CONDITIONS

In the laboratory, mussels exposed to low salinity sustained lower heart rates and were closed more often than mussels exposed to low DO. In the field, mussels appeared to close their valves and lower their heart rates more strongly in response to low DO than to low salinity. While seasonality may have influenced the strength of responses observed in the laboratory, the overall contrast in trends between laboratory and field remains evident. Repeating the trials during different seasons could provide further clarity. Furthermore, during the low salinity trials, salinity was manipulated in isolation, without the presence of additional stressors. Had hypoxia occurred simultaneously, it is possible that DO would have emerged as a more dominant predictor of physiological response. Additionally, the lab

hypoxia trials did not include true anoxic conditions. At the TRE, the presence of prolonged anoxia likely drove more extreme behavioral shifts, including widespread valve closure, which was not observed in the lab where oxygen levels remained sufficient for partial gaping to occur.

FURTHER EVIDENCE OF EXTREME ENVIRONMENTAL STRESS AT THE TRE

Multiple additional lines of evidence point to the extreme environmental stress experienced by mussels at the TRE. Mortality was a significant issue for mussels at the surface of the TRE. Conditions were so stressful that within the first month of deployment, all surface mussels had died (Figure 19A). Mussels at the bottom were able to survive until the mooring, unfortunately, became detached from the bottom weight and washed up on Imperial Beach, CA.

Stressful conditions were further exemplified by the notable lack of biofouling on the TRE mooring (Figure 42A). In contrast, at both LPL and SDB, invertebrate and algal growth was substantial, indicating more favorable conditions (Figure 42B-C). There were also iron deposits collecting on the magnets of mussels from the TRE, which could be an additional indicator of chronic runoff.

Differences in size and growth rates also highlighted the intensely stressful conditions at the TRE. Mussels from the TRE tended to be the smallest while mussels from LPL tended to be the largest (Table A1). Larger, positive growth rates observed in mussels at SDB and LPL suggest that environmental conditions at these sites were favorable enough to support energy allocation toward growth. The smaller positive growth rate for bottom mussels and the negative growth rate for surface mussels at the TRE are likely the result of metabolic depression, shell erosion, and short lifespan. The combination of smaller overall size and decreased growth rates is further evidence that conditions at the TRE are highly unfavorable. Severe stress conditions at the TRE elicited an energy-conserving response in mussels, likely restricting physiological activity to vital functions only.

Figure 42. Biofouling condition of biosentinel moorings recovered from A) the TRE after two months of deployment, B) SDB after several months since cleaning, and C) LPL after eight months of deployment. At LPL, the pictured mussels settled within the final three months of the deployment and grew rapidly.

IMPLICATIONS OF BIOSENTINEL APPLICATION IN THE FIELD

The implementation of biosentinel bivalves within San Diego estuaries has broad and valuable applications. Primarily, biosentinel bivalves can provide biological response metrics for an ecosystem that has traditionally been monitored through abiotic parameters. This expands monitoring beyond physical parameters to include real-time indicators of physiological stress, which offers a more ecologically relevant insight. With this information, estuary managers can implement conservation measures—such as manually breaching the

tidal inlet—more effectively. Manually breaching the mouth of the estuary can help alleviate flooding, improve water quality, allow for fish migration, and prevent excessive mosquito breeding and other public health risks (Crooks et al., 2016 Goodrich et al., 2020). Reopening an estuary is a very time-consuming, laborious, and expensive process. There is also a risk of inducing negative environmental impacts, such as rapid water quality changes, poor nearshore ocean water quality, the flushing or stranding of organisms, and loss of habitat (Largier et al., 2019). Applying bivalve biosentinels as a biological monitoring system allows estuary managers to make more informed decisions regarding manual breaching. By fully understanding how those bivalves respond to stressful environmental conditions, managers can be better informed on the timing and necessity of such interventions.

Biosentinels also show promise in public health contexts, especially in estuaries like the TRE that are chronically impacted by sewage flows. For the past few decades, transboundary sewage flows across the Mexican border have threatened the health of local, often marginalized, communities and created lethal conditions for wildlife. Lack of governmental oversight and collaborative efforts have prolonged the issue. Biosentinel bivalves can help mitigate the problem by providing an early warning system to alert local communities when water quality conditions are poor. This will help protect the health of both people and wildlife in the area.

There is also great promise in using bivalve biosentinels within the aquaculture industry. Traditionally, assessment of commercial stock relies on measurements of mortality and growth to discern health (Andrewartha et al., 2015). Additionally, due to being labor-intensive and costly, the process does not occur frequently. As a result, it is impossible to predict and mitigate stressors that can lead to a loss of product. Equipping bivalves with physiological sensors and deploying them alongside relevant water quality sensors can create a predictive monitoring system, helping to reduce stock loss, increase profitability, and improve customer satisfaction.

CONCLUSION

My study highlights the effectiveness of bivalve biosentinels—specifically *M. galloprovincialis*—for monitoring estuarine water quality within San Diego. This tool is particularly useful in conjunction with existing abiotic monitoring efforts and stress response

validations conducted through controlled laboratory experiments. Laboratory experiments demonstrated that both valve-gaping and heart rate are sensitive to hypoxia and low salinity, and mussels respond differently to each stressor. The location from which the mussels were collected appeared to have only a minimal effect on the responses. This lack of difference mirrors evidence supporting genetic mixing across the estuaries, which limits potential differences in response (Becker et al., 2007). Field deployments showed that mussels respond strongly to environmental stress, particularly at the TRE where anoxia is a chronic issue. Overall, DO was the most consistent environmental driver of both heart rate and gaping behavior, even in estuaries where stress was limited (SDB and LPL).

These findings provide a critical foundation for expanding biosentinel-based monitoring in San Diego estuaries. As this was the first set of experiments related to the existing biosentinel monitoring project (Miller, 2021), some of the most common stressors needed to be assessed first. Future laboratory experiments exposing bivalves to additional single stressors (e.g., chlorophyll *a*, temperature, pCO2, pH, and heavy metals), varying levels of stress, seasonal fluctuations in stress, and combinations of stressors will amplify the long-term success of the biosentinel program. Testing multiple stressors in tandem is especially important in light of the field conditions observed at the TRE, where mussels were exposed not only to prolonged hypoxia and anoxia, but also to chronic low salinity and elevated turbidity.

An admitted limitation of the lab experiments was the limited number of replicates combined with the high potential for individual variation. It is possible that exposing a larger number of mussels from each location would result in more power to reveal differences in gape and heart rate responses. Future studies should focus on increasing replication within each location.

Continuing to implement bivalve biosentinels in local estuaries is essential for fully understanding the dynamics and impacts of poor estuarine water quality. The incorporation of continuous and real-time physiological data alongside existing abiotic monitoring efforts enhances our ability to detect early signs of ecological stress and inform estuary management decisions. As a result, harmful estuarine conditions can be prevented and mitigated more efficiently.

ACKNOWLEDGEMENTS

This thesis would not be possible without everyone who helped me along the way. I'd like to begin by thanking my advisor, Luke Miller, for seeing my potential and teaching me not only how to be a better ecologist but also how to be a better writer, thinker, and mentor. I would also like to thank my committee members, Kevin Hovel and Trent Biggs, for offering their time, wisdom, and novel perspectives throughout the research and writing process.

I'd also like to acknowledge the generous funding provided by the National Oceanic and Atmospheric Administration (NOAA) through the National Estuarine Research Reserve System Science Collaborative (NA19NOS4190058), as well as support from the CSU Council on Ocean Affairs, Science, and Technology (COAST), both of which made my research possible. The former funding source also introduced me to Sarah Giddings, Jeff Crooks, and Kristen Goodrich, all of whom served as valuable collaborators.

Next, I'd like to express my everlasting gratitude to my lab mates, Lily McIntire, Lauren Strope, Bailey McKernan, and Gabby Kalbach, for creating such a welcoming environment and supporting me through it all. I am especially grateful for Lily, who was the best lab mom I could ask for! I am also incredibly grateful for the amazing undergraduates (Arianna Dial, Neenah Mendez, Maritere Rodriguez Rivera, Miles Ghannadian, and Simone Parsons) who stuck with me through the most tedious parts of this research (apologies for the mountains of heart data processing!). Watching you learn, grow, and develop as scientists has been one of the most rewarding parts of this experience. I am so proud of you all!

My experience at SDSU would not have been the same without the MEBSA team. A huge thank you to Xavius Boone, Lily McIntire, Lily Jorrick, Erin Horkan, Elisabeth Rotschedl, Jacob Ogawa, and Alyssa Dueñas for all that you've done to make MEBSA (and Marine Science Day!) run like a well-oiled machine. I also want to express my deepest gratitude for the (former) CMIL lab managers, Renee Angwin and Alexander Carsh, for

helping run Marine Science Day and for setting me up for success during my lab experiments.

On a personal note, thank you, thank you, thank you, Mom and Dad. I truly don't know how I got so lucky to have parents as supportive and loving as you. Thank you for always pushing me to dream big and for standing beside me through it all. And (like I said in the dedication), thank you for signing me up for marine science camp all those years ago. Finally, I want to thank my boyfriend, Ethan, for sticking with me and loving me through it all. And, of course, thank you to the Cat Distribution System for sending us Ruby, the world's best study buddy.

DATA AVAILABILITY

More information on the data logger and specific components is available at https://github.com/millerlp/BivalveBit and https://github.com/millerlp/BivalveBit_lib. Data and analysis code associated with this thesis are available in a permanent archive at (https://doi.org/10.5281/zenodo.17420812).

REFERENCES

Addis, P., Angioni, A., Pasquini, V., Giglioli, A., Andreotti, V., Carboni, S. and Secci, M. (2021). Flash flood simulation and valve behavior of *Mytilus galloprovincialis* measured with Hall sensors. *Integr. Zool.* **16**, 138–148.

Altieri, A. H. (2006). Inducible variation in hypoxia tolerance across the intertidal–subtidal distribution of the blue mussel *Mytilus edulis*. *Mar. Ecol. Prog. Ser.* **325**, 295–300.

Altieri, A. H. and Diaz, R. J. (2019). Chapter 24 - Dead zones: oxygen depletion in coastal ecosystems. In *World Seas: An Environmental Evaluation (Second Edition)* (ed. C. Sheppard), pp. 453–473. Academic Press.

Ameyaw-Akumfi, C. and Naylor, E. (1987). Temporal patterns of shell-gape in *Mytilus edulis*. *Mar. Biol.* **95**, 237–242.

Andrewartha, S., Elliott, N., Mcculloch, J., and Frappell, P. (2015). Aquaculture sentinels: smart-farming with biosensor equipped stock. *J. Aquac. Res. Dev*. **7**, 393.

Andrews, J., Haven, D., and Quayle, D. (1959). Fresh-water kill of oysters (*Crassostrea virginica*) in James River, Virginia, 1958. *J Shellfish Res.* **49**, 29–49.

Armstrong, D. A., Rooper, C. and Gunderson, D. (2003). Estuarine production of juvenile dungeness crab (*Cancer magister*) and contribution to the Oregon-Washington coastal fishery. *Estuaries* **26**, 1174–1188.

Ayad, M., Li, J., Holt, B. and Lee, C. (2020). Analysis and classification of stormwater and wastewater runoff from the Tijuana River using remote sensing imagery. *Front. Environ. Sci.* **8**.

Bakdash J., Marusich L. (2024). rmcorr: Repeated measures correlation. R package version 0.7.0, https://CRAN.R-project.org/package=rmcorr.

Baker, S. M. and Mann, R. (1992). Effects of hypoxia and anoxia on larval settlement, juvenile growth, and juvenile survival of the oyster *Crassostrea virginica*. *Biol. Bull.* **182**, 265–269.

Bakhmet, I. N., Berger, V. Ja. and Khalaman, V. V. (2005). The effect of salinity change on the heart rate of *Mytilus edulis* specimens from different ecological zones. *J. Exp. Mar. Biol. Ecol.* **318**, 121–126.

Ballesta-Artero, I., Witbaard, R., Carroll, M. L. and van der Meer, J. (2017). Environmental factors regulating gaping activity of the bivalve *Arctica islandica* in Northern Norway. *Mar. Biol.* **164**, 116.

Bamber, S. D. (2018). Does sustained tolerance of reduced salinity seawater alter phagocytosis efficiency in haemocytes of the blue mussel *Mytilus edulis* (L.)? *J. Exp. Mar. Biol. Ecol.* **500**, 132–139.

Bamber, S. D. (2023). Valve gaping behaviour in the European oyster (*Ostrea edulis*) in response to changes in light intensity when combined with variations in salinity and seawater temperature. *J. Exp. Mar. Biol. Ecol.* **568**, 151943.

Barbier, E. B., Hacker, S. D., Kennedy, C., Koch, E. W., Stier, A. C. and Silliman, B. R. (2011). The value of estuarine and coastal ecosystem services. *Ecol. Monogr.* **81**, 169–193.

Bartoń, K. (2025). MuMIn: Multi-model inference. R package version 1.48.11, https://CRAN.R-project.org/package=MuMIn.

Bates, D., Mächler, M., Bolker, B., and Walker, S. (2015). Fitting linear mixed-effects models using lme4. *J. Stat. Softw.* **67**, 1–48.

Bayne, B. L. (2000). Relations between variable rates of growth, metabolic costs and growth efficiencies in individual Sydney rock oysters (*Saccostrea commercialis*). *J. Exp. Mar. Biol. Ecol.* **251**, 185–203.

Becker, B. J., Levin, L. A., Fodrie, F. J. and McMillan, P. A. (2007). Complex larval connectivity patterns among marine invertebrate populations. *PNAS* **104**, 3267–3272.

Behrens, D. K., Bombardelli, F. A. and Largier, J. L. (2016). Landward propagation of saline waters following closure of a bar-built estuary: Russian River (California, USA). *Estuaries Coasts* **39**, 621–638.

Biggs, T., Zeigler, A. and Taniguchi-Quan, K. T. (2022). Runoff and sediment loads in the Tijuana River: dam effects, extreme events, and change during urbanization. *J. Hydrol.* **42**, 101162.

Borcherding, J. (2006). Ten years of practical experience with the Dreissena-Monitor, a biological early warning system for continuous water quality monitoring. *Hydrobiologia* **556**, 417–426.

Borchers, H. (2022). Pracma: practical numerical math functions. R package version 2.4.2. https://CRAN.R-project.org/package=pracma

Boukadida, K., Mlouka, R., Abelouah, M. R., Chelly, S., Romdhani, I., Conti, G. O., Ferrante, M., Cammarata, M., Parisi, M. G., AitAlla, A., et al. (2024). Unraveling the interplay between environmental microplastics and salinity stress on *Mytilus*

galloprovincialis larval development: a holistic exploration. *Sci. Total Environ.* **927**, 172177.

Boyer, J. N., Kelble, C. R., Ortner, P. B. and Rudnick, D. T. (2009). Phytoplankton bloom status: chlorophyll *a* biomass as an indicator of water quality condition in the southern estuaries of Florida, USA. *Ecol. Indic.* **9**, S56–S67.

Braby, C. E. and Somero, G. N. (2006). Following the heart: temperature and salinity effects on heart rate in native and invasive species of blue mussels (genus *Mytilus*). *J. Exp. Biol.* **209**, 2554–2566.

Brand, A. R. and Roberts, D. (1973). The cardiac responses of the scallop *Pecten maximus* (L.) to respiratory stress. *J. Exp. Mar. Biol. Ecol.* **13**, 29–43.

Breitburg, D., Levin, L. A., Oschlies, A., Grégoire, M., Chavez, F. P., Conley, D. J., Garçon, V., Gilbert, D., Gutiérrez, D., Isensee, K., et al. (2018). Declining oxygen in the global ocean and coastal waters. *Science* **359**, eaam7240.

Brown, J. A. (2006). Using the chemical composition of otoliths to evaluate the nursery role of estuaries for English sole *Pleuronectes vetulus* populations. *Mar. Ecol. Prog. Ser.* **306**, 269–281.

Burnett, N. P., Seabra, R., de Pirro, M., Wethey, D. S., Woodin, S. A., Helmuth, B., Zippay, M. L., Sarà, G., Monaco, C. and Lima, F. P. (2013). An improved noninvasive method for measuring heartbeat of intertidal animals. *Limnol. Oceanogr. Methods* **11**, 91–100.

Byrne, R. A., Gnaiger, E., McMahon, R. F. and Dietz, T. H. (1990). Behavioral and metabolic responses to emersion and subsequent reimmersion in the freshwater bivalve, *Corbicula fluminea*. *Biol. Bull.* **178**, 251–259.

Cheng, M. C. F., Ericson, J. A., Ragg, N. L. C., Dunphy, B. J. and Zamora, L. N. (2025). Mussels, *Perna canaliculus*, as biosensors for climate change: concurrent monitoring of heart rate, oxygen consumption and gaping behaviour under heat stress. *N. Z. J. Mar. Freshwater Res.* **59**, 1621–1639.

Clements, J. C., Comeau, L. A., Carver, C. E., Mayrand, É., Plante, S. and Mallet, A. L. (2018). Short-term exposure to elevated *p*CO2 does not affect the valve gaping response of adult eastern oysters, *Crassostrea virginica*, to acute heat shock under an *ad libitum* feeding regime. *J. Exp. Mar. Biol. Ecol.* **506**, 9–17.

Coats, R., Swanson, M. and Williams, P. (1989). Hydrologic analysis for coastal wetland restoration. *Environ. Manag.* **13**, 715–727.

Comeau, L. A., Babarro, J. M. F., Longa, A. and Padin, X. A. (2018). Valve-gaping behavior of raft-cultivated mussels in the Ría de Arousa, Spain. *Aquac. Reports* **9**, 68–73.

Cousins, M., Stacey, M. T. and Drake, J. L. (2010). Effects of seasonal stratification on turbulent mixing in a hypereutrophic coastal lagoon. *Limnol. Oceanogr.* **55**, 172–186.

Crooks, J., Talley, D., Cordrey, M., Whitcraft, C., Lorda, J., Uyeda, K., Bellringer, H., Mccullough, J. and Almeida, M. (2016). Unnatural history: biological invasions into coastal ecosystems. U.S.-Iran Symposium on Wetlands.

Curtis, T. M., Williamson, R. and Depledge, M. H. (2000). Simultaneous, long-term monitoring of valve and cardiac activity in the blue mussel *Mytilus edulis* exposed to copper. *Mar. Biol.* **136**, 837–846.

Davenport, J. (1979). The isolation response of mussels (*Mytilus edulis* L.) exposed to falling sea-water concentrations. *J. Mar. Biol. Assoc. U. K.* **59**, 123–132.

Davis, M. J., Woo, I., Ellings, C. S., Hodgson, S., Beauchamp, D. A., Nakai, G. and De La Cruz, S. E. W. (2022). A climate-mediated shift in the estuarine habitat mosaic limits prey availability and reduces nursery quality for juvenile salmon. *Estuaries Coasts* **45**, 1445–1464.

Davis, A. M., Plough, L. V. and Paynter, K. T. (2023). Intraspecific patterns of mortality and cardiac response to hypoxia in the eastern oyster, *Crassostrea virginica*. *J. Exp. Mar. Biol. Ecol.* **566**, 151921.

de Zwart, D., Kramer, K. J. M. and Jenner, H. A. (1995). Practical experiences with the biological early warning system “mosselmonitor.” *Environ. Toxicol. Water Qual.* **10**, 237–247.

Diaz, R. J. and Rosenberg, R. (2008). Spreading dead zones and consequences for marine ecosystems. *Science* **321**, 926–929.

Doughty, C. L., Cavanaugh, K. C., Ambrose, R. F. and Stein, E. D. (2019). Evaluating regional resiliency of coastal wetlands to sea level rise through hypsometry-based modeling. *Glob. Chang. Biol.* **25**, 78–92.

Dowd, W. W. and Somero, G. N. (2013). Behavior and survival of *Mytilus* congeners following episodes of elevated body temperature in air and seawater. *J. Exp. Biol.* **216**, 502–514.

D’Avanzo, C., and Kremer, J. N. (1994). Diel oxygen dynamics and anoxic events in an eutrophic estuary of Waquoit Bay, Massachusetts. *Estuaries* **17**, 131–139.

Ellis, J., Cummings, V., Hewitt, J., Thrush, S. and Norkko, A. (2002). Determining effects of suspended sediment on condition of a suspension feeding bivalve (*Atrina zelandica*): results of a survey, a laboratory experiment and a field transplant experiment. *J. Exp. Mar. Biol. Ecol.* **267**, 147–174.

Fahey, B. D. and Coker, R. J. (1992). Sediment production from forest roads in Queen Charlotte Forest and potential impact on marine water quality, Marlborough Sounds, New Zealand. *N. Z. J. Mar. Freshwater Res.* **26**, 187–195.

Fox, J. and Weisberg, S. (2019). *An R companion to applied regression*, Third edition. Sage, Thousand Oaks CA. https://www.john-fox.ca/Companion/.

Frank, D. M., Hamilton, J. F., Ward, J. E. and Shumway, S. E. (2007). A fiber optic sensor for high resolution measurement and continuous monitoring of valve gape in bivalve molluscs. *J. Shellfish Res.* **26**, 575–580.

Gale, E., Pattiaratchi, C. and Ranasinghe, R. (2006). Vertical mixing processes in intermittently closed and open lakes and lagoons, and the dissolved oxygen response. *Estuar. Coast. Shelf Sci.* **69**, 205–216.

Geller, J. B. (1999). Decline of a native mussel masked by sibling species invasion. *Conserv. Biol.* **13**, 661–664.

Geller, J. B., Carlton, J. T. and Powers, D. A. (1994). PCR-based detection of mtDNA haplotypes of native and invading mussels on the northeastern Pacific coast: latitudinal pattern of invasion. *Mar. Biol.* **119**, 243–249.

Goodrich, K. A., Basolo, V., Feldman, D. L., Matthew, R. A., Schubert, J. E., Luke, A., Eguiarte, A., Boudreau, D., Serrano, K., Reyes, A. S., et al. (2020). Addressing pluvial flash flooding through community-based collaborative research in Tijuana, Mexico. *Water* **12**, 1257.

Gosling, E. (2008). *Bivalve Molluscs: Biology, Ecology and Culture*. Hoboken: John Wiley and Sons.

Gostyukhina, O. L., Kladchenko, E. S., Chelebieva, E. S., Tkachuk, A. A., Lavrichenko, D. S., and Andreyeva, A. Y. (2023). Short-time salinity fluctuations are strong activators of oxidative stress in Mediterranean mussel (*Mytilus galloprovincialis*). *Ecol. Montenegrina* **63**, 46–58.

Guerreiro, M. A., Martinho, F., Baptista, J., Costa, F., Pardal, M. Â. and Primo, A. L. (2021). Function of estuaries and coastal areas as nursery grounds for marine fish early life stages. *Mar. Environ. Res.* **170**, 105408.

Gurr, S. J., Goleski, J., Lima, F. P., Seabra, R., Gobler, C. J. and Volkenborn, N. (2018). Cardiac responses of the bay scallop *Argopecten irradians* to diel-cycling hypoxia. *J. Exp. Mar. Biol. Ecol.* **500**, 18–29.

Gurr, S. J., Dwyer, I. P., Goleski, J., Lima, F. P., Seabra, R., Gobler, C. J. and Volkenborn, N. (2021). Acclimatization in the bay scallop *Argopecten irradians* along a eutrophication gradient: insights from heartbeat rate measurements during a simulated hypoxic event. *Mar. Freshw. Behav. and Physiol*. **54**, 23–49.

Hamer, B., Jakšić, Ž., Pavičić-Hamer, D., Perić, L., Medaković, D., Ivanković, D., Pavičić, J., Zilberberg, C., Schröder, H. C., Müller, W. E. G., et al. (2008). Effect of hypoosmotic stress by low salinity acclimation of Mediterranean mussels *Mytilus galloprovincialis* on biological parameters used for pollution assessment. *Aquat. Toxicol.* **89**, 137–151.

Hartig, F. (2024). *DHARMa: Residual diagnostics for hierarchical (multi-level/mixed) regression models* [Computer software]. https://cran.r-project.org/web/packages/DHARMa/vignettes/DHARMa.html

Harvey, M. E., Giddings, S. N., Stein, E. D., Crooks, J. A., Whitcraft, C., Gallien, T., Largier, J. L., Tiefenthaler, L., Meltzer, H., Pawlak, G., et al. (2020). Effects of elevated sea levels and waves on southern California estuaries during the 2015–2016 El Niño. *Estuaries Coasts* **43**, 256–271.

Harvey, M. E., Giddings, S. N., Pawlak, G. and Crooks, J. A. (2023). Hydrodynamic variability of an intermittently closed estuary over interannual, seasonal, fortnightly, and tidal timescales. *Estuaries Coasts* **46**, 84–108.

Hazen, E. L., Abrahms, B., Brodie, S., Carroll, G., Jacox, M. G., Savoca, M. S., Scales, K. L., Sydeman, W. J. and Bograd, S. J. (2019). Marine top predators as climate and ecosystem sentinels. *Front. Ecol. Environ.* **17**, 565–574.

Hellicar, A. D., Rahman, A., Smith, D. V., Smith, G., McCulloch, J., Andrewartha, S., and Morash, A. (2015). An algorithm for the automatic analysis of signals from an oyster heart rate sensor. *IEEE Sens. J.* **15**, 4480–4487.

Hofmann, G. E. and Somero, G. N. (1996). Interspecific variation in thermal denaturation of proteins in the congeneric mussels *Mytilus trossulus* and *M. galloprovincialis*: evidence from the heat-shock response and protein ubiquitination. *Mar. Biol.* **126**, 65–75.

Hui, T. Y., Dong, Y., Han, G., Lau, S. L. Y., Cheng, M. C. F., Meepoka, C., Ganmanee, M. and Williams, G. A. (2020). Timing metabolic depression: predicting thermal stress in extreme intertidal environments. *Am. Nat.* **196**, 501–511.

Hyndman, R., Athanasopoulos, G., Bergmeir, C., Caceres, G., Chhay, L., O'Hara-Wild, M., Petropoulos, F., Razbash, S., Wang, E., and Yasmeen, F. (2023). Forecast: forecasting functions for time series and linear models. R package version 8.21.1. https://pkg.robjhyndman.com/forecast/

Isani, G., Cattani, O., Zurzolo, M., Pagnucco, C. and Cortesi, P. (1995). Energy metabolism of the mussel, *Mytilus galloprovincialis*, during long-term anoxia. *Comp. Biochem. Physiol. Biochem. Mol. Biol.* **110**, 103–113.

Jou, L.-J., Lin, S.-C., Chen, B.-C., Chen, W.-Y. and Liao, C.-M. (2013). Synthesis and measurement of valve activities by an improved online clam-based behavioral monitoring system. *Comput. Electron. Agric.* **90**, 106–118.

Kennish, M. J. (2002). Environmental threats and environmental future of estuaries. *Environ. Conserv.* **29**, 78–107.

Komoroske, L. M., Lewison, R. L., Seminoff, J. A., Deustchman, D. D. and Deheyn, D. D. (2012). Trace metals in an urbanized estuarine sea turtle food web in San Diego Bay, CA. *Sci. Total Environ.* **417–418**, 108–116.

Kuznetsova A., Brockhoff P. B., Christensen R. H. B. (2017). lmerTest package: tests in linear mixed effects models. *J. Stat. Softw.* **82**, 1-26.

Landes, A., Dolmer, P., Poulsen, L. K., Petersen, J. K. and Vismann, B. (2015). Growth and respiration in blue mussels (*Mytilus spp.*) from different salinity regimes. *J. Shellfish Res.* **34**, 373–382.

Largier, J. L. (2023). Recognizing low-inflow estuaries as a common estuary paradigm. *Estuaries Coasts* **46**, 1949–1970.

Largier, J., O'Connor, K. and Clark, R. (2019). Considerations for management of the mouth state of California's bar-built estuaries. National Marine Fisheries Service - West Coast Region.

Lenth, R. (2025). emmeans: estimated marginal means, aka least-squares means. R package version 1.11.0, https://CRAN.R-project.org/package=emmeans

Levin, L. A., Mendoza, G. F., Neira, C., Giddings, S. N. and Crooks, J. A. (2023). Consequences of mouth closure and hypoxia-induced state changes in low-inflow estuaries: benthic community and trait-based response. *Estuaries Coasts* **46**, 2128–2147.

Livingston, R. J., Lewis, F. G., Woodsum, G. C., Niu, X.-F., Galperin, B., Huang, W., Christensen, J. D., Monaco, M. E., Battista, T. A., Klein, C. J., et al. (2000). Modelling oyster population response to variation in freshwater input. *Estuar. Coast. Shelf Sci.* **50**, 655–672.

Lockwood, B. L. and Somero, G. N. (2011). Invasive and native blue mussels (genus *Mytilus*) on the California coast: The role of physiology in a biological invasion. *J. Exp. Mar. Biol. Ecol.* **400**, 167–174.

Lowe, G. (1974). Effect of temperature change on the heart rate of *Crassostrea gigas* and *Mya arenaria* (Bivalvia). *J. Molluscan Stud.* **41**, 29–36.

Ludka, B. C., Guza, R. T. and O'Reilly, W. C. (2018). Nourishment evolution and impacts at four southern California beaches: a sand volume analysis. *Coast. Eng.* **136**, 96–105.

Luković, J., Chiang, J. C. H., Blagojević, D., and Sekulić, A. (2021). A later onset of the rainy season in California. *Geophys. Res. Lett.* **48**, e2020GL090350.

McClain, A. M., Field, C. L., Norris, T. A., Borremans, B., Duignan, P. J., Johnson, S. P., Whoriskey, S. T., Thompson-Barbosa, L. and Gulland, F. M. D. (2023). The symptomatology and diagnosis of domoic acid toxicosis in stranded California sea lions (*Zalophus californianus*): a review and evaluation of 20 years of cases to guide prognosis. *Front. Vet. Sci.* **10**.

McDonald, J. H. and Koehn, R. K. (1988). The mussels *Mytilus galloprovincialis* and *M. trossulus* on the Pacific coast of North America. *Mar. Biol.* **99**, 111–118.

McLamb, F., Feng, Z., Shea, D., Bozinovic, K., Vasquez, M. F., Stransky, C., Gersberg, R. M., Wang, W., Kong, X., Xia, X.-R., et al. (2024). Evidence of transboundary movement of chemicals from Mexico to the U.S. in Tijuana River Estuary sediments. *Chemosphere* **348**, 140749.

Melwani, A. R., Gregorio, D., Jin, Y., Stephenson, M., Ichikawa, G., Siegel, E., Crane, D., Lauenstein, G. and Davis, J. A. (2014). Mussel watch update: long-term trends in selected contaminants from coastal California, 1977–2010. *Mar. Pollut. Bull.* **81**, 291–302.

Meng, J., Wang, T., Li, L. and Zhang, G. (2018). Inducible variation in anaerobic energy metabolism reflects hypoxia tolerance across the intertidal and subtidal distribution of the Pacific oyster (*Crassostrea gigas*). *Mar. Environ. Res.* **138**, 135–143.

Miller, L. P. (2021). Habitat heartbeats: incorporating bivalve biosensors into estuary monitoring infrastructure. NERRS Science Collaborative. https://nerrssciencecollaborative.org/project/LMiller2021

Miller, L. P. (2022). Monitoring bivalve behavior and physiology in the laboratory and field using open-source tools. *Integr. Comp. Biol.* **62**, 1096–1110.

Miller, L. P. and Dowd, W. W. (2017). Multimodal in situ datalogging quantifies inter-individual variation in thermal experience and persistent origin effects on gaping behavior among intertidal mussels (*Mytilus californianus*). *J. Exp. Biol.* **220**, 4305–4319.

Miller, L. P. and Dowd, W. W. (2019). Repeatable patterns of small-scale spatial variation in intertidal mussel beds and their implications for responses to climate change. *Comp. Biochem. Physiol. Mol. Integr. Physiol.* **236**, 110516.

Newell, C. R., Wildish, D. J. and MacDonald, B. A. (2001). The effects of velocity and seston concentration on the exhalant siphon area, valve gape and filtration rate of the mussel *Mytilus edulis*. *J. Exp. Mar. Biol. Ecol.* **262**, 91–111.

Nicholson, S. (2002). Ecophysiological aspects of cardiac activity in the subtropical mussel *Perna viridis* (L.) (Bivalvia: Mytilidae). *J. Exp. Mar. Biol. Ecol.* **267**, 207–222.

Nordby, C. S. and Zedler, J. B. (1991). Responses of fish and macrobenthic assemblages to hydrologic disturbances in Tijuana Estuary and Los Peñasquitos Lagoon, California. *Estuaries* **14**, 80–93.

O'Higgins, T. and Rumril, S. (2007). Tidal and watershed forcing of nutrients and dissolved oxygen stress within four pacific coast estuaries: analysis of time-series data collected by the National Estuarine Research Reserve System-Wide Monitoring Program (2000-2006) within Padilla Bay (WA), South Slough (OR), Elkhorn Slough (CA) and the Tijuana River estuary (CA). The NOAA/UNH Cooperative Institute for Coastal and Estuarine Environmental Technology (CICEET).

Peterson, E. A., Keur, M. C., Yeboah, M., van de Grootevheen, T., Moth, L., Kamermans, P., Murk, T., Peck, M. A. and Foekema, E. (2025). Determining physiological responses of mussels (*Mytilus edulis*) to hypoxia by combining multiple sensor techniques. *Conserv. Physiol.* **13**, coaf023.

Porter, E. T. and Breitburg, D. L. (2016). Eastern oyster, *Crassostrea virginica*, valve gape behavior under diel-cycling hypoxia. *Mar. Biol.* **163**, 218.

Porter, E. T. and Porter, F. S. (2018). A strain gauge monitor (SGM) for continuous valve gape measurements in bivalve molluscs in response to laboratory induced diel-cycling hypoxia and pH. *J. Vis. Exp*. **138**, 57404.

R Development Core Team. (2025). R: a language and environment for statistical computing.

Reiber, C. L. and McMahon, B. R. (1998). The effects of progressive hypoxia on the crustacean cardiovascular system: a comparison of the freshwater crayfish, (*Procambarus clarkii*), and the lobster (*Homarus americanus*). *J. Comp. Physiol. B* **168**, 168–176.

Riisgård, H. U. (1991). Filtration rate and growth in the blue mussel, *Mytilus edulis* Linneaus, 1758: dependence on algal concentration. *J. Shellfish Res*. **10**, 29–35.

Riisgård, H. U., Lassen, J. and Kittner, C. (2006). Valve-gape response times in mussels (*Mytilus edulis*)—effects of laboratory preceding-feeding conditions and in situ tidally induced variation in phytoplankton biomass. *J. Shellfish Res.* **25**, 901–911.

Roberts, E. A. and Carrington, E. (2023). Energetic scope limits growth but not byssal thread production of two mytilid mussels. *J. Exp. Mar. Biol. Ecol.* **567**, 151927.

Scrivner, E., Mladenov, N., Biggs, T., Grant, A., Piazza, E., Garcia, S., Lee, C. M., Ade, C., Tufillaro, N., Grötsch, P., et al. (2025). Hyperspectral characterization of wastewater in the Tijuana River Estuary using laboratory, field, and EMIT satellite spectroscopy. *Sci. Total Environ.* **981**, 179598.

Seibel, B. A. (2023). Animal response to hypoxia in estuaries and effects of climate change. In *Climate Change and Estuaries* (ed. M. J. Kennish, H. W. Paerl and J. R. Crosswell), pp. 544–562. CRC Press.

Shen, X., Detenbeck, N. and You, M. (2022). Spatial and temporal variations of estuarine stratification and flushing time across the continental U.S. *Estuar. Coast. Shelf Sci.* **279**, 108–147.

Shinen, J. S. and Morgan, S. G. (2009). Mechanisms of invasion resistance: competition among intertidal mussels promotes establishment of invasive species and displacement of native species. *Mar. Ecol. Prog. Ser.* **383**, 187–197.

Shumway, S. E. (1977). Effect of salinity fluctuation on the osmotic pressure and Na+, Ca2+ and Mg2+ ion concentrations in the hemolymph of bivalve molluscs. *Mar. Biol*. **41**, 153–177.

Shurova, N. M. (2001). Influence of salinity on the structure and the state of bivalve *Mytilus galloprovincialis* Populations. *Russ. J. Mar. Biol.* **27**, 151–155.

Signal Developers. (2013). signal: signal processing. http://r-forge.r-project.org/projects/signal/

Sokolova, I. M., Frederich, M., Bagwe, R., Lannig, G. and Sukhotin, A. A. (2012). Energy homeostasis as an integrative tool for assessing limits of environmental stress tolerance in aquatic invertebrates. *Mar. Environ. Res.* **79**, 1–15.

Sparrow, B. D., Edwards, W., Munroe, S. E. M., Wardle, G. M., Guerin, G. R., Bastin, J.-F., Morris, B., Christensen, R., Phinn, S. and Lowe, A. J. (2020). Effective ecosystem monitoring requires a multi-scaled approach. *Biol. Rev.* **95**, 1706–1719.

Stevens, A. M. and Gobler, C. J. (2018). Interactive effects of acidification, hypoxia, and thermal stress on growth, respiration, and survival of four North Atlantic bivalves. *Mar. Ecol. Prog. Ser.* **604**, 143–161.

Talley, T. S., Loflen, C., Gossett, R., Pedersen, D., Venuti, N., Nguyen, J., and Gersberg, R. (2022). Contaminant concentrations and risks associated with the Pacific oyster in the highly urbanized San Diego Bay. *Mar. Pollut. Bull.* **174**, 113–132.

Tomanek, L. and Zuzow, M. J. (2010). The proteomic response of the mussel congeners *Mytilus galloprovincialis* and *M. trossulus* to acute heat stress: implications for thermal tolerance limits and metabolic costs of thermal stress. *J. Exp. Biol.* **213**, 3559–3574.

Tomanek, L., Zuzow, M. J., Hitt, L., Serafini, L. and Valenzuela, J. J. (2012). Proteomics of hyposaline stress in blue mussel congeners (genus *Mytilus*): implications for biogeographic range limits in response to climate change. *J. Exp. Biol*. **215**, 3905–3916.

Tran, D., Ciret, P., Ciutat, A., Durrieu, G. and Massabuau, J. (2003). Estimation of potential and limits of bivalve closure response to detect contaminants: application to cadmium. *Environ. Toxicol. Chem.* **22**, 914–920.

Tran, D., Haberkorn, H., Soudant, P., Ciret, P. and Massabuau, J.-C. (2010). Behavioral responses of *Crassostrea gigas* exposed to the harmful algae *Alexandrium minutum*. *Aquac.* **298**, 338–345.

Tronske, N. B., Parker, T. A., Henderson, H. D., Burnaford, J. L. and Zacherl, D. C. (2018). Densities and zonation patterns of native and non-indigenous oysters in southern California bays. *Wetlands* **38**, 1313–1326.

Trueman, E. R. (1967). Activity and heart rate of bivalve molluscs in their natural habitat. *Nature* **214**, 832–833.

Trueman, E. R., Lowe, G. A. (1971). The effect of temperature and littoral exposure on the heart rate of a bivalve mollusc, *Isognomum alatus*, in tropical conditions. *Comp. Biochem. Physiol. A Physiol.* **38**, 555–564.

Vaquer-Sunyer, R. and Duarte, C. M. (2008). Thresholds of hypoxia for marine biodiversity. *PNAS* **105**, 15452–15457.

Vasquez, M. C., Houston, C. T., Alcantar, C. Y., Milshteyn, L., Brazil, C. A. and Zepeda, O. G. (2022). Interactive effects of multiple stressors on the physiological performance of the invasive mussel *Mytilus galloprovincialis*. *Mar. Environ. Res.* **178**, 105665.

White, M. D. and Greer, K. A. (2006). The effects of watershed urbanization on the stream hydrology and riparian vegetation of Los Peñasquitos Creek, California. *Landsc. Urban Plan.* **74**, 125–138.

Widdows, J. (1973). Effect of temperature and food on the heart beat, ventilation rate and oxygen uptake of *Mytilus edulis*. *Mar. Biol*. **20**, 269–276.

Wilhm, J. L. and Dorris, T. C. (1968). Biological parameters for water quality criteria. *BioSci.* **18**, 477–481.

Wolfe, M. L., Bowers-Doerning, C. M., Espinosa, A., Frantz, T., Hoese, W. J., Lam, J. G., Lamp, K. R., Lyons, R. A., Nguyen, J. K., Keyes, B. D., et al. (2024). Intra-decadal increase in globally-spread *Magallana gigas* in southern California estuaries. *PLoS One* **19**, e0302935.

Wonham, M. J. (2004). Mini-review: distribution of the Mediterranean mussel *Mytilus galloprovincialis* (bivalvia: Mytilidae) and hybrids in the Northeast Pacific. *J. Shellfish Res*. **23**, 535–543.

Zedler, J. B. (2010). How frequent storms affect wetland vegetation: a preview of climate-change impacts. *Front. Ecol. Environ.* **8**, 540–547.

APPENDIX

SUPPLEMENTAL TABLES AND FIGURES

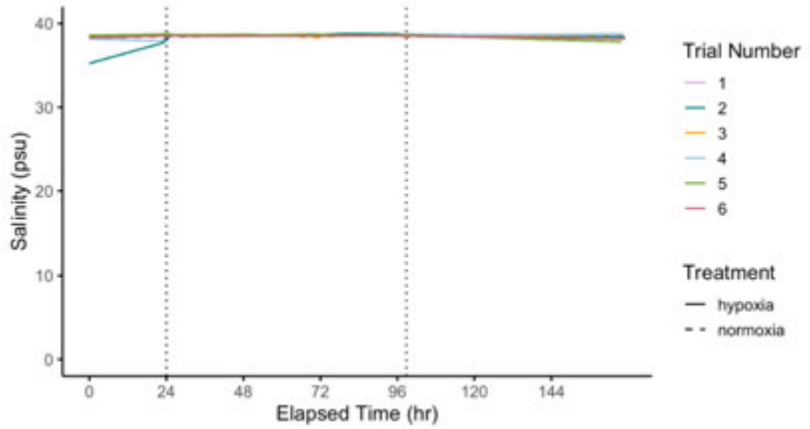

Figure A1. Change in salinity (psu) over time (elapsed hours) for the hypoxia trials. Solid lines represent the mean salinity levels in containers where mussels were exposed to hypoxia. Dashed lines represent control (unmanipulated seawater) containers. Line colors correspond to different trials. Vertical dotted lines indicate the average onset of DO decline and subsequent recovery to baseline conditions.

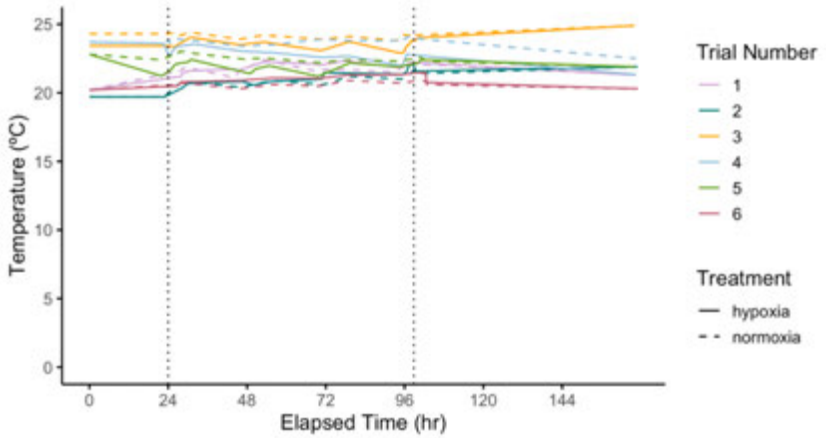

Figure A2. Change in temperature (ºC) over time (elapsed hours) for the hypoxia trials. Solid lines represent the mean temperatures in containers where mussels were exposed to hypoxia. Dashed lines represent control (unmanipulated seawater) containers. Line colors correspond to different trials. Vertical dotted lines indicate the average onset of DO decline and subsequent recovery to baseline conditions.

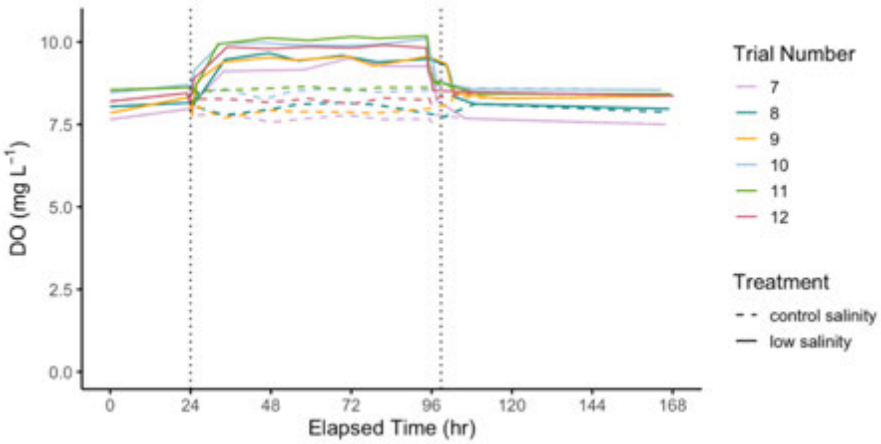

Figure A3. Change in DO (mg L^{-1}) over time (elapsed hours) for the low salinity trials. Solid lines represent the mean DO levels in containers where mussels were exposed to low salinity. Dashed lines represent control (unmanipulated seawater) containers. Line colors correspond to different trials. Vertical dotted lines indicate the average onset of salinity decline and subsequent recovery to baseline conditions.

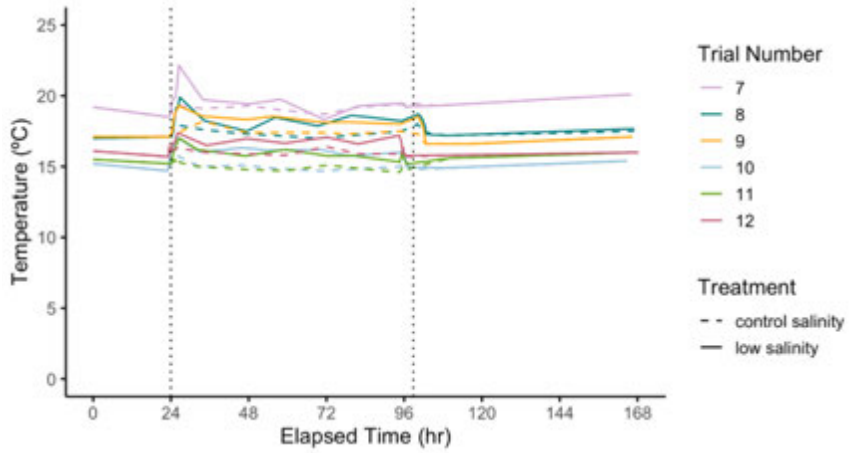

Figure A4. Change in temperature (°C) over time (elapsed hours) for the low salinity trials. Solid lines represent the mean temperatures in containers where mussels were exposed to low salinity. Dashed lines represent control (unmanipulated seawater) containers. Line colors correspond to different trials. Vertical dotted lines indicate the average onset of salinity decline and subsequent recovery to baseline conditions.

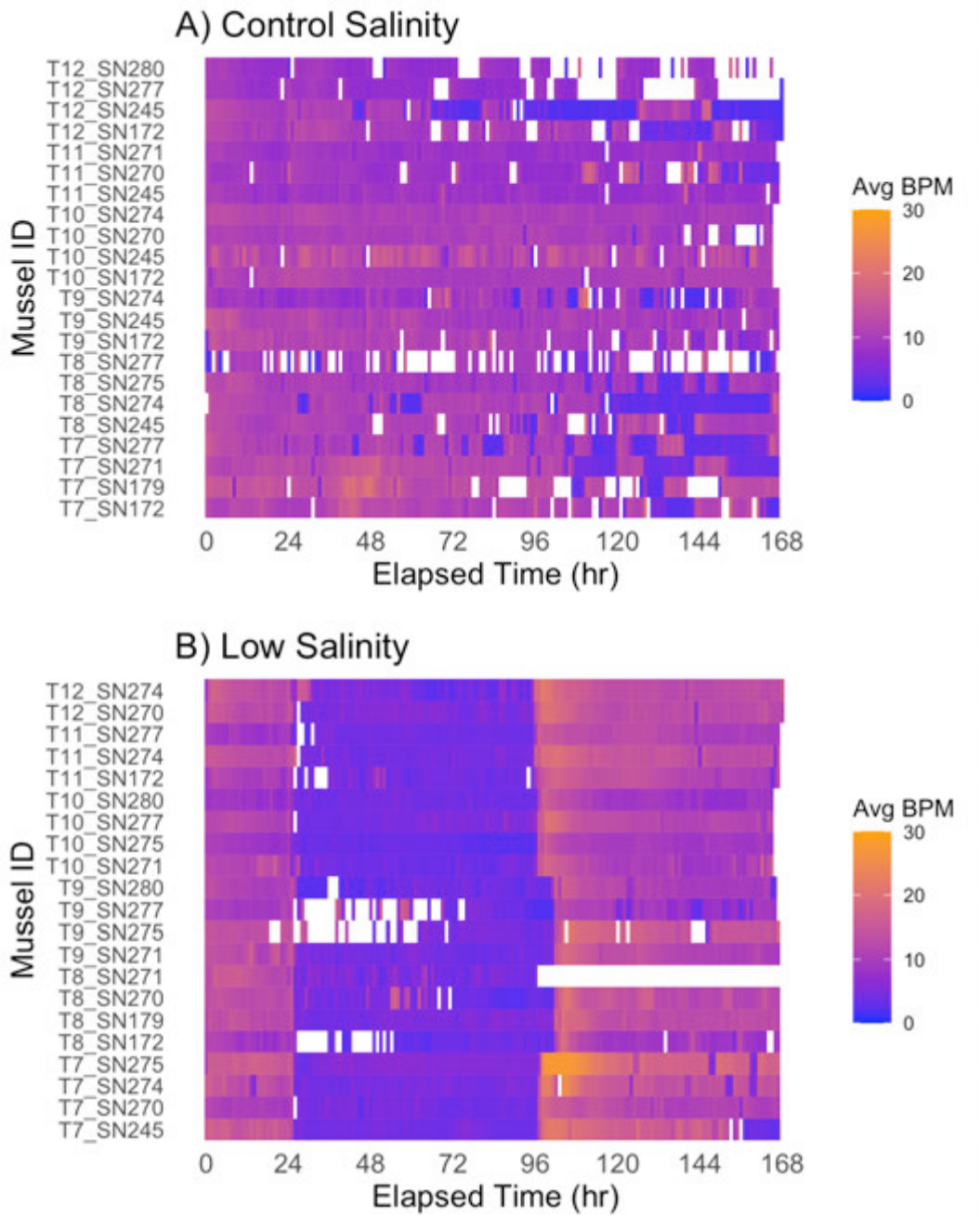

Figure A5. Heatmaps of A) the average heart rate (bpm) of all individual mussels exposed to control salinity and B) the average heart rate (bpm) of all individual mussels exposed to low salinity as trial time (hr) elapses. Treatment begins at 24 hours and ends at 96 hours.

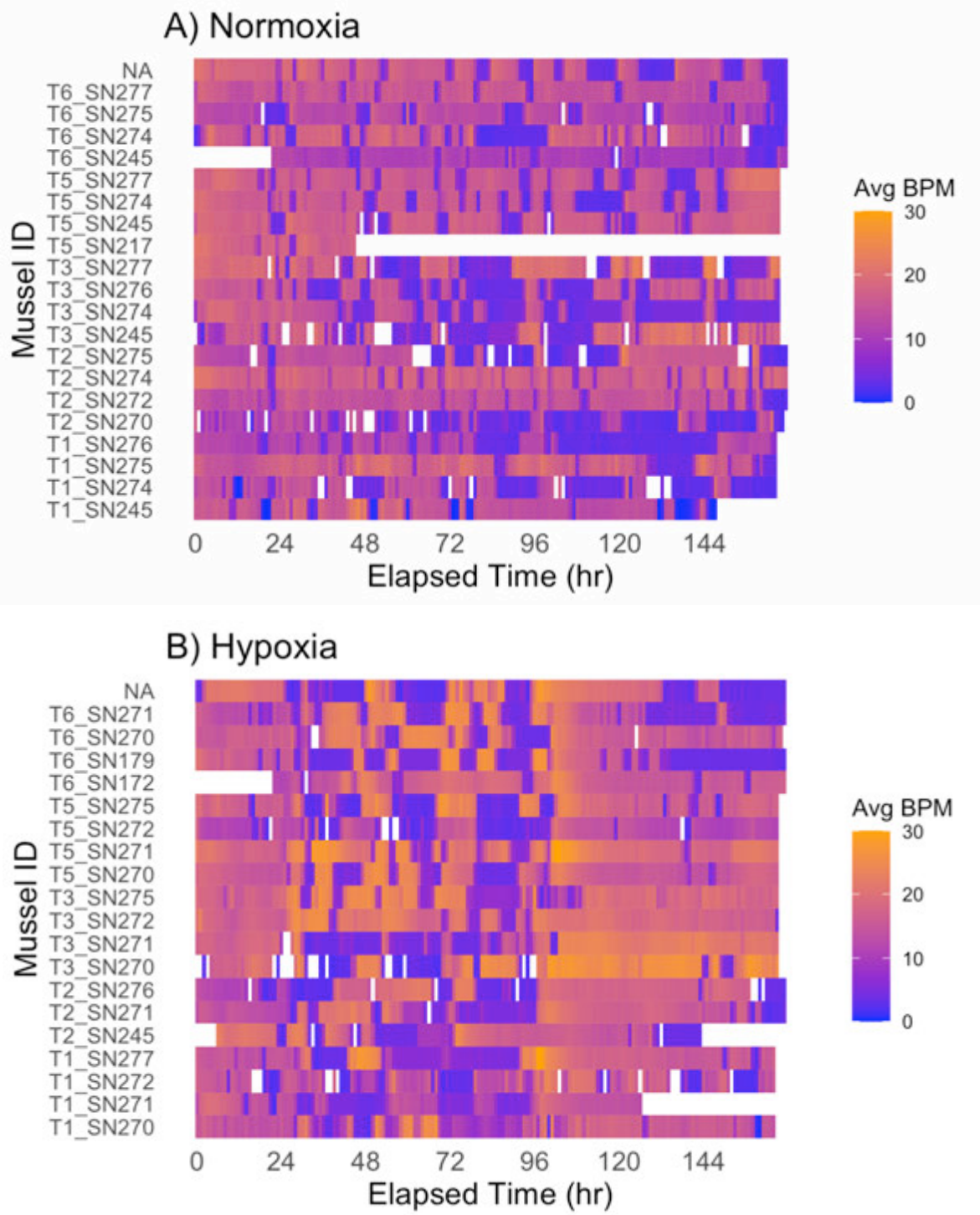

Figure A6. Heatmaps of A) the average heart rate (bpm) of all individual mussels exposed to normoxia and B) the average heart rate (bpm) of all individual mussels exposed to hypoxia as trial time (hr) elapses. Treatment begins at 24 hours and ends at 96 hours.

Table A1. Beginning length of all field mussels and end length, number of days deployed, and growth rate of mussels collected at the end of deployment. Growth rate calculated as the difference between the beginning and end shell lengths divided by the number of days deployed.

Individual mussel	Beginning Length (mm)	End Length (mm)	Days Deployed	Growth Rate (mm/day)
SDB_surface_01	68	74	487	0.012
SDB_surface_02	59	66	487	0.014
SDB_surface_03	50	68	487	0.037
SDB_surface_04	73.5	74	172	0.003
SDB_surface_05	73	76	315	0.009
SDB_bottom_01	77			
SDB_bottom_02	61			
SDB_bottom_03	79	90	412	0.027
SDB_bottom_04	68	80	412	0.029
TRE_surface_01	58	57	64	-0.016
TRE _surface_02	55	54	64	-0.016
TRE _surface_03	65	63	64	-0.031
TRE _surface_04	66	65	64	-0.016
TRE _surface_05	55	54	64	-0.016
TRE _surface_06	52	52	64	0
TRE _surface_07	57	58	64	0.016
TRE _surface_08	55	55	64	0
TRE _bottom_01	61	61	64	0
TRE _bottom_02	76	76	64	0
TRE _bottom_03	56	57	64	0.016
TRE _bottom_04	46	47	64	0.016
TRE _bottom_05	48	49	64	0.016
TRE _bottom_06	66	66	64	0
TRE _bottom_07	64	65	64	0.016
TRE _bottom_08	71	71	64	0

LPL_surface_01	65	79.5	251	0.058
LPL_surface_02	82	86	251	0.016
LPL_surface_03	62	65	251	0.012
LPL_surface_04	76	82	251	0.024
LPL_bottom_01	75			
LPL_bottom_02	88			
LPL_bottom_03	82			
LPL_bottom_04	64			

Table A2. Length, location, and trial type of mussels collected for lab trials.

Individual mussel	Length (mm)	Location	Trial type
T7_SN275	70	LPL	Salinity
T7_SN172	71	LPL	Salinity
T7_SN270	66	LPL	Salinity
T7_SN277	82	LPL	Salinity
T8_SN274	66	LPL	Salinity
T8_SN179	74	LPL	Salinity
T9_SN245	65.5	LPL	Salinity
T9_SN271	72	LPL	Salinity
T10_SN270	65	LPL	Salinity
T10_SN277	64	LPL	Salinity
T10_SN274	57	LPL	Salinity
T10_SN280	73	LPL	Salinity
T11_SN270	78.5	LPL	Salinity
T11_SN277	67	LPL	Salinity
T12_SN245	88.5	LPL	Salinity
T12_SN271	61	LPL	Salinity
T7_SN274	56.5	SDB	Salinity
T7_SN179	56	SDB	Salinity
T8_SN245	45	SDB	Salinity
T8_SN271	56	SDB	Salinity
T9_SN275	44	SDB	Salinity
T9_SN172	47	SDB	Salinity
T10_SN275	53	SDB	Salinity
T10_SN172	65.5	SDB	Salinity
T11_SN274	62.5	SDB	Salinity
T11_SN280	59	SDB	Salinity
T11_SN245	54	SDB	Salinity

T11_SN271	57	SDB	Salinity
T12_SN275	59	SDB	Salinity
T12_SN172	58	SDB	Salinity
T12_SN270	59	SDB	Salinity
T12_SN277	49	SDB	Salinity
T7_SN245	57	TRE	Salinity
T7_SN271	52	TRE	Salinity
T8_SN275	53.5	TRE	Salinity
T8_SN172	52	TRE	Salinity
T8_SN270	55	TRE	Salinity
T8_SN277	61.5	TRE	Salinity
T9_SN270	56.5	TRE	Salinity
T9_SN277	59	TRE	Salinity
T9_SN274	54	TRE	Salinity
T9_SN280	51	TRE	Salinity
T10_SN245	53	TRE	Salinity
T10_SN271	47	TRE	Salinity
T11_SN275	64	TRE	Salinity
T11_SN172	65.5	TRE	Salinity
T12_SN274	53	TRE	Salinity
T12_SN280	52	TRE	Salinity
T1_SN275	89	LPL	DO
T1_SN276	78	LPL	DO
T1_SN270	73	LPL	DO
T1_SN277	86	LPL	DO
T2_SN274	80	LPL	DO
T2_SN272	81	LPL	DO
T2_SN245	68	LPL	DO

T2_SN271	67	LPL	DO
T3_SN275	77	LPL	DO
T3_SN276	84	LPL	DO
T4_SN274	78	LPL	DO
T4_SN272	82	LPL	DO
T5_SN270	68	LPL	DO
T5_SN277	79	LPL	DO
T6_SN245	87	LPL	DO
T6_SN271	60	LPL	DO
T1_SN274	68	SDB	DO
T1_SN272	70	SDB	DO
T2_SN275	54	SDB	DO
T2_SN276	51	SDB	DO
T3_SN270	56	SDB	DO
T3_SN277	66	SDB	DO
T3_SN245	71	SDB	DO
T3_SN271	62	SDB	DO
T4_SN270	47	SDB	DO
T4_SN277	51	SDB	DO
T4_SN245	66	SDB	DO
T4_SN271	74	SDB	DO
T5_SN275	59	SDB	DO
T5_SN217	56	SDB	DO
T6_SN274	57	SDB	DO
T6_SN179	60	SDB	DO
T1_SN245	57	TRE	DO
T1_SN271	65	TRE	DO
T2_SN270	67	TRE	DO

T2_SN277	63	TRE	DO
T3_SN274	59	TRE	DO
T3_SN272	58	TRE	DO
T4_SN275	58	TRE	DO
T4_SN217	55	TRE	DO
T5_SN274	55	TRE	DO
T5_SN272	51	TRE	DO
T5_SN245	70	TRE	DO
T5_SN271	55	TRE	DO
T6_SN275	69	TRE	DO
T6_SN172	59	TRE	DO
T6_SN270	72	TRE	DO
T6_SN277	69.5	TRE	DO